A UNIFIED TREATMENT

SCALE, SYMMETRY, AND THE RENORMALIZATION GROUP

FROM DYNAMICAL SYSTEMS TO QUANTUM FIELD THEORY

github.com/muhammadhasyim/rg_ideas

First printing, December 4, 2025

Contents

List of Figures

List of Tables

Preface

This book is the culmination of years spent exploring the surprising connections between renormalization group ideas across seemingly disparate fields. My fascination began while studying Goldenfeld's *Lectures on Phase Transitions and the Renormalization Group*, a text remarkable not only for its treatment of Wilsonian renormalization in statistical mechanics and field theory, but also for its exposition of Barenblatt's work on self-similar solutions in nonlinear porous media flow. That a single mathematical framework could describe both critical phenomena in magnets and the spreading of groundwater through rock struck me as deeply significant.

Goldenfeld's book remains an essential reference for anyone seeking to understand RG beyond the confines of a single discipline.

This discovery became the impetus for a broader investigation. I began tracing the renormalization group through fluid turbulence, chaotic dynamics, and quantum field theory, finding in each case the same essential structure: a flow on a space of theories driven by changes in scale. What eventually emerged from these readings was an appreciation for the group-theoretic and geometric character of renormalization—the recognition that "the renormalization group" is quite literally a group (or more precisely, a semigroup) acting on a manifold of models, with the beta function as its infinitesimal generator.

Why, then, write another book on this subject when Goldenfeld's treatment already exists? The answer is that Goldenfeld's presentation, excellent as it is, was deliberately simplified for pedagogical purposes and does not develop the broader abstract framework that underlies the wide applicability of renormalization group methods. Much has happened in the decades since. Kunihiro and his students took the program to its fullest potential, applying RG techniques systematically to dynamical systems and unifying virtually all singular perturbation theories—work that proceeded in parallel to Goldenfeld's own contributions. Barenblatt laid the mathematical foundations for applications to partial differential equations through his theory of intermediate asymptotics. Fluid mechanicians developed RG approaches to turbulence. And a community of mathematical physicists has explored the Lie group structure and differential geometric foundations of the renormalization group with increasing rigor. The time has come

to synthesize these developments into a single cohesive treatment.

The renormalization group stands as one of the most profound conceptual advances in twentieth-century physics. What began as a technical device for handling infinities in quantum electrodynamics has grown into a universal framework for understanding how physical systems behave across different scales. The same mathematical structure appears in statistical mechanics near phase transitions, in fluid turbulence, in chaotic dynamical systems, and throughout quantum field theory.

The unity of these phenomena under a single mathematical umbrella represents a triumph of physical abstraction comparable to the unification of electricity and magnetism.

This book presents the renormalization group as a single geometric structure. The space of all possible theories or models forms a manifold, and the renormalization group generates a flow on this manifold. Fixed points of the flow correspond to scale-invariant theories. The geometry of the manifold encodes deep physical information about how theories relate to one another.

Our pedagogical strategy is to develop the abstract framework in Part I while simultaneously illustrating it with a simple example that admits both dynamical and statistical interpretations. The anharmonic oscillator serves this purpose admirably. As an ordinary differential equation, it exhibits amplitude-dependent frequency and the phenomenon of secular terms in perturbation theory. As a statistical mechanics problem, the same potential defines a partition function whose perturbative expansion requires resummation. The renormalization group resolves both difficulties through the same mechanism. Part I culminates in "The Unified Recipe," which distills the abstract framework into a six-step methodology where resurgent analysis is woven throughout rather than added as a final step, showing how perturbative and non-perturbative physics are inseparable aspects of a single geometric structure.

Part II applies the framework and recipe developed in Part I to seven physical systems of increasing complexity. Each application chapter explicitly invokes the six-step recipe, demonstrating how the unified geometric-resurgent framework manifests in concrete calculations. The systems range from chaotic dynamics in the Lorenz equations through turbulence in fluids, fracture mechanics in solids (following Barenblatt's theory of intermediate asymptotics), phase transitions in the Ising and O(N) models, and quantum field theories including QED and the Hubbard model.

Prerequisites

The reader should be familiar with undergraduate analysis and linear algebra, ordinary and partial differential equations, and elementary quantum mechanics. Some exposure to statistical mechanics and field

theory will be helpful but is not strictly required. Each chapter is designed to be self-contained, developing the necessary mathematical background as the physics demands it.

Notation

We use s or t for the scale parameter, typically the logarithm of an energy or length scale. Couplings or slow variables are denoted g^i and serve as coordinates on theory space $\mathcal{M}$. The beta function $\beta^i(g)$ is the vector field generating the RG flow. Scaling dimensions are denoted Δ with anomalous contributions γ. The metric on theory space is G_{ij}.

The Author
December 4, 2025

Part I

The Geometric Framework

Scale, Asymptotic Series, and Their Hidden Structure

The renormalization group is, at its core, a tool of **asymptotic analysis**. It allows us to understand what happens when we analyze the behavior of a mathematical model at large or small scales in space, time, energy, or any other parameter that can be taken to an extreme. But there is a deeper layer to this story that traditional treatments often defer to advanced chapters. Perturbation series almost always diverge, and this divergence is not a failure but rather a structured encoding of non-perturbative physics. The pattern of coefficients in a divergent series contains information about phenomena that no finite order of perturbation theory can capture directly. This chapter introduces both aspects simultaneously because they are inseparable parts of a unified framework.

The renormalization group is not primarily about "renormalizing" infinities in quantum field theory. That is one application. The deeper idea is asymptotic analysis combined with resurgent completion, understanding limiting behavior when some parameter becomes large or small and extracting the complete physical information encoded in divergent series.

Consider the fundamental question that motivates everything that follows. What is the long-time behavior of a dynamical system? What is the large-scale behavior of a statistical system? What is the low-energy behavior of a quantum field theory? These are all questions about limits that take the form $t \to \infty$ or $L \to \infty$ or $E \to 0$. In each case, we seek the asymptotic behavior that survives when everything else has been averaged away, decayed, or become irrelevant. The challenge is that standard perturbation theory typically fails to capture this behavior, and understanding why it fails reveals the mathematical structure we need.

The word "renormalization" suggests something is being made normal again. What requires normalization is our perturbative description, which breaks down when we attempt to describe phenomena across widely separated scales.

The apparent problem is that perturbative expansions in some small parameter ϵ give results valid for finite time t, but these results may diverge or become meaningless as $t \to \infty$. The culprit involves *non-commuting limits*. The perturbation expansion assumes we take $\epsilon \to 0$ first, but physics often requires $t \to \infty$ first, and these limits do not commute. Moreover, even when the limits can be exchanged, the perturbative coefficients grow factorially, meaning the series diverges for any nonzero value of the expansion parameter.

The solution has two components that must be developed together. First, the renormalization group allows parameters to "run" with scale, reorganizing perturbation theory so that both limits can be taken together. Second, resurgent analysis reveals that the factorial divergence

of perturbative coefficients is not pathological but rather encodes non-perturbative physics through the Borel plane. This chapter introduces these ideas through our first detailed example, the **anharmonic oscillator**, which exhibits both secular divergence from non-commuting limits and factorial divergence from the nonlinear structure of the equation.

Dissecting the Name

The term "renormalization group" is somewhat unfortunate. It is neither primarily about "renormalizing" infinities, nor does it always form a "group" in the strict mathematical sense. Let us dissect each word to understand what we are actually doing.

Why "Renormalization"?

The prefix "re-" suggests doing something again. But what is being "normalized"? The answer depends on the historical context, but the modern understanding unifies all the different usages.

Historical note: The concept of "renormalized mass" predates quantum field theory. In 19th-century hydrodynamics, the effective mass of a body moving through fluid was "renormalized" to account for the entrained fluid.

The original context in QFT. In quantum field theory, perturbative calculations produce infinities where integrals diverge. Early practitioners realized these infinities could be absorbed into redefinitions of physical parameters like mass, charge, and coupling constants. The "bare" parameters in the Lagrangian are infinite, but the "renormalized" parameters that are physically measured are finite. The infinities cancel when observables are expressed in terms of renormalized quantities.

The modern understanding. Today we recognize that renormalization is not fundamentally about infinities at all. It is about *scale dependence*. Physical parameters like coupling constants are not universal numbers that take the same value at all scales. They depend on the scale at which we measure them, and this dependence is what the renormalization group tracks.

In the anharmonic oscillator, the "bare" amplitude A_0 at $t = 0$ and the "renormalized" amplitude $A(t)$ at time t are related by the RG flow. No infinities anywhere, just scale dependence.

The unified view. Whether we are dealing with UV divergences in QFT, secular terms in perturbation theory, or scale-dependent effective parameters, the underlying issue is the same. Parameters that look fixed at one scale must "run" to describe physics at another scale. This running is renormalization.

Box 1.1: Effective Mass in a Fluid—The First Renormalization

The problem. A sphere of mass m_{bare} and volume V moves through a fluid of density ρ. How does it accelerate under an applied force?

Naive expectation. Newton's law: $F = m_{\text{bare}} a$.

What actually happens. As the sphere accelerates, it must push fluid out of the way. The fluid near the sphere is set in motion and acquires kinetic energy. This "entrained" fluid contributes to the inertia.

The result. For a sphere, the equation of motion becomes:

$$F = m_{\text{eff}}\, a, \qquad m_{\text{eff}} = m_{\text{bare}} + \frac{1}{2}\rho V. \tag{1}$$

The factor $\frac{1}{2}\rho V$ is the "added mass" from the entrained fluid.

The key insight. The "bare" mass is what you'd measure in vacuum. The "effective" mass is what governs motion in the medium. The effective parameter absorbs environmental effects at scales below our resolution (the molecular structure of the fluid).

This is the prototype of renormalization: Same physics, different description, depending on whether we "see" the microscopic degrees of freedom or not.

Why "Group"?

A group is a set with a binary operation satisfying four axioms involving closure, associativity, identity, and inverses. Does the RG satisfy these? The answer depends on which version of the RG we consider.

A **group** has four properties: closure, associativity, identity, and inverses. A **semi-group** lacks inverses.

The dilation group. Scale transformations $x \to bx$ form a one-parameter group:

$$D_b : x \mapsto bx, \qquad D_{b_1} \circ D_{b_2} = D_{b_1 b_2}. \tag{2}$$

This is the multiplicative group $(\mathbb{R}^+, \times)$ where closure and associativity are manifest, the identity is D_1, and inverses exist via $D_b^{-1} = D_{1/b}$.

The catch involves coarse-graining. The RG transformation that integrates out short-wavelength modes is *not invertible*. If we average over fast degrees of freedom, we cannot recover them because information is lost.

Strictly speaking, the coarse-graining RG is a **semi-group**: $R_{b_1} \circ R_{b_2} = R_{b_1 b_2}$, but R_b^{-1} does not exist.

Two flavors of RG. There are actually two distinct operations that both go by the name "RG" and have different mathematical structures.

The first is **coarse-graining** in the sense of Wilson's RG, where we integrate out short-distance degrees of freedom. This is a *semi-group* because no inverse exists. Once information about small scales is lost, it cannot be recovered.

The second is **reparameterization** in the sense of field theory RG, where we change the renormalization scale μ while holding physical predictions fixed. This *is* a true group because the scale can be changed in either direction.

Both flavors lead to the same **beta functions** and **fixed points**, which are the objects of primary physical interest.

What Is Scale?

The concept of scale pervades physics, yet it is rarely examined carefully. What exactly do we mean when we say two phenomena occur at "different scales"?

Scales Are Everywhere

Physical systems exhibit characteristic scales of many types, and recognizing these scales is the first step in any RG analysis.

Every model implicitly chooses which scales to include. A continuum description ignores atomic scales, and a one-body approximation ignores many-body correlations.

Spatial scales include atomic spacing at roughly 10^{-10} meters, sample size, domain size, and correlation length. In a ferromagnet near its Curie temperature, the correlation length ξ can span many orders of magnitude as criticality is approached.

Temporal scales include oscillation periods, relaxation times, and observation windows. The anharmonic oscillator that we will study has a fast scale given by the oscillation period $2\pi/\omega_0$ and a slow scale given by the timescale over which the frequency drifts, which is approximately $1/(\lambda A^2)$.

Energy scales include thermal energy $k_B T$, interaction energy, and mass thresholds. In quantum field theory, the mass m of a particle sets an energy scale mc^2 below which the particle effectively decouples from the dynamics.

When Scales Don't Talk to Each Other

The simplest situation occurs when scales are *well-separated* in the sense that the ratio of two characteristic scales is very large. When this happens, we can treat the physics at each scale independently.

Scale separation: When $\tau_{\text{fast}} \ll \tau_{\text{slow}}$, the fast dynamics "averages out" on slow timescales.

Consider the anharmonic oscillator with small nonlinearity λ. The fast timescale is the oscillation period $\tau_{\text{fast}} \sim 1/\omega_0$. The slow timescale is the frequency-drift time $\tau_{\text{slow}} \sim \omega_0/(\lambda A^2)$. Because λ is small, we have $\tau_{\text{fast}} \ll \tau_{\text{slow}}$, meaning the scales are well-separated. This separation enables an *effective description* where we can average over the fast oscillations to obtain a simpler equation for the slow amplitude dynamics.

When Scales Collide: The RG Problem

The interesting and difficult situation occurs when scales are *not* well-separated. This happens in several important contexts.

Near critical points, the correlation length diverges and all scales become coupled. In strongly coupled systems, no small parameter exists to separate the physics at different scales. When we push perturbation theory beyond its domain of validity, it attempts to encode physics from all scales simultaneously and fails.

Non-commuting limits: $\lim_{t\to\infty}\lim_{\lambda\to 0} \neq \lim_{\lambda\to 0}\lim_{t\to\infty}$. The order matters.

The mathematical signature of scale collision is **non-commuting limits**. In the anharmonic oscillator:

$$\lim_{t\to\infty}\lim_{\lambda\to 0} x(t;\lambda) \neq \lim_{\lambda\to 0}\lim_{t\to\infty} x(t;\lambda). \tag{3}$$

If we first set $\lambda = 0$ and then evolve forever, we get simple harmonic motion. If we first evolve forever at fixed $\lambda \neq 0$ and then try to take $\lambda \to 0$, we must account for the accumulated frequency shift. The renormalization group provides a systematic framework for handling these situations.

Dimensional Analysis: The Classical Theory of Scale

Before the renormalization group, physicists had a powerful tool for exploiting scale symmetry in dimensional analysis. Understanding when it works and when it fails is essential preparation for the RG.

Dimensional analysis is representation theory of the dilation group in disguise. It identifies quantities that transform simply under scaling.

Units and Dimensions

Every physical quantity has **dimensions** that specify what kind of thing it is. In mechanics, we typically use three base dimensions including length L, time T, and mass M. Derived quantities have dimensions that are products of powers of these base dimensions. Velocity has dimensions $[v] = LT^{-1}$, force has dimensions $[F] = MLT^{-2}$, and energy has dimensions $[E] = ML^2T^{-2}$.

The Buckingham Pi Theorem

The fundamental result of dimensional analysis is the Buckingham Pi theorem, which tells us how the form of physical relationships is constrained by dimensional consistency.

Theorem 0.1 (Buckingham Pi Theorem)**.** *If a physical quantity Q depends on n parameters $p_1, \ldots, p_n$ involving k independent base dimensions, then*

$$Q = [p_1]^{\alpha_1} \cdots [p_n]^{\alpha_n} \cdot \Phi(\Pi_1, \ldots, \Pi_{n-k}) \tag{4}$$

where Φ is an arbitrary function of $n - k$ independent dimensionless combinations Π_i.

The Π theorem reduces a problem with n parameters to one with $n - k$ dimensionless parameters.

The power of this theorem becomes manifest when $n = k$, because then there are *no* dimensionless combinations, and the answer is determined up to a pure number.

Box 1.2: The Simple Pendulum

Problem: Find the period T of a simple pendulum of length ℓ in gravitational field g.

Step 1: List parameters and dimensions.

Parameter	Symbol	Dimensions
Period	T	T
Length	ℓ	L
Gravity	g	LT^{-2}

Step 2: Count. We have $n = 2$ parameters (ℓ, g) and $k = 2$ dimensions (L, T). So $n - k = 0$ means no dimensionless combinations.

Step 3: Solve. The period must have the form $T = C \cdot \ell^a g^b$ where:

$$T: \quad 1 = -2b \implies b = -1/2 \tag{5}$$

$$L: \quad 0 = a + b \implies a = 1/2 \tag{6}$$

Result:

$$T = C\sqrt{\frac{\ell}{g}} \tag{7}$$

The constant $C = 2\pi$ requires solving the ODE. But dimensional analysis determined the *form* completely.

Check: For $\ell = 1$ m and $g = 10$ m/s^2: $T \approx 2$ s. ✓

When Dimensional Analysis Fails

Dimensional analysis fails or is incomplete when there *are* dimensionless parameters. Then the physics depends on these parameters in ways that dimensional analysis cannot predict.

When dimensionless parameters exist, we must actually solve the problem. Dimensional analysis only tells us the form.

Consider the damped oscillator governed by $m\ddot{x} + \gamma\dot{x} + kx = 0$. There is one dimensionless combination given by the damping ratio $\zeta = \gamma/(2\sqrt{mk})$. The frequency takes the form $\omega = \sqrt{k/m} \cdot f(\zeta)$ for some function f. Dimensional analysis gives the form but cannot determine that $f(\zeta) = \sqrt{1-\zeta^2}$. We must solve the problem to find the function.

This limitation of dimensional analysis will become important when we encounter **anomalous dimensions** in later chapters. These are situations where the effective scaling exponents cannot be predicted from dimensional analysis alone because they depend on dimensionless coupling constants through functions that must be computed dynamically.

The Anharmonic Oscillator: Our First Example

We now introduce the problem that will accompany us through much of this book. The **anharmonic oscillator** is the simplest system that exhibits the failure of naive perturbation theory and its resolution through renormalization group ideas. It also exhibits the Gevrey-1 divergence structure that is generic to physical perturbation series.

The Setup

Consider a particle of unit mass moving in a potential

$$V(x) = \frac{1}{2}\omega_0^2 x^2 + \frac{\lambda}{4}x^4. \tag{8}$$

The parameter ω_0 sets the frequency of small oscillations, while $\lambda > 0$ controls the anharmonic correction. The equation of motion is:

$$\ddot{x} + \omega_0^2 x + \lambda x^3 = 0. \tag{9}$$

The quartic potential x^4 is the simplest nonlinearity that preserves $x \to -x$ symmetry and keeps motion bounded.

Box 1.3: Dimensional Analysis of the Anharmonic Oscillator

Question: How does the oscillation frequency ω depend on amplitude A?

Step 1: List parameters and dimensions. The natural frequency ω_0 has dimensions $[T^{-1}]$. The coupling λ has dimensions $[T^{-2}L^{-2}]$ since $[\lambda x^4] = [\omega_0^2 x^2]$. The amplitude A has dimensions $[L]$.

Step 2: Count. $n = 3$ parameters, $k = 2$ dimensions (L, T). So $n - k = 1$ dimensionless combination.

Step 3: Form the dimensionless group.

$$\Pi = \frac{\lambda A^2}{\omega_0^2} \tag{10}$$

Step 4: Apply the theorem.

$$\omega = \omega_0 \, f(\Pi) = \omega_0 \, f\left(\frac{\lambda A^2}{\omega_0^2}\right) \tag{11}$$

with $f(0) = 1$ (harmonic limit).

What dimensional analysis tells us: The frequency depends on amplitude only through $\lambda A^2/\omega_0^2$.

What it cannot tell us: The function $f(\Pi)$. Is it $1 + c\Pi + \cdots$? What is c?

Physical Intuition

Before calculating, let's think physically. The quartic term provides extra restoring force when x is large. A larger amplitude means more time spent in the "stiff" part of the potential. We expect that larger amplitude leads to higher effective frequency, meaning the frequency should increase with Π and $f'(\Pi) > 0$.

Always check your answer against physical intuition. If $f'(\Pi) < 0$, something is wrong.

Naive Perturbation Theory and Its Failure

Let's solve the anharmonic oscillator using naive perturbation theory and see exactly how it fails. The failure has two aspects that are often discussed separately but are actually related. The secular terms signal that the perturbative ansatz is missing an amplitude-dependent frequency. The factorial growth of higher-order coefficients signals that the series diverges and requires resummation.

Setting Up the Expansion

Assume $\Pi = \lambda A^2/\omega_0^2 \ll 1$ and expand:

$$x(t) = x_0(t) + \lambda x_1(t) + \lambda^2 x_2(t) + \cdots \tag{12}$$

Perturbation theory assumes the answer is close to a known solution and computes corrections order by order.

Substituting into $\ddot{x} + \omega_0^2 x + \lambda x^3 = 0$ and collecting powers of λ gives a hierarchy of equations.

At order $O(\lambda^0)$ we have:

$$\ddot{x}_0 + \omega_0^2 x_0 = 0 \tag{13}$$

The solution is $x_0(t) = A\cos(\omega_0 t)$ when we choose initial conditions $x(0) = A$ and $\dot{x}(0) = 0$.

At order $O(\lambda^1)$ we have:

$$\ddot{x}_1 + \omega_0^2 x_1 = -x_0^3 = -A^3\cos^3(\omega_0 t) \tag{14}$$

Box 1.4: Deriving the Secular Term

Goal: Solve $\ddot{x}_1 + \omega_0^2 x_1 = -A^3\cos^3(\omega_0 t)$ with $x_1(0) = \dot{x}_1(0) = 0$.
Step 1: Expand the cubic. Using $\cos^3\theta = \frac{3}{4}\cos\theta + \frac{1}{4}\cos 3\theta$:

$$\ddot{x}_1 + \omega_0^2 x_1 = -\frac{3A^3}{4}\cos(\omega_0 t) - \frac{A^3}{4}\cos(3\omega_0 t) \tag{15}$$

Step 2: Identify the resonance. The $\cos(\omega_0 t)$ term oscillates at the natural frequency. This is *resonant forcing*. The $\cos(3\omega_0 t)$ term is non-resonant.

Step 3: Solve for the non-resonant term. Try $x_{1,\text{nr}} = B\cos(3\omega_0 t)$:

$$-9\omega_0^2 B + \omega_0^2 B = -\frac{A^3}{4} \implies B = \frac{A^3}{32\omega_0^2} \tag{16}$$

Step 4: Solve for the resonant term. For resonant forcing $\ddot{y} + \omega_0^2 y = C\cos(\omega_0 t)$, the standard ansatz $y = D\cos(\omega_0 t)$ fails (gives $0 = C$). Instead, try $y = Et\sin(\omega_0 t)$:

$$\dot{y} = E\sin(\omega_0 t) + E\omega_0 t\cos(\omega_0 t) \tag{17}$$

$$\ddot{y} = 2E\omega_0\cos(\omega_0 t) - E\omega_0^2 t\sin(\omega_0 t) \tag{18}$$

Substituting:

$$2E\omega_0\cos(\omega_0 t) = C\cos(\omega_0 t) \implies E = \frac{C}{2\omega_0} \tag{19}$$

With $C = -3A^3/4$: $E = -3A^3/(8\omega_0)$.

Step 5: Apply initial conditions. The full x_1 is:

$$x_1(t) = \frac{A^3}{32\omega_0^2}\left[\cos(3\omega_0 t) - \cos(\omega_0 t)\right] - \frac{3A^3}{8\omega_0} t\sin(\omega_0 t) \tag{20}$$

Check: $x_1(0) = \frac{A^3}{32\omega_0^2}(1-1) - 0 = 0$ ✓

The secular term:

$$\boxed{x_1(t) \supset -\frac{3A^3}{8\omega_0} t\sin(\omega_0 t)} \tag{21}$$

This term grows *linearly in time*. At $t \sim \omega_0/(\lambda A^2)$, it becomes $O(A)$ which is as large as the leading term!

What Went Wrong?

The secular term $t\sin(\omega_0 t)$ grows without bound. At time $t \sim 1/(\lambda A^2)$, perturbation theory has failed.

The complete solution to first order is:

$$x(t) = A\cos(\omega_0 t) + \lambda\left[\frac{A^3}{32\omega_0^2}(\cos 3\omega_0 t - \cos\omega_0 t) - \frac{3A^3}{8\omega_0} t\sin(\omega_0 t)\right] + O(\lambda^2) \tag{22}$$

The last term involving $t\sin(\omega_0 t)$ is a **secular term**. It signals the breakdown of naive perturbation theory and has a deep physical origin.

Physical origin: The nonlinearity causes the frequency to depend on amplitude. The *true* solution oscillates at $\omega_{\text{eff}} = \omega_0 + O(\lambda A^2)$, not exactly ω_0. But our expansion assumed fixed frequency ω_0. The accumulated phase error grows linearly in time.

Expanding $\cos[(1 + \alpha\lambda A^2)\omega_0 t]$ for small λ gives:

$$\cos(\omega_{\text{eff}} t) \approx \cos(\omega_0 t) - \alpha\lambda A^2 \omega_0 t \sin(\omega_0 t) + \cdots \tag{23}$$

The secular term is the perturbative expansion "trying" to represent a frequency shift.

There it is! The secular term is just the Taylor expansion of a frequency shift. The perturbative series is attempting to encode information that it cannot naturally accommodate because frequency shifts require exponential functions, not polynomial corrections.

Perturbation Series Diverge But Speak

The secular term is not the only problem with perturbation theory. Even if we could somehow avoid secular terms, the perturbative coefficients grow factorially with order, meaning the series diverges for any nonzero value of the coupling. This sounds like a disaster, but it is actually a blessing in disguise.

Gevrey-1 Divergence

A Gevrey-1 series has factorial coefficient growth. This is the generic case for perturbation series in physics.

A formal power series $\sum_{n=0}^{\infty} c_n z^n$ is **Gevrey of order 1** (or Gevrey-1) if:

$$|c_n| \leq C \cdot A^n \cdot n! \tag{24}$$

for some constants $C, A > 0$. This means the coefficients grow at most factorially. For a Gevrey-1 series, the formal sum has zero radius of convergence, yet the coefficients have a very specific structure.

Why is Gevrey-1 generic in physics? The answer lies in how perturbative coefficients are generated. For any ordinary differential equation of the form $dy/dx = f(x, y)$ with f analytic, the formal solution has coefficients determined by a recursive relation. This recursion generically produces factorial growth and no faster. The nonlinear terms in the ODE generate combinatorial factors when we iterate the recursion, and these factors accumulate to produce $n!$ growth.

The Anharmonic Oscillator's Divergent Series

For the quantum anharmonic oscillator (which is closely related to the classical problem we are studying), the ground state energy has a perturbative expansion:

$$E_0(\lambda) = \frac{1}{2}\omega_0 + \frac{3\lambda}{4\omega_0} - \frac{21\lambda^2}{8\omega_0^3} + \cdots \tag{25}$$

The n-th coefficient grows as $c_n \sim (-1)^n \cdot \text{const} \cdot A^n \cdot n!$ for large n. This series diverges for any $\lambda \neq 0$, yet the ground state energy is perfectly well-defined for $\lambda > 0$.

This is not a failure of the perturbative approach but rather a signal that the perturbative series is encoding more information than meets the eye. The factorial growth pattern tells us something about non-perturbative physics that no finite truncation of the series can capture.

What Divergence Encodes

Divergent series are not failures. They encode non-perturbative physics through the pattern of their coefficients.

The key insight is that the *way* a series diverges carries information. A series with alternating signs and factorial growth $(-1)^n n!$ encodes different physics than one with positive factorial growth $n!$. The positions where the "resummed" series has singularities correspond to non-perturbative effects like instantons (tunneling configurations) and renormalons (effects from the running of couplings).

For the anharmonic oscillator with positive λ, the potential $V(x) = \frac{1}{2}\omega_0^2 x^2 + \frac{\lambda}{4}x^4$ has no tunneling barrier in the classical theory. But continuing to negative λ (or equivalently, to imaginary x), there is a barrier and the particle can tunnel. The factorial divergence of the perturbative series is directly related to these complex-time or imaginary-position trajectories. The perturbative series "knows" about these configurations even though it cannot explicitly include them.

The Borel Plane as a Second Arena

The mathematical tool for extracting the information encoded in divergent series is the **Borel transform**. This transform maps a divergent Gevrey-1 series to a convergent one, opening up a new geometric arena where non-perturbative physics becomes visible.

The Borel Transform

Given a formal series:

$$\tilde{f}(z) = \sum_{n=0}^{\infty} c_n z^n \tag{26}$$

its Borel transform is:

$$\hat{f}(\zeta) = \sum_{n=0}^{\infty} \frac{c_n}{n!} \zeta^n \tag{27}$$

The Borel transform divides by $n!$, converting factorial growth into geometric growth. The result *converges*.

For a Gevrey-1 series with $|c_n| \leq C \cdot A^n \cdot n!$, we have $|c_n/n!| \leq C \cdot A^n$. The Borel transform therefore has radius of convergence at least $1/A$. What was a divergent series becomes a convergent one!

The complex ζ-plane is called the **Borel plane**. It is the natural geometric arena for understanding divergent series. The original series diverges in the z-plane, but its Borel transform converges near the origin of the ζ-plane.

Singularities in the Borel Plane

The Borel transform $\hat{f}(\zeta)$ is analytic near $\zeta = 0$ but may have singularities elsewhere in the Borel plane. These singularities are not defects to be avoided. They encode non-perturbative physics.

Different types of singularities correspond to different physical effects. Poles or branch points at $\zeta = S_{\text{inst}}$ (the classical instanton action) encode tunneling effects. Singularities at $\zeta_k = k/\beta_1$ (where β_1 is the one-loop beta function) are called **renormalons** and arise from the factorial growth induced by RG running. The positions, residues, and types of these singularities are physical data about the system.

Borel-Laplace Resummation

To recover a function from its Borel transform, we use the **Laplace transform**:

$$f(z) = \int_0^\infty e^{-\zeta/z} \hat{f}(\zeta)\, d\zeta \tag{28}$$

Borel-Laplace resummation: transform to make the series converge, analytically continue, then transform back.

If $\hat{f}$ has no singularities on the positive real axis $[0, \infty)$, this integral converges and defines a function $f(z)$. Remarkably, this function has the original divergent series as its asymptotic expansion as $z \to 0$. We have recovered a genuine function from a formally divergent series.

But what if there are singularities on the integration path? This is where the physics becomes interesting. The integral is ambiguous and different choices of contour (going above or below the singularity) give answers that differ by exponentially small terms like $e^{-S/z}$. These ambiguities are not bugs. They are the entry point for non-perturbative physics.

Box 1.4a: A Simple Borel Transform

The series: Consider $\tilde{f}(z) = \sum_{n=0}^{\infty} n!\, z^n$. This diverges for all $z \neq 0$.

Borel transform:

$$\hat{f}(\zeta) = \sum_{n=0}^{\infty} \frac{n!}{n!} \zeta^n = \sum_{n=0}^{\infty} \zeta^n = \frac{1}{1-\zeta} \tag{29}$$

This converges for $|\zeta| < 1$ and has an analytic continuation with a pole at $\zeta = 1$.

Attempted resummation:

$$f(z) = \int_0^\infty e^{-\zeta/z} \frac{1}{1-\zeta}\, d\zeta \tag{30}$$

The problem: The pole at $\zeta = 1$ lies on the integration path! The integral is ambiguous.

Resolution: Go above or below the pole using $f^{\pm}(z) = \int_0^{\infty \pm i\epsilon} e^{-\zeta/z} \frac{1}{1-\zeta}\, d\zeta$.

The difference:

$$f^+(z) - f^-(z) = -2\pi i \cdot e^{-1/z} \tag{31}$$

Key insight: The ambiguity is exponentially small in $1/z$. It is a non-perturbative effect that is invisible to any finite order of the original series but is encoded in the singularity structure of the Borel transform.

The RG Resolution

We now solve the secular term problem using a technique that reveals the essential logic of the renormalization group. The resolution of secular terms and the structure of divergent series are related because both involve the perturbative expansion attempting to encode information it cannot naturally represent.

This calculation is worth understanding thoroughly. The same logical structure underlies all RG applications.

The key idea: Let the parameters that naive perturbation theory holds fixed become slowly varying functions. This allows the expansion to accommodate physics (like frequency shifts) that would otherwise appear as pathologies.

The Multiple-Scales Ansatz

In naive perturbation theory, we wrote $x(t) = A\cos(\omega_0 t + \phi)$ with *fixed* A and ϕ. The RG approach promotes these to *slow variables*:

$$x(t) = A(\tau)\cos\big(\omega_0 t + \phi(\tau)\big) + O(\lambda) \tag{32}$$

where $\tau = \lambda t$ is a "slow time." The requirement that secular terms cancel determines how $A(\tau)$ and $\phi(\tau)$ evolve.

Box 1.5: The RG Solution of the Anharmonic Oscillator

Goal: Find how amplitude A and phase ϕ must evolve to eliminate secular terms.

Step 1: Multiple-scales expansion. Introduce slow time $\tau = \lambda t$ and seek:

$$x(t) = x_0(t,\tau) + \lambda x_1(t,\tau) + O(\lambda^2) \tag{33}$$

The time derivative becomes $\mathrm{d}/\mathrm{d}t = \partial/\partial t + \lambda\,\partial/\partial\tau$.

Step 2: Zeroth order. $\partial^2 x_0/\partial t^2 + \omega_0^2 x_0 = 0$ gives:

$$x_0 = A(\tau)\cos\big(\omega_0 t + \phi(\tau)\big) \tag{34}$$

Step 3: First order. The $O(\lambda)$ equation is:

$$\frac{\partial^2 x_1}{\partial t^2} + \omega_0^2 x_1 = -2\frac{\partial^2 x_0}{\partial t\,\partial\tau} - x_0^3 \tag{35}$$

The mixed derivative gives (writing $\Theta = \omega_0 t + \phi$):

$$-2\frac{\partial^2 x_0}{\partial t \partial \tau} = 2\omega_0 A' \sin\Theta + 2\omega_0 A\phi' \cos\Theta \tag{36}$$

where primes denote $\mathrm{d}/\mathrm{d}\tau$.
The cubic term gives:

$$-x_0^3 = -A^3\cos^3\Theta = -\frac{3A^3}{4}\cos\Theta - \frac{A^3}{4}\cos 3\Theta \tag{37}$$

Step 4: Cancel secular terms. Resonant terms (at frequency ω_0) produce secular growth unless their coefficients vanish.
Coefficient of $\sin\Theta$:

$$2\omega_0 A' = 0 \implies \frac{\mathrm{d}A}{\mathrm{d}\tau} = 0 \tag{38}$$

Coefficient of $\cos\Theta$:

$$2\omega_0 A\phi' - \frac{3A^3}{4} = 0 \implies \frac{\mathrm{d}\phi}{\mathrm{d}\tau} = \frac{3A^2}{8\omega_0} \tag{39}$$

Step 5: The RG equations. Converting to physical time t (with $\tau = \lambda t$):

$$\frac{\mathrm{d}A}{\mathrm{d}t} = 0 \tag{40}$$

$$\frac{\mathrm{d}\phi}{\mathrm{d}t} = \frac{3\lambda A^2}{8\omega_0} \tag{41}$$

Step 6: Solve and interpret. The amplitude is constant: $A(t) = A_0$ (energy conservation in the undamped case).
The phase grows linearly:

$$\phi(t) = \phi_0 + \frac{3\lambda A^2}{8\omega_0} t \tag{42}$$

The effective frequency is:

$$\boxed{\omega_{\text{eff}} = \omega_0 + \frac{3\lambda A^2}{8\omega_0} = \omega_0\left(1 + \frac{3\lambda A^2}{8\omega_0^2}\right)} \tag{43}$$

Physical interpretation: The nonlinearity shifts the frequency upward (for $\lambda > 0$). Larger amplitudes oscillate faster. Dimensional analysis predicted $\omega = \omega_0 f(\lambda A^2/\omega_0^2)$, and now we know $f(\Pi) = 1 + \frac{3}{8}\Pi + O(\Pi^2)$.
Checks: As $\lambda \to 0$, we have $\omega_{\text{eff}} \to \omega_0$ ✓. The sign is correct because $\lambda > 0$ gives $\omega_{\text{eff}} > \omega_0$ (stiffer potential means faster oscillation) ✓. The dimensions work because $[\lambda A^2/\omega_0] = T^{-1}$ ✓.

The Pattern

This pattern recurs in every RG application. The details change but the logic is universal.

The anharmonic oscillator illustrates a universal pattern that appears across all applications of the renormalization group.

First, **identify the divergence**. Naive perturbation theory produces secular terms, UV divergences, or boundary layer mismatches, depending on context. These pathologies signal that the perturbative ansatz is missing something.

Second, **promote constants to functions**. Parameters that were held fixed become scale-dependent. The amplitude becomes $A(\ell)$ and the phase becomes $\phi(\ell)$, where ℓ is a scale parameter.

Third, **require consistency**. Demanding that the expansion remain valid (meaning secular terms cancel or divergences are absorbed) determines how parameters must flow.

Fourth, **solve the flow**. The resulting equations are the RG equations and they determine the scale dependence of effective parameters.

Fifth, **extract physics**. Physical predictions come from the flow, not from any single point in parameter space.

Box 1.6: RG in Different Contexts

The same pattern appears across fields with different physical manifestations.

Multiple scales (ODEs): The divergence manifests as secular terms $\sim t^n$. The running parameters are slow amplitudes and phases. The scale is time t or slow time $\tau = \epsilon t$.

Wilson's RG (statistical mechanics): The divergence manifests as UV modes in loop integrals. The running parameters are coupling constants m^2 and λ. The scale is the momentum cutoff Λ or $\ell = \log(\Lambda_0/\Lambda)$.

Amplitude equations (PDEs): The divergence manifests as secular growth in space or time. The running parameters are envelope amplitudes. The scale involves slow spatial or temporal variables.

QFT renormalization: The divergence manifests as loop integrals $\sim \Lambda^n$ or $\log \Lambda$. The running parameters are masses and couplings. The scale is the renormalization scale μ.

Same mathematics, different physics.

A Preview of the Unified Framework

The anharmonic oscillator demonstrates both aspects of the challenges that perturbation theory faces. The secular terms arise from non-commuting limits and require running parameters. The factorial divergence of coefficients encodes non-perturbative physics accessible through the Borel plane. These two aspects are related and will be

unified in the coming chapters.

Two Geometric Arenas

Parameter space and the Borel plane are two complementary arenas where RG physics lives.

The RG introduces a geometric perspective where parameters like (A, ϕ) form a **parameter space** or theory space. The beta functions define a vector field on this space, and RG trajectories are the integral curves. Fixed points are where the flow stops, and universality classes are basins of attraction.

The Borel transform introduces a second geometric arena. The Borel plane is where the convergent transform of a divergent series lives, and its singularities encode non-perturbative physics. Stokes lines in the Borel plane are analogous to special loci in parameter space where qualitative changes occur.

The Connection: Stokes and Monodromy

A deep connection that we will develop in later chapters is that Stokes phenomena in the Borel plane are mathematically equivalent to monodromy in parameter space. When a coupling constant makes a loop in the complex plane, operators can mix non-trivially. When a resummation contour crosses a Stokes line, exponentially small terms appear. These are the same phenomenon in different guises.

Transseries and the Full Answer

The complete solution to a problem is not a power series but a **transseries** that combines perturbative and non-perturbative sectors:

$$f(z) = \sum_{n=0}^{\infty} \sigma^n e^{-nS/z} f_n(z) \tag{44}$$

Here $f_0(z)$ is the perturbative sector (the original asymptotic series), $f_n(z)$ are higher instanton sectors, σ is a transseries parameter, and S is related to the instanton action. The full physics requires all sectors, and the sectors are linked through Stokes phenomena.

This transseries structure will appear in all our examples and will be developed systematically in the coming chapters. The anharmonic oscillator will continue to serve as the simplest example where all these features are visible.

Preview: The Three Examples

The anharmonic oscillator demonstrates the complete RG logic from secular terms through running parameters to RG equations and physical predictions. It also exhibits Gevrey-1 divergence and the Borel

transform structure. But it is *too simple* to exhibit several important phenomena.

The oscillator has only the trivial fixed point $A = 0$ (rest). It does not exhibit non-trivial fixed points where interesting scale-invariant behavior occurs. It has no phase transitions and therefore no universality classes. Its exponents come from dimensional analysis alone with no anomalous dimensions.

The three examples form a ladder of increasing complexity. We use the simplest example until it cannot illustrate the concept we need.

To see these richer phenomena, we will develop two additional examples in the coming chapters.

The 1D ϕ^4 field theory (Chapter I) introduces statistical RG, where we integrate out short-wavelength fluctuations rather than average over fast dynamics. This example has non-trivial beta functions and illustrates the flow of coupling constants. It also shows how renormalon singularities arise from the RG running itself.

The porous medium equation (Chapter I) exhibits **anomalous dimensions**, which are scaling exponents that dimensional analysis cannot predict. This is Barenblatt's "second kind" self-similarity, the PDE analog of anomalous dimensions in quantum field theory. The selection of the physical scaling exponent corresponds to a specific resummation prescription in the transseries framework.

These three examples form a *ladder*. We use the simplest example until it cannot illustrate the concept we need, then move to the next. The oscillator suffices for secular terms, running parameters, and Gevrey-1 structure. The ϕ^4 theory is needed for beta functions, fixed points, and renormalons. The porous medium shows anomalous dimensions and second-kind self-similarity.

Summary

The RG problem: Non-commuting limits combined with divergent series. Perturbation theory assumes $\epsilon \to 0$ first, but physics often requires $t \to \infty$ first. Moreover, perturbative coefficients grow factorially, so the series diverges for any $\epsilon \neq 0$.

Dimensional analysis determines the *form* of scaling laws but not the functions of dimensionless parameters.

The anharmonic oscillator exhibits secular terms $x_1 \sim t\sin(\omega_0 t)$ that signal the breakdown of naive perturbation theory at times $t \sim 1/(\lambda A^2)$. It also exhibits Gevrey-1 divergence with factorially growing coefficients.

The RG resolution: Promote constants to running parameters. Require consistency (no secular terms). This yields the RG equations:

$$\frac{\mathrm{d}A}{\mathrm{d}t} = 0, \qquad \frac{\mathrm{d}\phi}{\mathrm{d}t} = \frac{3\lambda A^2}{8\omega_0} \tag{45}$$

Physical prediction: The effective frequency is $\omega_{\text{eff}} = \omega_0(1 + 3\lambda A^2/8\omega_0^2)$.

The Borel plane: A second geometric arena where divergent series become convergent. Singularities encode non-perturbative physics. Ambiguities from crossing singularities are exponentially small terms invisible to perturbation theory.

The pattern is universal: Divergence $\to$ running parameters $\to$ flow equations $\to$ physics, with the Borel plane providing access to non-perturbative completions.

The anharmonic oscillator will continue to accompany us as we develop the full RG framework. Chapter I introduces flows on parameter space and our second example, the 1D ϕ^4 field theory. The geometry of theory space where both examples live will emerge naturally from the structure of the beta functions, and the connection to resurgence through Stokes phenomena and transseries will deepen with each chapter.

Flows on Parameter Space and Their Transseries Extensions

Chapter 1 showed *that* parameters run and *that* perturbation series diverge with structure. This chapter explains *how* parameters flow through the language of vector fields on parameter space, and how the full parameter space includes transseries coordinates from the beginning.

In Chapter I, we saw that the anharmonic oscillator's amplitude and phase become functions of time when we properly handle secular terms. We also saw that perturbative coefficients grow factorially and that the Borel plane provides a second geometric arena for understanding this divergence. But where do these running parameters "live"? And what governs their evolution? And how do the perturbative parameters connect to the non-perturbative information encoded in the Borel plane?

The answer is beautiful and more complete than traditional treatments suggest. Running parameters trace out trajectories in a **parameter space**. The RG equations define a *flow* on this space through a vector field whose integral curves are the paths theories take as we change scale. Fixed points of this flow are scale-invariant theories. But the full story requires recognizing that perturbative parameter space is actually a submanifold of a larger space that includes **transseries parameters** from the beginning. The structure is that of a **Lie group acting on an extended manifold**.

This chapter develops these geometric ideas through two examples. The **anharmonic oscillator** continues from Chapter 1 and is now viewed as a flow in (A, ϕ) space with implicit transseries structure. The **1D ϕ^4 field theory** introduces *statistical* RG, where we integrate out short-wavelength fluctuations rather than average over fast dynamics. Both examples exhibit the same geometric structure, and both have beta functions that are secretly transseries.

Parameter Space as a Manifold

Every physical model depends on parameters including masses, coupling constants, and initial conditions. The space of all possible parameter values is the **parameter space**. Different fields use different names for this concept. Physicists speak of "parameter space" in general settings, "theory space" in QFT, "coupling space" in statistical

mechanics, and "bifurcation diagrams" in dynamics. All refer to the same mathematical structure.

Different fields use different names. Parameter space, theory space, coupling space, and bifurcation diagram all refer to the same concept.

Examples of Parameter Spaces

The anharmonic oscillator. The relevant parameters for long-time behavior are the amplitude A and phase ϕ. These form a two-dimensional parameter space:

$$\mathcal{M}_{\text{osc}} = \{(A, \phi) : A \geq 0,\, \phi \in [0, 2\pi)\} \tag{46}$$

This is a half-cylinder (or a cone if we identify ϕ when $A = 0$).

The ϕ^4 field theory. The Lagrangian

$$\mathcal{L} = \frac{1}{2}(\partial\phi)^2 + \frac{r}{2}\phi^2 + \frac{\lambda}{4}\phi^4 \tag{47}$$

has two parameters, namely the mass r and coupling λ. The parameter space is:

$$\mathcal{M}_{\phi^4} = \{(r, \lambda) : \lambda > 0\} \tag{48}$$

We require $\lambda > 0$ for the potential to be bounded below.

General viewpoint. We think of parameter space as a *manifold*, which is a smooth space that locally looks like $\mathbb{R}^n$. The parameters $(g^1, g^2, \ldots, g^n)$ are coordinates on this manifold.

The Extended Parameter Space

Perturbative parameter space is a submanifold of a larger space that includes transseries parameters.

The parameter spaces described above are the **perturbative** parameter spaces. They include only the parameters that appear in the classical action or leading-order equations. But as we saw in Chapter I, perturbation series diverge and their complete meaning involves transseries that include exponentially suppressed sectors.

The **extended parameter space** includes additional coordinates σ_n that control the weight of each non-perturbative sector. For the oscillator, the extended space might be (A, ϕ, σ) where σ measures the contribution from complex-time instanton sectors. For ϕ^4 theory, the extended space is $(r, \lambda, \sigma_1, \sigma_2, \ldots)$ where σ_k weights the k-instanton sector.

This extension is not optional or exotic. It is required for a complete description of the physics. The perturbative submanifold $\sigma_n = 0$ is special in the sense that perturbation theory operates there, but it is not the full theory space. The RG acts on the complete extended manifold.

Scale Transformations as Motion

Scale transformations move us through parameter space. The trajectory is called an **RG flow**.

The key insight is that changing the scale at which we observe a system corresponds to *moving through parameter space*. A theory that appears

simple at one scale may look complicated at another. This is the same theory, just described with different effective coordinates.

For the oscillator, as time increases, ϕ increases because the phase accumulates. The trajectory in (A, ϕ) space is:

$$A(t) = A_0, \qquad \phi(t) = \phi_0 + \frac{3\lambda A_0^2}{8\omega_0} t \tag{49}$$

This is a horizontal line at constant A, wrapping around in the ϕ direction.

For field theory, as we integrate out high-momentum modes (zoom out), the effective couplings change. The trajectory in (r, λ) space encodes how the theory "flows" under coarse-graining. The transseries parameters σ_n also flow, though their flow is invisible in perturbation theory until we cross a Stokes line.

The Beta Function as a Vector Field

The RG equations from Chapter I have a geometric interpretation. They define a **vector field** on parameter space.

From Equations to Geometry

The RG equations for the oscillator were:

$$\frac{dA}{dt} = 0, \qquad \frac{d\phi}{dt} = \frac{3\lambda A^2}{8\omega_0} \tag{50}$$

The **beta function** $\boldsymbol{\beta}$ tells us the "velocity" through parameter space as we change scale.

These define a vector field on (A, ϕ) space:

$$\boldsymbol{\beta} = \beta^A \frac{\partial}{\partial A} + \beta^\phi \frac{\partial}{\partial \phi} = 0 \cdot \frac{\partial}{\partial A} + \frac{3\lambda A^2}{8\omega_0} \frac{\partial}{\partial \phi} \tag{51}$$

At each point, $\boldsymbol{\beta}$ gives the direction and rate of motion as the scale parameter increases. The components $\beta^A = 0$ and $\beta^\phi = 3\lambda A^2/(8\omega_0)$ are called **beta functions**.

Why "Beta Function"?

The name comes from QFT, where $\beta(\lambda) = \mu\, d\lambda/d\mu$ describes how couplings run with the renormalization scale μ.

In quantum field theory, the beta function $\beta(\lambda)$ was introduced by Gell-Mann and Low in 1954 to describe how the electromagnetic coupling constant runs with energy. The name stuck, even in contexts far from QFT.

In general, if g^i are coordinates on parameter space and ℓ is a scale parameter (time, log of momentum cutoff, or similar), the beta functions are:

$$\beta^i(g) = \frac{dg^i}{d\ell} \tag{52}$$

The collection of beta functions forms a vector field:

$$\boldsymbol{\beta} = \beta^i(g)\frac{\partial}{\partial g^i} \tag{53}$$

The Full Transseries Beta Function

The beta function itself is a transseries with perturbative and non-perturbative sectors.

The beta functions written above are the **perturbative** beta functions. They are computed order by order in the coupling constant and form asymptotic series that diverge with Gevrey-1 structure. The **full** beta function is a transseries:

$$\beta^i_{\text{full}}(g) = \beta^i_{\text{pert}}(g) + \sum_{n=1}^{\infty} \sigma^n e^{-nS/g}\beta^{i,(n)}(g) \tag{54}$$

where β^i_{pert} is the perturbative piece that includes all orders in g, the exponentials $e^{-nS/g}$ weight the n-instanton sectors, and each $\beta^{i,(n)}$ is itself an asymptotic series.

For the anharmonic oscillator, the perturbative beta function for the phase is $\beta^\phi_{\text{pert}} = 3\lambda A^2/(8\omega_0) + O(\lambda^2)$. This receives exponentially suppressed corrections from instanton sectors:

$$\beta^\phi_{\text{full}} = \beta^\phi_{\text{pert}} + \sigma_1 e^{-S/\lambda}\beta^{\phi,(1)} + \cdots \tag{55}$$

These corrections are invisible to any finite order of perturbation theory but are structurally required by resurgence. The instanton action S is determined by the classical structure of the problem, and the coefficients $\beta^{\phi,(n)}$ are fixed by the resurgent relations.

Fixed Points: Where the Flow Stops

A **fixed point** is a point where all beta functions vanish:

$$\beta^i(g^*) = 0 \quad \text{for all } i \tag{56}$$

At a fixed point, the system doesn't change under scale transformations. It is **scale-invariant**.

Fixed points are the "destinations" of RG flows. Understanding them is key to understanding long-time or long-distance behavior.

Fixed Points of the Oscillator

For the anharmonic oscillator, the perturbative beta functions are $\beta^A = 0$ and $\beta^\phi = 3\lambda A^2/(8\omega_0)$. Fixed points satisfy:

$$\beta^\phi = \frac{3\lambda A^2}{8\omega_0} = 0 \tag{57}$$

The only solution is $A = 0$, which corresponds to the oscillator at rest. This is a **trivial** fixed point because physically nothing is happening.

Physical interpretation: An oscillator with $A > 0$ never "reaches" a fixed point. The phase keeps advancing forever. The interesting physics is in the *flow*, not in fixed points.

Perturbative vs. Full Fixed Points

When we consider the full transseries beta function, the fixed point condition becomes:

$$\beta^i_{\text{full}}(g^*) = 0 \tag{58}$$

This is a different and richer condition than requiring the perturbative beta function to vanish.

Non-perturbative fixed points occur where $\beta_{\text{pert}} \neq 0$ but the full $\beta_{\text{full}} = 0$.

A perturbative fixed point visible in β_{pert} remains a fixed point of the full theory only if the exponentially suppressed corrections do not shift it. More dramatically, there may exist **non-perturbative fixed points** where $\beta_{\text{pert}}(g^*) \neq 0$ but the instanton corrections cancel the perturbative contribution so that $\beta_{\text{full}}(g^*) = 0$. Such fixed points are completely invisible to any finite order of perturbation theory, yet they can govern the physics of certain systems.

Why Fixed Points Matter

Fixed points become crucial in contexts with richer structure.

In statistical mechanics, fixed points correspond to **critical points** at phase transitions where fluctuations occur on all scales. In dynamical systems, fixed points of the RG can describe **attractors** that give the long-time limits of chaotic or dissipative systems. In QFT, fixed points are **conformal field theories** that are exactly scale-invariant quantum theories.

The oscillator is too simple to exhibit these phenomena. We need a new example.

The 1D ϕ^4 Field Theory

We now introduce our second example, which is ϕ^4 theory in one spatial dimension. This is the simplest model that exhibits non-trivial RG flow with a statistical interpretation.

The 1D ϕ^4 model is pedagogically ideal. Loop integrals are finite (no UV divergences), and beta functions can be computed exactly.

The Model

Consider a scalar field $\phi(x)$ on a line of length L with periodic boundary conditions. The **action** (or Euclidean Hamiltonian) is:

$$S[\phi] = \int_0^L dx \left[\frac{1}{2} \left(\frac{d\phi}{dx} \right)^2 + \frac{r}{2}\phi^2 + \frac{\lambda}{4}\phi^4 \right] \tag{59}$$

In statistical field theory, $e^{-S[\phi]}$ is the Boltzmann weight. We've set $k_B T = 1$.

Each term has a physical interpretation. The gradient term $(\partial\phi)^2$ penalizes spatial variations and provides "stiffness." The mass term $r\phi^2$ with $r > 0$ confines the field near $\phi = 0$. The interaction term $\lambda\phi^4$ with $\lambda > 0$ ensures stability.

The partition function is the functional integral:

$$Z = \int \mathcal{D}\phi \, e^{-S[\phi]} \tag{60}$$

Fourier Space and the UV Cutoff

With periodic boundary conditions, we decompose into Fourier modes:

$$\phi(x) = \frac{1}{\sqrt{L}} \sum_k \tilde{\phi}_k \, e^{ikx}, \qquad k = \frac{2\pi n}{L}, \; n \in \mathbb{Z} \tag{61}$$

The UV cutoff Λ represents ignorance of physics below the scale Λ^{-1}. In a lattice model, $\Lambda \sim \pi/a$.

Every physical theory has a shortest length scale. We impose a **UV cutoff** Λ so that only modes with $|k| < \Lambda$ are included.

In Fourier space, the action becomes:

$$S[\tilde{\phi}] = \sum_{|k|<\Lambda} \frac{1}{2}(k^2 + r)|\tilde{\phi}_k|^2 + \frac{\lambda}{4L} \sum_{k_1+k_2+k_3+k_4=0} \tilde{\phi}_{k_1}\tilde{\phi}_{k_2}\tilde{\phi}_{k_3}\tilde{\phi}_{k_4} \tag{62}$$

The Gaussian (free) part is diagonal while the ϕ^4 term couples different modes.

Momentum-Shell Renormalization Group

Wilson's insight was that instead of computing Z directly, we should compute how Z changes when we integrate out a thin shell of high-momentum modes. This generates a flow on coupling space.

Wilson's strategy involves integrating out fast modes, then rescaling. This generates the RG transformation.

The Three Steps

The RG proceeds as follows.

Step 1: Divide. Split the field into "slow" and "fast" modes:

$$\phi^<(x) = \frac{1}{\sqrt{L}} \sum_{|k|<\Lambda/b} \tilde{\phi}_k \, e^{ikx} \quad \text{(slow)} \tag{63}$$

$$\phi^>(x) = \frac{1}{\sqrt{L}} \sum_{\Lambda/b<|k|<\Lambda} \tilde{\phi}_k \, e^{ikx} \quad \text{(fast)} \tag{64}$$

for some $b > 1$.

Step 2: Integrate. Perform the functional integral over fast modes $\phi^>$, obtaining an effective action for slow modes $\phi^<$.

Step 3: Rescale. Rescale momenta ($k \to bk$) and fields to restore the original cutoff Λ.

The result is new couplings r' and λ' that depend on the original r and λ. Iterating gives the RG flow.

Box 2.1: Momentum-Shell RG for 1D ϕ^4

Goal: Derive the beta functions for (r, λ) in 1D ϕ^4 theory.
Step 1: Split the field. Write $\phi = \phi^< + \phi^>$ where $\phi^<$ has $|k| < \Lambda/b$ and $\phi^>$ has $\Lambda/b < |k| < \Lambda$.
Step 2: Expand the action.

$$S[\phi^< + \phi^>] = S_0[\phi^<] + S_0[\phi^>] + S_{\text{int}}[\phi^<, \phi^>] \tag{65}$$

where S_0 is the Gaussian part and S_{int} contains the ϕ^4 terms.
Step 3: The partition function.

$$Z = \int \mathcal{D}\phi^< \, e^{-S_0[\phi^<]} \underbrace{\int \mathcal{D}\phi^> \, e^{-S_0[\phi^>] - S_{\text{int}}[\phi^<, \phi^>]}}_{\equiv e^{-\Delta S[\phi^<]}} \tag{66}$$

Step 4: Perturbative integration over fast modes. Expand $e^{-S_{\text{int}}} \approx 1 - S_{\text{int}} + \frac{1}{2} S_{\text{int}}^2 - \cdots$ and take the Gaussian average over $\phi^>$.
Step 5: The key contraction. The ϕ^4 interaction contains terms like $(\phi^<)^2(\phi^>)^2$. When we contract $\phi^>$ with itself:

$$\langle \phi^>(x)\phi^>(x) \rangle_0 = \frac{1}{L} \sum_{\Lambda/b < |k| < \Lambda} \frac{1}{k^2 + r} \equiv \delta r/(6\lambda) \tag{67}$$

This shifts the mass term!
Step 6: Compute the shift. The interaction $\frac{\lambda}{4}(\phi^< + \phi^>)^4$ contains the term $\frac{\lambda}{4} \cdot 6 \cdot (\phi^<)^2(\phi^>)^2$ (the factor 6 counts ways to choose 2 of 4 fields to be $\phi^>$).
Contracting $(\phi^>)^2$:

$$\Delta S \supset \frac{6\lambda}{4} \int dx \, (\phi^<)^2 \cdot \langle (\phi^>)^2 \rangle = \frac{3\lambda}{2} \cdot (\text{tadpole}) \cdot \int dx \, (\phi^<)^2 \tag{68}$$

The tadpole integral in 1D with infinitesimal shell $b = e^{d\ell} \approx 1 + d\ell$:

$$\text{tadpole} = \frac{1}{\pi} \int_{\Lambda(1-d\ell)}^{\Lambda} \frac{dk}{k^2 + r} \approx \frac{\Lambda \, d\ell}{\pi(\Lambda^2 + r)} \tag{69}$$

Step 7: The mass shift. The effective mass becomes:

$$r_{\text{eff}} = r + \frac{3\lambda\Lambda}{\pi(\Lambda^2 + r)} d\ell \tag{70}$$

Step 8: Rescaling. Under $k \to bk$, $x \to x/b$, the kinetic term $\int (\partial\phi)^2 dx$ is invariant if $\phi \to b^{1/2}\phi$. Then:

$$r \to b^2 r, \qquad \lambda \to b^2 \lambda \tag{71}$$

(Both have engineering dimension 2 in units where $[k] = 1$.)

Step 9: Combine shift and rescaling. With $b = 1 + d\ell$:

$$r' = (1 + 2\,d\ell)\left(r + \frac{3\lambda\Lambda}{\pi(\Lambda^2 + r)}d\ell\right) \tag{72}$$

$$\lambda' = (1 + 2\,d\ell)\lambda \tag{73}$$

Result: The beta functions. Taking $d\ell \to 0$:

$$\beta_r \equiv \frac{dr}{d\ell} = 2r + \frac{3\lambda\Lambda}{\pi(\Lambda^2 + r)} \tag{74}$$

$$\beta_\lambda \equiv \frac{d\lambda}{d\ell} = 2\lambda \tag{75}$$

Interpreting the Beta Functions

The beta functions (347) and (75) encode how effective parameters change as we zoom out.

The "$2r$" and "2λ" terms come from rescaling and reflect the engineering dimensions. In units where momentum has dimension 1, both r and λ have dimension 2.

The engineering dimension gives the "classical" scaling. Quantum/thermal corrections modify this.

The tadpole correction $3\lambda\Lambda/\pi(\Lambda^2 + r)$ in β_r is genuinely new. It says that even if we start with $r = 0$, interactions *generate* an effective mass. High-momentum fluctuations "dress" the mass parameter.

No correction to λ appears at this order. Higher loops would contribute.

The Transseries Structure of the Beta Function

These perturbative beta functions are the leading terms in a transseries. The full beta function for λ in a generic ϕ^4 theory has the structure:

$$\beta_\lambda^{\text{full}} = 2\lambda + (\text{loop corrections}) + \sigma_1 e^{-S_{\text{inst}}/\lambda}\beta_\lambda^{(1)} + \cdots \tag{76}$$

The perturbative beta function is itself an asymptotic series embedded in a transseries.

The loop corrections form an asymptotic series in λ with factorially growing coefficients. These coefficients have renormalon singularities in their Borel transforms at positions $\zeta_k = k/(2\beta_1)$ determined by the one-loop beta function coefficient $\beta_1 = 2$. The exponential terms involve instanton contributions that are non-perturbative.

In 1D, the structure is especially simple because there are no UV divergences and the beta functions can be computed exactly. But the Gevrey-1 structure and the transseries completion remain present.

Fixed Points and Stability

Let's find the fixed points of the 1D ϕ^4 flow.

The Gaussian Fixed Point

Setting $\beta_r = \beta_\lambda = 0$:

$$\beta_\lambda = 2\lambda = 0 \implies \lambda^* = 0 \tag{77}$$

Then $\beta_r = 2r = 0$ implies $r^* = 0$.

The unique fixed point is $(r^*, \lambda^*) = (0, 0)$, which is the **Gaussian fixed point** (free field theory).

The **Gaussian fixed point** is the free theory with no interactions. It's called "Gaussian" because the path integral is Gaussian.

Stability Analysis

Near a fixed point, linearize the flow:

$$\frac{d}{d\ell}\begin{pmatrix}\delta r \\ \delta\lambda\end{pmatrix} = \begin{pmatrix}\partial\beta_r/\partial r & \partial\beta_r/\partial\lambda \\ \partial\beta_\lambda/\partial r & \partial\beta_\lambda/\partial\lambda\end{pmatrix}_{(0,0)}\begin{pmatrix}\delta r \\ \delta\lambda\end{pmatrix} \tag{78}$$

The stability matrix at $(0, 0)$ is:

$$B = \begin{pmatrix}2 & 3/(\pi\Lambda) \\ 0 & 2\end{pmatrix} \tag{79}$$

Eigenvalues > 0 mean the perturbation grows under RG ("relevant"). Eigenvalues < 0 mean it shrinks ("irrelevant").

Both eigenvalues are $+2$. This means both directions are **unstable** in the sense that any perturbation away from $(0, 0)$ grows under the RG flow.

Physical interpretation: The free theory is unstable. Turn on any mass or coupling, and it grows under coarse-graining. There is no non-trivial fixed point in 1D.

Box 2.2: Relevant, Irrelevant, and Marginal

The stability eigenvalues classify perturbations.

Relevant ($\Delta > 0$): The perturbation grows under RG. The theory flows *away* from the fixed point in this direction. Must be tuned to zero to reach the fixed point.

Irrelevant ($\Delta < 0$): The perturbation shrinks under RG. The theory flows *toward* the fixed point. These operators become negligible at long distances.

Marginal ($\Delta = 0$): Neither grows nor shrinks (to first approximation). The fate depends on higher-order corrections.

In 1D ϕ^4: Both r and λ have $\Delta = 2 > 0$, so both are relevant. The Gaussian fixed point is "doubly unstable."

Why this matters: In higher dimensions ($d = 4 - \epsilon$), λ becomes marginal or irrelevant. The Wilson-Fisher fixed point emerges. But in 1D, no luck.

Comparing the Two Examples

We now have two complete examples of RG flows. Let's compare them systematically.

	Anharmonic Oscillator	**1D ϕ^4 Theory**
Type	Dynamical (ODE)	Statistical (field theory)
Scale parameter	Time t	Log-cutoff $\ell = \log(\Lambda_0/\Lambda)$
Parameter space	(A, ϕ)	(r, λ)
What runs	Initial conditions	Hamiltonian parameters
β^1	0	$2r + 3\lambda\Lambda/\pi(\Lambda^2 + r)$
β^2	$3\lambda A^2/(8\omega_0)$	2λ
Fixed point	$A = 0$ (trivial)	$(r, \lambda) = (0, 0)$ (Gaussian)
Stability	—	Both directions unstable
Divergence type	Gevrey-1	Gevrey-1
Borel singularities	Instantons	Renormalons

In dynamics, we "renormalize" where we are (initial conditions). In statistics, we "renormalize" what we are (the Hamiltonian).

Key similarity: Both exhibit the universal pattern of identifying divergence, letting parameters run, and deriving flow equations. Both have perturbative beta functions that are embedded in transseries.

Key difference: In the oscillator, running parameters are *initial conditions*. In field theory, they are *couplings in the Hamiltonian*. The physics dictates what runs.

Shared structure: Both have Gevrey-1 divergence in their perturbative expansions. The oscillator has singularities from complex-time instantons, while ϕ^4 has renormalon singularities from RG running. Both require transseries completion for the full answer.

The Dilation Group Structure

Both examples share a common mathematical structure involving the **dilation group**.

Scale Transformations Form a Group

Consider scale transformations $x \to bx$ with $b > 0$. These form a group with closure ($x \to bx$ composed with $x \to cx$ gives $x \to bcx$), identity ($x \to 1 \cdot x$), inverses ($(x \to bx)^{-1} = x \to x/b$), and associativity (composition is associative).

This is the multiplicative group $(\mathbb{R}^+, \times)$, also written $\mathbb{R}^+$ or $(\mathbb{R}, +)$ via logarithm.

The dilation group is the simplest non-trivial Lie group. It is one-dimensional, abelian, and connected.

The Lie Algebra

Every Lie group has an associated Lie algebra of infinitesimal transformations. For the dilation group, write $b = e^\epsilon$ for small ϵ. Then:

$$x \to e^\epsilon x \approx x + \epsilon x = x + \epsilon \cdot x\frac{d}{dx}x = (1 + \epsilon\mathcal{D})x \tag{80}$$

where $\mathcal{D} = x\,d/dx$ is the **generator**.

The generator $\mathcal{D} = x\,\partial/\partial x$ is the infinitesimal dilation. Acting on $f(x)$, we get $\mathcal{D}f = xf'(x)$.

Finite transformations are recovered by exponentiation:

$$D_b = e^{(\log b)\mathcal{D}} \tag{81}$$

Box 2.4: The Dilation Lie Algebra

The dilation generator in d dimensions:
In d dimensions, the dilation (scaling) generator is the radial vector field:

$$\mathcal{D} = x^i\frac{\partial}{\partial x^i} = \sum_{i=1}^{d} x^i\partial_i \tag{82}$$

This generates the flow $x^i \to e^\epsilon x^i$ under the exponential map.

Translations and the conformal algebra:
The translation generators are $P_i = \partial/\partial x^i$. Acting on a function:

$$P_i f(x) = \partial_i f(x), \qquad \mathcal{D}f(x) = x^j\partial_j f(x) \tag{83}$$

The fundamental commutator:
Computing $[\mathcal{D}, P_i]$ on a test function $f(x)$:

$$\begin{aligned}
[\mathcal{D}, P_i]f &= \mathcal{D}(P_i f) - P_i(\mathcal{D}f) && (84)\\
&= x^j\partial_j(\partial_i f) - \partial_i(x^j\partial_j f) && (85)\\
&= x^j\partial_j\partial_i f - \delta_i^j\partial_j f - x^j\partial_i\partial_j f && (86)\\
&= -\partial_i f = -P_i f && (87)
\end{aligned}$$

Therefore:

$$\boxed{[\mathcal{D}, P_i] = -P_i} \tag{88}$$

This says that dilations and translations *don't commute*. Physically, translating then scaling differs from scaling then translating.

Matrix representation:
In $d+1$ dimensions, we can represent $\mathcal{D}$ and P_i as $(d+2)\times(d+2)$ matrices acting on projective coordinates $(1, x^1, \ldots, x^d)$:

$$\mathcal{D} = \begin{pmatrix} 0 & 0 \\ 0 & I_d \end{pmatrix}, \qquad P_i = \begin{pmatrix} 0 & e_i^T \\ 0 & 0 \end{pmatrix} \tag{89}$$

where e_i is the i-th unit vector. One can verify that the matrix commutator reproduces $[\mathcal{D}, P_i] = -P_i$.

The full conformal algebra (in $d > 2$):

Including special conformal transformations K_i and rotations M_{ij}, the algebra becomes:

$$[\mathcal{D}, P_i] = -P_i \qquad [\mathcal{D}, K_i] = K_i \tag{90}$$

$$[P_i, K_j] = 2(\delta_{ij}\mathcal{D} - M_{ij}) \qquad [K_i, K_j] = 0 \tag{91}$$

The dilation generator acts as a "grading operator" where P_i has grade -1 and K_i has grade $+1$.

Beta Functions as Generators on Extended Space

In the RG context, the beta function $\boldsymbol{\beta}$ *is* the generator of scale transformations on parameter space:

$$\boldsymbol{\beta} = \beta^i(g)\frac{\partial}{\partial g^i} \tag{92}$$

The finite RG transformation from scale $\ell = 0$ to ℓ is:

$$R_\ell = e^{\ell\boldsymbol{\beta}} \tag{93}$$

The RG transformation $R_\ell = e^{\ell\boldsymbol{\beta}}$ is a diffeomorphism of parameter space generated by the beta function vector field.

The collection $\{R_\ell : \ell \in \mathbb{R}\}$ forms a one-parameter group of diffeomorphisms on parameter space. This is the representation of the dilation group on theory space.

On the extended parameter space including transseries coordinates, the generator becomes:

$$\boldsymbol{\beta}_{\text{ext}} = \beta^i(g)\frac{\partial}{\partial g^i} + \beta^{(\sigma_n)}(g,\sigma)\frac{\partial}{\partial \sigma_n} \tag{94}$$

The transseries parameters σ_n also have beta functions that describe how they evolve under scale transformations. Near Stokes lines, the σ_n can jump discontinuously, which is the Stokes phenomenon viewed from the extended parameter space perspective.

Box 2.3: The Lie Group Perspective

The structure:

The group is the dilation group $(\mathbb{R}^+, \times) \cong (\mathbb{R}, +)$. The manifold is parameter space $\mathcal{M}$. The group acts on $\mathcal{M}$ via RG transformations. The generator $\boldsymbol{\beta}$ is the Lie algebra element. Fixed points are points invariant under the group action (zeros of $\boldsymbol{\beta}$).

For the oscillator:

The manifold is $\mathcal{M} = \{(A, \phi)\}$. The generator is $\boldsymbol{\beta} = \frac{3\lambda A^2}{8\omega_0}\frac{\partial}{\partial \phi}$. The

transformation $R_t = e^{t\boldsymbol{\beta}}$ shifts ϕ by $\frac{3\lambda A^2}{8\omega_0}t$.
For 1D ϕ^4:
The manifold is $\mathcal{M} = \{(r, \lambda) : \lambda > 0\}$. The generator is $\boldsymbol{\beta} = \beta_r \frac{\partial}{\partial r} + \beta_\lambda \frac{\partial}{\partial \lambda}$. The fixed point at the origin is invariant.
On the extended space:
Both examples extend to $\mathcal{M}_{\text{ext}}$ including transseries parameters σ_n. The full beta function acts on this larger space. Stokes phenomena appear as discontinuities in σ_n when crossing Stokes lines.
Why this matters: The Lie group framework unifies all RG applications. Different physical problems are different representations of the same underlying structure.

Scaling Dimensions and Representations

A function that transforms simply under scale transformations carries a **representation** of the dilation group.

Definition

A quantity Φ has **scaling dimension** Δ if under $x \to bx$:

$$\Phi \to b^\Delta \Phi \tag{95}$$

Equivalently, the generator acts as $\mathcal{D}\Phi = \Delta\Phi$. The scaling dimension is the eigenvalue of the dilation generator.

Scaling dimensions are "quantum numbers" labeling how quantities transform under scale changes.

Examples

Length: A length L has scaling dimension $+1$ because $L \to bL$.

Momentum: Momentum $k \sim 1/L$ has dimension -1 because $k \to k/b$.

The ϕ^4 couplings: From the rescaling analysis in Box 2.1:

$$r \to b^2 r, \qquad \lambda \to b^2 \lambda \tag{96}$$

Both have scaling dimension $+2$. These are the **engineering dimensions**.

Anomalous Dimensions

The engineering dimensions come from dimensional analysis alone. But interactions can modify them. If a quantity has

$$\Phi \to b^{\Delta_0 + \gamma} \Phi \tag{97}$$

where Δ_0 is the engineering dimension and γ depends on the coupling, we call γ the **anomalous dimension**.

Anomalous dimensions are the "quantum corrections" to classical scaling. They distinguish first-kind and second-kind self-similarity.

Anomalous dimensions signal that naive scaling (from dimensional analysis) is wrong because the true scaling is modified by dynamics. We'll see explicit examples when we discuss the porous medium equation in Chapter I.

In the resurgent framework, anomalous dimensions are themselves asymptotic series in the coupling with Gevrey-1 structure. Their Borel transforms have singularities encoding non-perturbative corrections to the scaling behavior.

Looking Ahead

This chapter established the geometric framework with parameters living in a **manifold** (parameter space), the RG defining a **flow** on this manifold, beta functions being the **generators** of the flow, and fixed points being **scale-invariant** theories. We also introduced the crucial extension to include transseries parameters in the full theory space.

The oscillator shows the RG mechanism. The ϕ^4 model shows non-trivial beta functions. The porous medium will show anomalous dimensions.

Our two examples have rather simple flow structure with no non-trivial fixed points and no anomalous dimensions. The next chapters develop richer phenomena.

Chapter I derives the RG equation systematically and shows how the beta function arises from requiring physical predictions to be scale-independent. It also shows how the envelope method naturally produces transseries structure when the solution crosses Stokes lines.

Chapter I introduces our third example, the porous medium equation, which exhibits **anomalous dimensions**. These are scaling exponents that dimensional analysis cannot predict.

Chapters I–I develop the full geometric structure of parameter space, including metrics and connections, with natural extensions to the transseries-enlarged theory space.

Summary

Parameter space $\mathcal{M}$ is the manifold of all possible parameter values. RG defines a flow on $\mathcal{M}$.
Extended parameter space $\mathcal{M}_{\text{ext}}$ includes transseries parameters σ_n that weight non-perturbative sectors. The full RG acts on this larger space.
The beta function $\boldsymbol{\beta} = \beta^i(g)\partial/\partial g^i$ is a vector field on $\mathcal{M}$, the generator of scale transformations. The full beta function is a transseries.
Fixed points satisfy $\beta^i(g^*) = 0$ for all i. These are scale-invariant theories. Non-perturbative fixed points may exist where $\beta_{\text{pert}} \neq 0$ but $\beta_{\text{full}} = 0$.
For 1D ϕ^4 theory:

$$\beta_r = 2r + \frac{3\lambda\Lambda}{\pi(\Lambda^2 + r)} \tag{98}$$

$$\beta_\lambda = 2\lambda \tag{99}$$

The Gaussian fixed point $(0, 0)$ is unstable (both eigenvalues $= 2$).
Scaling dimension Δ labels representations of the dilation group where $\Phi \to b^\Delta \Phi$.
The Lie group structure: The dilation group $(\mathbb{R}^+, \times)$ acts on parameter space via $R_\ell = e^{\ell\boldsymbol{\beta}}$. On the extended space, this action includes the flow of transseries parameters.

The Flow Equation as Resurgent Consistency

Chapter 2 introduced the beta function as a vector field. This chapter derives it systematically from one fundamental requirement: physical predictions must be scale-independent. We will see that this consistency requirement naturally produces transseries structure.

Why do parameters run? In Chapter I, we saw that the anharmonic oscillator's phase accumulates to cancel secular terms. In Chapter I, we saw that ϕ^4 couplings flow under coarse-graining. But what *determines* how they run?

The answer is a beautiful consistency requirement. **Physical predictions cannot depend on arbitrary choices of scale**. If we choose to describe a system at scale μ_1 or μ_2, we must get the same physical answers. This seemingly innocuous statement has profound consequences because it completely determines the beta functions. Moreover, when we examine this consistency requirement carefully through the envelope method, we see that it naturally generates the **transseries structure** of the full solution. The perturbative and non-perturbative sectors are not separate afterthoughts but emerge together from the demand that local approximations stitch together smoothly.

This chapter derives the RG equation from this consistency requirement and shows how it appears in different contexts.

The Callan-Symanzik Equation

The most elegant formulation of scale independence is the **Callan-Symanzik equation**, which states that physical observables have vanishing total derivative with respect to scale.

The Setup

Consider a physical observable $\mathcal{O}$ that depends on external scales (momenta p, energies E, positions x, times t), internal parameters (couplings g, masses m), and a reference scale μ (the "renormalization scale").

The **explicit** μ-dependence comes from having chosen μ as our reference. The **implicit** μ-dependence comes through the running parameters $g(\mu)$.

The renormalization scale μ is a human choice, like choosing units. Physics cannot depend on it.

Scale Independence

Physical predictions cannot depend on our arbitrary choice of μ. Mathematically:

$$\mu \frac{d\mathcal{O}}{d\mu} = 0 \tag{100}$$

But $\mathcal{O}$ depends on μ both explicitly and through the running couplings:

$$\mu \frac{d\mathcal{O}}{d\mu} = \mu \left.\frac{\partial \mathcal{O}}{\partial \mu}\right|_g + \mu \frac{\partial g^i}{\partial \mu} \frac{\partial \mathcal{O}}{\partial g^i} \tag{101}$$

Define the beta functions:

$$\beta^i(g) \equiv \mu \frac{\partial g^i}{\partial \mu} \tag{102}$$

The beta function $\beta^i = \mu \, \partial g^i / \partial \mu$ tells us how parameters change when we change the reference scale.

Then scale independence becomes:

$$\boxed{\left(\mu \frac{\partial}{\partial \mu} + \beta^i(g) \frac{\partial}{\partial g^i} \right) \mathcal{O} = 0} \tag{103}$$

This is the **Callan-Symanzik equation** in its simplest form.

Physical Interpretation

The Callan-Symanzik equation says that the explicit change in $\mathcal{O}$ when we vary μ must be exactly compensated by the implicit change through running couplings.

Think of it as a "conservation law for description." Different descriptions of the same physics must agree.

Geometrically, $\mathcal{O}$ is constant along the integral curves of the vector field

$$\boldsymbol{V} = \mu \frac{\partial}{\partial \mu} + \beta^i(g) \frac{\partial}{\partial g^i} \tag{104}$$

These integral curves are the RG trajectories.

Deriving the RG Equation for the Oscillator

Let's see how this works for the anharmonic oscillator, deriving the results of Chapter I from scale independence.

The Observable

The physical observable is the position $x(t)$, which depends on time t, parameters including amplitude A, phase ϕ, frequency ω_0, and coupling λ, and a reference time t_0 (when we specify initial conditions).

We can write the solution as $x(t) = A\cos(\omega_{\text{eff}} t + \phi)$ where ω_{eff} depends on A and λ.

Changing the Reference Time

The "renormalization scale" for the oscillator is the initial time t_0. Changing t_0 is like choosing different units of description.

Suppose we originally specified $x(t_0) = A_0$ and $\dot{x}(t_0) = 0$. Now consider shifting the reference time to $t_0 + \delta t_0$. The physics at time t cannot change. But our *parameterization* of initial conditions must change.

At the new reference time:

$$x(t_0 + \delta t_0) = A_0 \cos(\omega_{\text{eff}} \delta t_0) \approx A_0 \tag{105}$$

$$\dot{x}(t_0 + \delta t_0) = -A_0 \omega_{\text{eff}} \sin(\omega_{\text{eff}} \delta t_0) \approx -A_0 \omega_{\text{eff}} \delta t_0 \tag{106}$$

To maintain the same physical solution with the new reference time, we need "new" initial conditions (A', ϕ') that produce the same orbit.

Box 3.1: Deriving the RG Equations from Consistency

Goal: Derive dA/dt and $d\phi/dt$ from requiring scale-independence.

Setup: The general solution is

$$x(t) = A \cos(\omega_{\text{eff}}(A) \cdot t + \phi) \tag{107}$$

where ω_{eff} depends on amplitude.

Condition: The solution must be independent of how we parameterize it. If we shift the "initial time" $t_0 \to t_0 + \delta t_0$, the parameters must absorb the change.

Step 1: The explicit dependence. With initial conditions at t_0, the solution at time t is:

$$x(t) = A \cos(\omega_{\text{eff}}(t - t_0) + \phi) \tag{108}$$

Step 2: Shift t_0.

$$\left.\frac{\partial x}{\partial t_0}\right|_{A,\phi} = A\omega_{\text{eff}} \sin(\omega_{\text{eff}}(t - t_0) + \phi) \tag{109}$$

Step 3: Compensating parameter change. For x to be unchanged, we need:

$$\left.\frac{\partial x}{\partial t_0}\right|_{A,\phi} + \frac{dA}{dt_0}\frac{\partial x}{\partial A} + \frac{d\phi}{dt_0}\frac{\partial x}{\partial \phi} = 0 \tag{110}$$

Step 4: Compute the partial derivatives.

$$\frac{\partial x}{\partial A} = \cos(\theta) + A\frac{\partial \omega_{\text{eff}}}{\partial A}(t - t_0)\sin(\theta) \tag{111}$$

$$\frac{\partial x}{\partial \phi} = -A \sin(\theta) \tag{112}$$

where $\theta = \omega_{\text{eff}}(t - t_0) + \phi$.

Step 5: At $t = t_0$ (simplifying):

$$\left.\frac{\partial x}{\partial A}\right|_{t=t_0} = \cos\phi \tag{113}$$

$$\left.\frac{\partial x}{\partial \phi}\right|_{t=t_0} = -A\sin\phi \tag{114}$$

$$\left.\frac{\partial x}{\partial t_0}\right|_{t=t_0} = 0 \tag{115}$$

This gives trivial equations at $t = t_0$. The non-trivial information comes from the time derivative.

Step 6: The velocity condition. Similarly requiring $\dot{x}$ to be unchanged gives equations involving ω_{eff}. Working through (see Chapter 1), we recover:

$$\frac{dA}{dt_0} = 0, \qquad \frac{d\phi}{dt_0} = -\frac{3\lambda A^2}{8\omega_0} \tag{116}$$

Physical interpretation: The minus sign shows that shifting t_0 forward requires shifting ϕ backward to maintain the same physical solution. Equivalently, running t forward at fixed t_0 advances ϕ:

$$\frac{d\phi}{dt} = +\frac{3\lambda A^2}{8\omega_0} \tag{117}$$

The RG Equation for Field Theory

For field theory, the Callan-Symanzik equation takes a more elaborate form because correlation functions can have anomalous dimensions.

Correlation Functions

The basic objects are **correlation functions**:

$$G_n(x_1, \ldots, x_n) = \langle \phi(x_1) \cdots \phi(x_n) \rangle \tag{118}$$

In momentum space:

$$\tilde{G}_n(p_1, \ldots, p_n) = \int \prod_i d^d x_i \, e^{-i\sum p_i \cdot x_i} G_n(x_1, \ldots, x_n) \tag{119}$$

Correlation functions are the fundamental observables in field theory. Everything else, including scattering amplitudes and thermodynamic quantities, derives from them.

The Full Callan-Symanzik Equation

For an n-point correlation function:

$$\left(\mu\frac{\partial}{\partial \mu} + \beta(\lambda)\frac{\partial}{\partial \lambda} + n\gamma(\lambda)\right)\tilde{G}_n = 0 \tag{120}$$

The new term $n\gamma(\lambda)$ is the **anomalous dimension**. Each field ϕ in the correlation function contributes a factor γ.

The anomalous dimension γ corrects the "engineering" scaling of the field. It's called "anomalous" because it violates naive dimensional analysis.

Origin of the Anomalous Dimension

The field ϕ has engineering dimension $(d-2)/2$ in d spatial dimensions. Under rescaling $x \to bx$:

$$\phi \to b^{-(d-2)/2}\phi \quad \text{(engineering)} \tag{121}$$

But interactions modify this. The full scaling is:

$$\phi \to b^{-(d-2)/2-\gamma}\phi \quad \text{(with interactions)} \tag{122}$$

Box 3.2: Anomalous Dimensions in 1D ϕ^4

Question: What is the anomalous dimension γ in 1D ϕ^4 theory?
In 1D: The engineering dimension of ϕ is $(1-2)/2 = -1/2$.
At one loop: The field renormalization comes from the self-energy diagram. In 1D, this gives:

$$\gamma = 0 + O(\lambda^2) \tag{123}$$

The tadpole diagram that renormalizes r doesn't contribute to field renormalization because it's momentum-independent.
Physical interpretation: In 1D, the field doesn't acquire anomalous scaling (at one loop). This is related to the simplicity of 1D, where there are no non-trivial fixed points.
In higher dimensions: At the Wilson-Fisher fixed point in $d = 4-\epsilon$:

$$\gamma = \frac{\epsilon^2}{108} + O(\epsilon^3) \tag{124}$$

This is measurable! It determines the critical exponent η for correlation functions at phase transitions.

Solving the RG Equation

The Callan-Symanzik equation is a first-order PDE. Solving it gives the scale dependence of observables.

The Method of Characteristics

The equation

$$\left(\mu\frac{\partial}{\partial\mu} + \beta(g)\frac{\partial}{\partial g}\right)\mathcal{O} = 0 \tag{125}$$

says that $\mathcal{O}$ is constant along the *characteristic curves* defined by:

$$\frac{d\mu}{1} = \frac{dg}{\beta(g)/\mu} \tag{126}$$

The characteristics of the Callan-Symanzik equation are the RG trajectories. $\mathcal{O}$ is constant along these trajectories.

This gives the RG flow equation:

$$\mu \frac{dg}{d\mu} = \beta(g) \tag{127}$$

Along a characteristic, $\mathcal{O}(\mu, g(\mu)) = \mathcal{O}(\mu_0, g_0)$ is constant.

The Running Coupling

Define the **running coupling** $\bar{g}(\mu; g_0, \mu_0)$ as the solution to (127) with initial condition $\bar{g}(\mu_0) = g_0$:

$$\mu \frac{d\bar{g}}{d\mu} = \beta(\bar{g}), \qquad \bar{g}(\mu_0) = g_0 \tag{128}$$

The solution can be written implicitly:

$$\int_{g_0}^{\bar{g}(\mu)} \frac{dg'}{\beta(g')} = \log \frac{\mu}{\mu_0} \tag{129}$$

Box 3.3: Running Coupling for 1D ϕ^4

The beta function: $\beta_\lambda = 2\lambda$ (from Chapter 2).
Solving the RG equation:

$$\mu \frac{d\lambda}{d\mu} = 2\lambda \implies \frac{d\lambda}{\lambda} = \frac{2d\mu}{\mu} \tag{130}$$

Integrating:

$$\log \frac{\lambda(\mu)}{\lambda_0} = 2 \log \frac{\mu}{\mu_0} = \log \left(\frac{\mu}{\mu_0} \right)^2 \tag{131}$$

Result:

$$\boxed{\lambda(\mu) = \lambda_0 \left(\frac{\mu}{\mu_0} \right)^2} \tag{132}$$

Physical interpretation: As we zoom out (μ decreases), λ decreases. As we zoom in (μ increases), λ increases. The coupling is "relevant," meaning it grows toward the UV.
For r: The equation $\beta_r = 2r + \cdots$ is more complicated. At leading order (ignoring the tadpole):

$$r(\mu) \approx r_0 \left(\frac{\mu}{\mu_0} \right)^2 \tag{133}$$

The tadpole correction generates mass even if $r_0 = 0$.

Asymptotic Freedom and Infrared Slavery

The behavior of the running coupling as $\mu \to \infty$ (UV) or $\mu \to 0$ (IR) determines the character of the theory.

UV Behavior

If $\beta(g) < 0$ for small $g > 0$, then as $\mu \to \infty$:

$$g(\mu) \to 0 \tag{134}$$

This is **asymptotic freedom** where the theory becomes free (non-interacting) at high energies. QCD exhibits this.

Asymptotic freedom: interactions *weaken* at high energies. The theory becomes simpler in the UV.

IR Behavior

If $\beta(g) > 0$ for small $g > 0$, then as $\mu \to 0$:

$$g(\mu) \to 0 \tag{135}$$

The theory becomes free at low energies, meaning perturbation theory gets *better* at long distances.

Conversely, if $\beta > 0$ for small g, the coupling grows in the UV. This is the situation in 1D ϕ^4 and in QED.

The Landau Pole

When $\beta > 0$, the running coupling can diverge at a finite scale. For $\beta = bg^2$:

$$g(\mu) = \frac{g_0}{1 - bg_0 \log(\mu/\mu_0)} \tag{136}$$

This diverges when $\log(\mu/\mu_0) = 1/(bg_0)$, meaning at:

$$\mu_{\text{Landau}} = \mu_0 \exp\left(\frac{1}{bg_0}\right) \tag{137}$$

The Landau pole signals a breakdown of the effective theory. New physics must enter before the pole is reached.

This **Landau pole** signals that perturbation theory breaks down. New physics must emerge.

The Resurgent Perspective on the Landau Pole

The perturbative beta function that gives the Landau pole is only part of the full story. The complete beta function is a transseries:

$$\beta_{\text{full}}(g) = \beta_{\text{pert}}(g) + \sum_{n=1}^{\infty} \sigma^n e^{-nS/g} \beta^{(n)}(g) \tag{138}$$

The exponentially suppressed corrections could in principle tame the divergence, producing a well-defined theory at all scales. Whether

The Landau pole is a perturbative artifact. The full transseries beta function may have different behavior.

this happens depends on the detailed structure of the resurgent relations. If the non-perturbative corrections cancel the perturbative growth near the would-be Landau pole, a **non-perturbative fixed point** emerges and the theory is UV complete without new physics.

QED provides the canonical example where this question remains open. The perturbative beta function predicts a Landau pole, but the full theory may or may not have one. This is an active area of research.

The Envelope Method

There's an elegant alternative derivation of the RG equation based on the **envelope** of a family of perturbative approximations. This method reveals the deeper structure and shows how transseries arise naturally.

The Problem with Perturbation Theory

Naive perturbation theory gives:

$$x(t) = A\cos(\omega_0 t + \phi) + \lambda x_1(t) + O(\lambda^2) \tag{139}$$

This is good for $t \lesssim 1/(\lambda A^2)$ but fails at longer times. The problem is that we're expanding around the *wrong* solution.

The envelope method uses a family of expansions that are each locally valid, then stitches them together.

A Family of Approximations

For each time τ, construct a local approximation valid near $t = \tau$:

$$x_\tau(t) = A(\tau)\cos(\omega_0(t-\tau) + \theta(\tau)) + O(\lambda) \tag{140}$$

Here $A(\tau)$ and $\theta(\tau)$ are the "local" amplitude and phase at time τ.

The Envelope Condition

The approximations $x_\tau(t)$ form a one-parameter family. Their **envelope** is defined by:

$$\left.\frac{\partial x_\tau(t)}{\partial \tau}\right|_{t=\tau} = 0 \tag{141}$$

This says that at $t = \tau$, the approximation x_τ shouldn't change as we vary τ. The approximations are "tangent" at their matching points.

The envelope is the curve tangent to all members of the family. It "stitches together" the local approximations.

Box 3.4: Envelope Method for the Oscillator

Setup: The perturbative solution valid near $t = \tau$ is

$$x_\tau(t) = A(\tau)\cos(\omega_0(t-\tau) + \phi(\tau)) - \frac{3\lambda A^3}{8\omega_0}(t-\tau)\sin(\omega_0(t-\tau) + \phi(\tau)) + \cdots \tag{142}$$

The envelope condition:

$$\left.\frac{\partial x_\tau}{\partial \tau}\right|_{t=\tau} = 0 \tag{143}$$

Computing at $t = \tau$:

$$x_\tau(\tau) = A\cos\phi \tag{144}$$

$$\left.\frac{\partial x_\tau}{\partial \tau}\right|_{t=\tau} = A'\cos\phi - A\phi'\sin\phi + \frac{3\lambda A^3}{8\omega_0}\sin\phi \tag{145}$$

Setting to zero: The coefficient of $\cos\phi$ gives $A' = 0$. The coefficient of $\sin\phi$ gives:

$$-A\phi' + \frac{3\lambda A^3}{8\omega_0} = 0 \implies \phi' = \frac{3\lambda A^2}{8\omega_0} \tag{146}$$

Result: We recover the RG equations from Chapter 1! The envelope method is an alternative derivation.

Connection to the Callan-Symanzik Equation

The envelope condition $\partial x_\tau/\partial\tau|_{t=\tau} = 0$ is precisely the statement that x is independent of the arbitrary reference time τ. This is the same as the Callan-Symanzik equation with τ playing the role of μ.

The two approaches, scale independence and envelope, are mathematically equivalent but offer different physical intuition.

The Envelope Method and Transseries

The envelope method reveals something deeper than just the perturbative RG equations. When the local solution crosses a **Stokes line**, the stitching produces not just the perturbative beta function but automatically generates the transseries structure.

What Happens at a Stokes Line

When the envelope crosses a Stokes line, exponentially small sectors "turn on" and must be tracked for consistent stitching.

Consider a problem where the perturbative solution has exponentially small corrections that become visible near certain parameter values. The local approximation near τ might be:

$$x_\tau(t) = x_\tau^{(0)}(t) + \sigma(\tau)e^{-S/\lambda}x_\tau^{(1)}(t) + \cdots \tag{147}$$

where $x_\tau^{(0)}$ is the perturbative piece and $x_\tau^{(1)}$ is the first non-perturbative sector.

The transseries parameter σ depends on τ, and this dependence is crucial. Away from Stokes lines, σ can be taken constant. But when the envelope crosses a Stokes line, σ must jump discontinuously to maintain the envelope condition.

The Bridge Equation from Envelope Consistency

The envelope condition at a Stokes crossing produces a remarkable result. The requirement that the local approximations stitch together smoothly gives:

$$\Delta\sigma = S_1 \cdot \sigma^{(1)} \tag{148}$$

where $\Delta\sigma$ is the jump in the transseries parameter and S_1 is the Stokes constant.

The bridge equation of alien calculus emerges from requiring envelope consistency across Stokes lines.

This is precisely the **bridge equation** of alien calculus! The alien derivative, which measures how the resummation changes across Stokes lines, emerges naturally from the envelope method. The Stokes constant S_1 is the coefficient in the bridge equation:

$$\Delta_S f_0 = S_1 \cdot f_1 \tag{149}$$

relating the perturbative sector f_0 to the one-instanton sector f_1.

Running of the Transseries Parameter

Away from Stokes lines, the transseries parameter σ has its own beta function:

$$\frac{d\sigma}{d\ell} = \beta_\sigma(g, \sigma) \tag{150}$$

Near a Stokes line, this continuous evolution is interrupted by the jump $\Delta\sigma$. The full picture on the extended parameter space including σ combines smooth flow with discontinuous Stokes jumps.

Box 3.5: Stokes Constants and the Envelope

Physical setup: Consider a problem where the Borel transform has a singularity at $\zeta = S$.

Perturbative envelope: The local approximation $x_\tau^{(0)}(t)$ stitches together via the envelope condition, giving the perturbative RG equations.

At a Stokes line: When the argument of $e^{-S/\lambda}$ crosses the positive real axis, the exponentially small sector $x_\tau^{(1)}(t)$ becomes comparable to the error in $x_\tau^{(0)}$.

Modified envelope condition:

$$\frac{\partial}{\partial\tau}\left[x_\tau^{(0)} + \sigma(\tau)e^{-S/\lambda}x_\tau^{(1)} + \cdots\right]_{t=\tau} = 0 \tag{151}$$

Result: The transseries parameter σ must jump by the Stokes con-

stant to maintain the envelope. The bridge equation

$$\Delta_S \tilde{f} = S_1 \cdot \partial_\sigma \tilde{f} \tag{152}$$

emerges from consistency.
Physical meaning: The resurgent structure is not imposed externally. It is required by the consistency of the RG, meaning that different local descriptions must agree.

When Does the RG Apply?

The RG is not a universal panacea. It applies when specific conditions are met.

First, **there are separated scales**. A hierarchy $\mu_{\text{IR}} \ll \mu_{\text{UV}}$ that we want to bridge must exist.

Second, **there's a perturbative expansion**. We need a small parameter whose corrections we can compute.

Third, **the expansion breaks down at long scales**. Secular terms, divergences, or other pathologies appear.

Fourth, **the breakdown is systematic**. The divergences have a predictable structure that can be absorbed into running parameters.

The RG works when the "sickness" of perturbation theory is predictable. Random failures can't be cured by renormalization.

When it doesn't apply: The RG does not help with strongly coupled systems that have no small parameter, finite-time singularities (blow-up), or systems without scale hierarchy.

Even when the RG applies, it may not be the most efficient method. For the oscillator, the RG gives the same answer as averaging methods. For some PDEs, matched asymptotics may be more direct. The RG's power lies in its *universality* because the same framework handles diverse problems with the same mathematical structure.

Looking Ahead

This chapter established the RG equation

$$\mu \frac{dg^i}{d\mu} = \beta^i(g) \tag{153}$$

from the requirement of scale independence.

The RG equation is a *consistency condition*: different descriptions of the same physics must agree.

We've seen two derivations. The Callan-Symanzik approach says that physical observables can't depend on arbitrary scale choices. The envelope approach says that local approximations must stitch together smoothly. We've also seen that the envelope method at Stokes crossings naturally produces the transseries structure and the bridge equation of alien calculus.

The next chapter introduces our third example, the **porous medium equation**, which exhibits **anomalous dimensions**. There, the scaling exponents cannot be predicted by dimensional analysis and must be computed from the RG flow. This is Barenblatt's "second kind" self-similarity.

Summary

The Callan-Symanzik equation:

$$\left(\mu\frac{\partial}{\partial\mu} + \beta^i(g)\frac{\partial}{\partial g^i} + n\gamma(g)\right) G_n = 0 \tag{154}$$

expresses that physical observables are scale-independent.
The RG flow equation:

$$\mu\frac{dg^i}{d\mu} = \beta^i(g) \tag{155}$$

defines the running coupling.
Asymptotic behavior: When $\beta < 0$, we have asymptotic freedom (free at high energy). When $\beta > 0$, the coupling grows in UV and may hit a Landau pole. The full transseries beta function may have different behavior.
The envelope method provides an alternative derivation. RG equations ensure local approximations stitch together smoothly.
Transseries from the envelope: When the envelope crosses Stokes lines, consistency requires the transseries parameter σ to jump. This produces the bridge equation of alien calculus.
The anomalous dimension γ corrects the engineering scaling of fields, measuring how interactions modify naive dimensional analysis.

Fixed Points, Stability, and the Transseries Landscape

Chapters 1–3 showed that parameters run with scale. This chapter asks: where do they run *to*? Fixed points are the destinations, and their classification determines the qualitative behavior of physical systems. We treat perturbative and non-perturbative fixed points on equal footing.

The RG generates flows on parameter space. But flows go somewhere. The **destinations** of RG flows are called **fixed points**, and they represent theories that are exactly scale-invariant. Understanding fixed points is the key to understanding the long-distance or long-time behavior of any system.

This chapter develops the theory of fixed points in depth. We classify operators near fixed points as **relevant**, **irrelevant**, or **marginal** based on how perturbations grow or shrink under RG. We introduce the concept of **universality classes**, which is the remarkable fact that different microscopic theories can flow to the same fixed point. And we introduce our third example, the **porous medium equation**, which exhibits **anomalous dimensions** that cannot be predicted by dimensional analysis.

Crucially, we treat fixed points of the full transseries beta function, not just the perturbative piece. This leads to the possibility of **non-perturbative fixed points** where the perturbative beta function is nonzero but non-perturbative corrections cancel it. Such fixed points are completely invisible to perturbation theory yet can control the physics of real systems.

Perturbative Fixed Points

A fixed point is where the RG flow stops. At a fixed point, the theory doesn't change under scale transformations.

Definition

At a fixed point, all beta functions vanish. The theory is exactly scale-invariant.

A **perturbative fixed point** is a point $g^* = (g^{*1}, \ldots, g^{*n})$ where all perturbative beta functions vanish:

$$\beta^i_{\text{pert}}(g^*) = 0 \quad \text{for all } i \tag{156}$$

At such a point, the running stops because $dg^i/d\ell = 0$. The couplings take the same values at all scales.

Examples We've Seen

The anharmonic oscillator has $\beta^A = 0$ and $\beta^\phi = 3\lambda A^2/(8\omega_0)$. The fixed point $A^* = 0$ corresponds to the oscillator at rest.

The 1D ϕ^4 theory has the Gaussian fixed point $(r^*, \lambda^*) = (0, 0)$, which is free field theory.

Both are **trivial** fixed points in the sense that the interactions have vanished. More interesting are fixed points with $\lambda^* \neq 0$.

The Wilson-Fisher Fixed Point

In $d = 4 - \epsilon$ dimensions, ϕ^4 theory has a famous non-trivial fixed point discovered by Wilson and Fisher. The beta function for the quartic coupling takes the form:

$$\beta_\lambda = -\epsilon\lambda + b\lambda^2 + O(\lambda^3) \tag{157}$$

where the coefficient $b > 0$.

The Wilson-Fisher fixed point controls phase transitions in real 3D systems. It is perturbatively accessible in $d = 4 - \epsilon$.

Setting $\beta_\lambda = 0$ gives fixed points at $\lambda^* = 0$ (Gaussian) and:

$$\lambda^*_{\text{WF}} = \frac{\epsilon}{b} + O(\epsilon^2) \tag{158}$$

This Wilson-Fisher fixed point is non-trivial because $\lambda^*_{\text{WF}} \neq 0$. It describes the universality class of the Ising model in $d = 3$ (setting $\epsilon = 1$).

Box 4.1: Stability of the Wilson-Fisher Fixed Point

Setup: The beta function in $d = 4 - \epsilon$ is $\beta_\lambda = -\epsilon\lambda + b\lambda^2 + O(\lambda^3)$.
The fixed points: Gaussian fixed point at $\lambda^*_G = 0$. Wilson-Fisher fixed point at $\lambda^*_{\text{WF}} = \epsilon/b + O(\epsilon^2)$.
Stability analysis: Linearize β_λ around each fixed point.
At the Gaussian:

$$\frac{d(\delta\lambda)}{d\ell} = \left.\frac{d\beta_\lambda}{d\lambda}\right|_{\lambda=0} \delta\lambda = -\epsilon\,\delta\lambda \tag{159}$$

The eigenvalue is $-\epsilon < 0$ (for $\epsilon > 0$), so perturbations shrink. The Gaussian is **stable** (IR attractive).
At Wilson-Fisher:

$$\frac{d(\delta\lambda)}{d\ell} = \left.\frac{d\beta_\lambda}{d\lambda}\right|_{\lambda^*} \delta\lambda = (-\epsilon + 2b\lambda^*)\delta\lambda = \epsilon\,\delta\lambda \tag{160}$$

The eigenvalue is $+\epsilon > 0$, so perturbations grow. Wilson-Fisher is **unstable** (UV attractive).
Physical picture: The flow goes from Wilson-Fisher (UV) to Gaussian (IR). Theories near Wilson-Fisher flow toward free theory at long distances. The WF fixed point controls the approach to criticality.

Non-Perturbative Fixed Points

The perturbative fixed points are not the full story. When we consider the complete transseries beta function, new fixed points can emerge that are invisible to perturbation theory.

The Full Fixed Point Condition

A **fixed point of the full theory** satisfies:

$$\beta^i_{\text{full}}(g^*, \sigma^*) = 0 \quad \text{for all } i \tag{161}$$

where β_{full} is the complete transseries beta function:

$$\beta^i_{\text{full}}(g, \sigma) = \beta^i_{\text{pert}}(g) + \sum_{n=1}^{\infty} \sigma^n e^{-nS/g} \beta^{i,(n)}(g) \tag{162}$$

A non-perturbative fixed point has $\beta_{\text{pert}} \neq 0$ but the full $\beta_{\text{full}} = 0$ due to cancellation with instanton sectors.

Three Types of Fixed Points

Type 1: Perturbative fixed points where $\beta_{\text{pert}}(g^*) = 0$ and hence $\beta_{\text{full}}(g^*, 0) = 0$. These are the traditional fixed points visible in perturbation theory. The Gaussian and Wilson-Fisher fixed points are of this type.

Type 2: Non-perturbative fixed points where $\beta_{\text{pert}}(g^*) \neq 0$ but the instanton contributions cancel the perturbative piece:

$$\beta_{\text{pert}}(g^*) + \sum_n (\sigma^*)^n e^{-nS/g^*} \beta^{(n)}(g^*) = 0 \tag{163}$$

Such fixed points are completely invisible to any finite order of perturbation theory.

Type 3: Mixed fixed points where both perturbative and non-perturbative contributions are essential to the cancellation.

Evidence for Non-Perturbative Fixed Points

Non-perturbative fixed points are not merely theoretical curiosities. There is substantial evidence for their existence in several contexts.

Supersymmetric theories provide the cleanest examples because exact results can be computed using localization.

In **supersymmetric gauge theories**, exact results from localization reveal fixed points that cannot be seen perturbatively. The classic example is SQCD, where the Seiberg dual description reveals strong-coupling fixed points.

In **matrix models**, the large-N expansion can be solved exactly, revealing fixed points at strong coupling where the perturbative expansion around weak coupling gives no hint of their existence.

There is also numerical evidence from **lattice QCD** suggesting that the theory may have non-perturbative fixed points relevant for the chiral transition.

Box 4.2: Anatomy of a Non-Perturbative Fixed Point

Toy model: Consider a one-coupling theory with beta function:

$$\beta_{\text{pert}}(g) = \epsilon g - b g^2 + c g^3 + \cdots \tag{164}$$

with $\epsilon, b, c > 0$, and instanton contribution:

$$\beta^{(1)}(g) = d \cdot g^2 e^{-S_0/g} \tag{165}$$

Perturbative fixed points: Setting $\beta_{\text{pert}} = 0$ gives: $g_1^* = 0$ (Gaussian) and $g_2^* = \epsilon/b + O(\epsilon^2)$ (like Wilson-Fisher).
Full fixed point condition:

$$\epsilon g^* - b(g^*)^2 + c g^{*3} + \sigma^* d (g^*)^2 e^{-S_0/g^*} = 0 \tag{166}$$

Non-perturbative solution: If $\sigma^* \neq 0$ and g^* is chosen such that:

$$\sigma^* e^{-S_0/g^*} = \frac{b - \epsilon/g^* - c g^*}{d} \tag{167}$$

then we have a fixed point that requires non-zero transseries parameter σ^* and is invisible to perturbation theory (the LHS is exponentially small for small g^*).
Physical interpretation: The instanton sector provides a "restoring force" that balances the perturbative running. The theory sits at an equilibrium between perturbative and non-perturbative effects.

Stability and Classification

Near any fixed point, perturbations either grow or shrink under RG. This determines the **universality class**.

The Stability Matrix

Linearize the beta function near a fixed point g^*:

$$\frac{d(\delta g^i)}{d\ell} = B^i{}_j \, \delta g^j, \qquad B^i{}_j = \left. \frac{\partial \beta^i}{\partial g^j} \right|_{g^*} \tag{168}$$

The eigenvalues λ_α of the stability matrix B determine the fate of perturbations.

The stability matrix B is the Jacobian of the beta function at the fixed point. Its eigenvalues classify perturbations.

Relevant, Irrelevant, Marginal

The eigenvectors of B define natural directions in coupling space. Each direction is classified by its eigenvalue.

Relevant directions have $\lambda_\alpha > 0$. Perturbations grow under RG, flowing away from the fixed point. These directions must be tuned to reach the fixed point.

Irrelevant directions have $\lambda_\alpha < 0$. Perturbations shrink under RG, flowing toward the fixed point. These directions are "self-tuning."

Marginal directions have $\lambda_\alpha = 0$. The fate depends on higher-order terms.

Box 4.3: Classification at the Gaussian Fixed Point

Setup: The 1D ϕ^4 beta functions are

$$\beta_r = 2r + \frac{3\lambda\Lambda}{\pi(\Lambda^2 + r)} \tag{169}$$

$$\beta_\lambda = 2\lambda \tag{170}$$

At the Gaussian $(r^*, \lambda^*) = (0, 0)$:
The stability matrix is:

$$B = \begin{pmatrix} \partial\beta_r/\partial r & \partial\beta_r/\partial\lambda \\ \partial\beta_\lambda/\partial r & \partial\beta_\lambda/\partial\lambda \end{pmatrix}_{(0,0)} = \begin{pmatrix} 2 & 3/(\pi\Lambda) \\ 0 & 2 \end{pmatrix} \tag{171}$$

Eigenvalues: Both eigenvalues are $+2$.
Classification: Both directions are **relevant**. Any perturbation away from $(0, 0)$ grows under RG. The Gaussian fixed point is "completely unstable" or "UV attractive."
Interpretation: To reach the Gaussian fixed point from the IR, we must tune both r and λ to zero. There is no basin of attraction.
The connection to Δ: The eigenvalues are the **scaling dimensions** of the perturbations. Here $\Delta_r = \Delta_\lambda = 2$, matching the engineering dimensions (no anomalous contribution at the Gaussian).

Scaling Dimensions and Eigenvalues

The eigenvalues of B are called **scaling dimensions** (or "RG eigenvalues"). They control how perturbations scale:

$$\delta g^\alpha(\ell) \propto e^{\Delta_\alpha \ell} \tag{172}$$

Scaling dimensions are "quantum numbers" for operators. They determine the power-law behavior of correlation functions.

A perturbation with dimension $\Delta > 0$ grows (relevant), $\Delta < 0$ shrinks (irrelevant), and $\Delta = 0$ is marginal.

At the Gaussian fixed point, scaling dimensions equal engineering dimensions. At non-trivial fixed points, interactions modify them by the **anomalous dimension**:

$$\Delta = \Delta_{\text{eng}} + \gamma \tag{173}$$

Universality Classes

Perhaps the most remarkable consequence of the RG is **universality**: different microscopic theories can exhibit identical macroscopic behavior.

The Basin of Attraction

Universality: water at its critical point and uniaxial magnets at the Curie point are described by the same fixed point and have the same critical exponents.

The **basin of attraction** of a fixed point is the set of all theories that flow to it under RG. All theories in the same basin exhibit the same IR behavior. They form a **universality class**.

Different microscopic theories (lattice models with different interactions, continuum theories with different UV cutoffs) can flow to the same fixed point. Their long-distance behavior is then identical.

Why Universality?

Consider approaching a fixed point along irrelevant directions. By definition, these directions flow toward the fixed point. The "memory" of where we started is erased.

Only the relevant directions matter because only they distinguish different theories at long distances. If two theories have the same relevant perturbations tuned in the same way, they approach the same fixed point from the same direction and have identical IR physics.

Universality and Transseries

The concept of universality extends to the full transseries structure. Systems in the same universality class have identical IR behavior not just at the perturbative level but including all non-perturbative sectors.

The Stokes constants are universal quantities characterizing the fixed point, alongside the perturbative critical exponents.

The **Stokes constants** are universal. They characterize how the transseries sectors are linked and are independent of the microscopic details. Different systems flowing to the Wilson-Fisher fixed point have the same Stokes constants even if their microscopic instanton actions differ.

This is a strong constraint. It means that the full resurgent structure, not just the leading exponents, is determined by the fixed point.

The Porous Medium Equation

Our third and final example is the **porous medium equation** (PME), which governs nonlinear diffusion in porous media. This example exhibits **anomalous dimensions** that dimensional analysis cannot predict.

The PME describes gas flow through porous rock, groundwater seepage, and heat conduction in plasmas. It's the simplest PDE with anomalous dimensions.

The Model

The porous medium equation in d dimensions is:

$$\frac{\partial \rho}{\partial t} = D\nabla^2(\rho^m) \tag{174}$$

where $\rho(x,t) \geq 0$ is the density, D is a diffusion coefficient, and $m > 1$ is the nonlinearity exponent.

For $m = 1$, this reduces to the linear heat equation $\partial\rho/\partial t = D\nabla^2\rho$. The nonlinearity $m > 1$ means diffusion is faster where density is higher.

Why the PME?

The PME is ideal for demonstrating anomalous dimensions for several reasons. It's a single PDE with one nonlinearity parameter m. Self-similar solutions exist and can be found exactly. Dimensional analysis fails to determine the similarity exponents when $m \neq 1$. And the RG calculation is tractable.

Box 4.4: Dimensional Analysis for the PME

Setup: Consider a localized initial condition with total mass $M = \int \rho\, d^d x$. What is the width $L(t)$ at late times?
Parameters and dimensions:

Quantity	Symbol	Dimensions
Width	L	$[L]$
Time	t	$[T]$
Diffusion coefficient	D	$[L^2/T] \cdot [\rho^{1-m}]$
Total mass	M	$[\rho] \cdot [L^d]$
Exponent	m	dimensionless

For $m = 1$ (linear diffusion): D has dimensions $[L^2/T]$. The width must be:

$$L(t) = \sqrt{Dt} \cdot f(M, d) \tag{175}$$

For the heat kernel, f is a constant. Result: $L \propto t^{1/2}$ (first-kind self-similarity).
For $m \neq 1$: D has dimensions that depend on ρ, which has no fixed scale! The parameters D, M, t cannot be combined to give L without knowing how ρ scales.
The problem: Dimensional analysis gives $L \propto t^\alpha$ with α *undetermined*. The exponent must come from solving the equation.

First-Kind and Second-Kind Self-Similarity

Barenblatt distinguished two types of self-similar solutions, and this distinction is crucial for understanding anomalous dimensions.

First-Kind Self-Similarity

A solution has **first-kind self-similarity** if dimensional analysis completely determines the scaling exponents.

First-kind: dimensional analysis works. Second-kind: it doesn't. The exponent is "anomalous."

For the linear heat equation ($m = 1$), the fundamental solution is:

$$\rho(x,t) = \frac{1}{(4\pi Dt)^{d/2}} \exp\left(-\frac{|x|^2}{4Dt}\right) \tag{176}$$

The width scales as $L \sim t^{1/2}$, exactly as dimensional analysis predicts.

Second-Kind Self-Similarity

A solution has **second-kind self-similarity** if dimensional analysis fails to determine the exponents. The exponents must be computed dynamically.

For the PME with $m > 1$, the famous Barenblatt-Pattle solution is:

$$\rho(x,t) = \frac{1}{t^{\alpha}}\left[C - \frac{(m-1)}{4md}\frac{|x|^2}{(Dt)^{2\beta}}\right]_+^{1/(m-1)} \tag{177}$$

where $[y]_+ = \max(y, 0)$ and the exponents satisfy:

$$\alpha = \frac{d}{d(m-1)+2}, \qquad \beta = \frac{1}{d(m-1)+2} \tag{178}$$

The Barenblatt exponents depend on m in a non-trivial way. They are "anomalous" in the RG sense.

The exponents depend on m in a way that dimensional analysis alone cannot predict. The exponent β is the **anomalous dimension** of this problem.

Box 4.5: Deriving the Barenblatt Exponents

Ansatz: Seek self-similar solutions of the form:

$$\rho(x,t) = t^{-\alpha} f(\xi), \qquad \xi = \frac{|x|}{t^{\beta}} \tag{179}$$

Step 1: Substitute into the PME.

$$-\alpha t^{-\alpha-1} f - \beta t^{-\alpha-1}\xi f' = D t^{-m\alpha-2\beta}\left[\frac{d-1}{\xi}(f^m)' + (f^m)''\right] \tag{180}$$

Step 2: Require self-consistency. For the equation to be satisfied for all t, the powers of t must match:

$$-\alpha - 1 = -m\alpha - 2\beta \tag{181}$$

Step 3: Conservation of mass. Total mass $M = \int \rho \, d^d x = t^{-\alpha+d\beta} \int f(\xi)\xi^{d-1} d\xi$ must be constant:

$$-\alpha + d\beta = 0 \tag{182}$$

Step 4: Solve the system. From mass conservation: $\alpha = d\beta$. Substituting into the self-consistency equation:

$$-d\beta - 1 = -md\beta - 2\beta = -\beta(md + 2) \tag{183}$$

$$\beta[(md + 2) - d] = 1 \implies \beta = \frac{1}{d(m-1)+2} \tag{184}$$

Result:

$$\boxed{\alpha = \frac{d}{d(m-1)+2}, \qquad \beta = \frac{1}{d(m-1)+2}} \tag{185}$$

Check: For $m = 1$: $\beta = 1/2$ (linear diffusion) ✓
The anomalous dimension: Compare to dimensional analysis, which would give $\beta = 1/2$ if it worked. The deviation $\gamma_\beta = \beta - 1/2$ is the anomalous dimension. Its existence signals second-kind self-similarity.

The PME as an RG Flow

The Barenblatt exponents have a natural interpretation in the RG language. The PME flows to a fixed point where the exponents are determined dynamically.

The Parameter Space

Consider the family of self-similar solutions parameterized by their exponents:

$$\rho_{\alpha,\beta}(x,t) = t^{-\alpha} f_{\alpha,\beta}(|x|/t^\beta) \tag{186}$$

Only special values of (α, β) give solutions to the PME. The Barenblatt values are a fixed point of the RG in the space of self-similar profiles.

The Barenblatt solution is an RG fixed point in the space of self-similar profiles.

Stability and Selection

Why does the Barenblatt solution emerge? Other self-similar forms might exist but are unstable. Under the RG (zooming out), generic initial conditions flow toward the stable self-similar profile.

The Barenblatt fixed point is **IR stable**: perturbations decay as $t \to \infty$. This is why the exponents (178) are observed experimentally.

The Transseries Structure

The self-similar exponent β is computed exactly in this case, but it can also be understood as the sum of a perturbative series plus non-perturbative corrections. Expanding around $m = 1$:

$$\beta = \frac{1}{2} - \frac{d}{4}(m-1) + \frac{d(d+2)}{8}(m-1)^2 - \cdots \tag{187}$$

Even for the PME, the exponents can be viewed as transseries with the expansion parameter $(m-1)$.

This series has Gevrey-1 structure if we consider it as an asymptotic expansion in $(m-1)$. The Borel transform has singularities corresponding to "instanton" configurations in the m-expansion. While these are less dramatic than QFT instantons, the mathematical structure is identical.

The selection of the physical exponent from among the formal solutions corresponds to a specific resummation prescription. Median resummation gives the real Barenblatt exponent.

The Wilson-Fisher Fixed Point Revisited

The epsilon expansion for the Wilson-Fisher fixed point has a deep resurgent structure that parallels the PME analysis.

The Expansion

The anomalous dimension η at the Wilson-Fisher fixed point has the expansion:

$$\eta = \frac{(n+2)}{2(n+8)^2}\epsilon^2 + O(\epsilon^3) \tag{188}$$

where n is the number of field components and $\epsilon = 4 - d$.

This series continues to high orders and is known to be asymptotic with factorially growing coefficients.

The epsilon expansion is Gevrey-1. Borel resummation is required for meaningful predictions at $\epsilon = 1$.

Resurgent Analysis

The Borel transform of the epsilon series has singularities that encode non-perturbative effects. For scalar ϕ^4 theory:

$$\hat{\eta}(\zeta) \sim \frac{1}{\zeta - \zeta_{\text{ren}}} + \cdots \tag{189}$$

where $\zeta_{\text{ren}} = 3/(n+8)$ is the leading renormalon position.

Renormalons are singularities in the Borel plane arising from the factorial growth of perturbative coefficients due to RG running. They are not related to tunneling (unlike instantons) but rather to the inherent ambiguity in defining the perturbative sum at large orders.

Physical Predictions

Despite the divergence, the epsilon expansion gives remarkably accurate predictions. For the 3D Ising model ($n = 1$, $\epsilon = 1$):

$$\eta_{\text{exp}} \approx 0.0363, \qquad \eta_{O(\epsilon^2)} = \frac{3}{242} \approx 0.0124 \tag{190}$$

Higher-order calculations with resummation give $\eta \approx 0.036$, in excellent agreement with experiment and numerical simulations.

Box 4.6: Renormalons and the Epsilon Expansion

Why the expansion diverges:
The k-th order contribution to η goes like:

$$\eta^{(k)} \sim (-1)^k c \cdot a^k \cdot k! \cdot \epsilon^k \tag{191}$$

The factorial $k!$ arises from counting the number of diagrams at high orders and from UV renormalon contributions.
Borel transform:

$$\hat{\eta}(\zeta) = \sum_k \frac{\eta^{(k)}}{k!} \zeta^k \sim \sum_k (-a\zeta)^k = \frac{1}{1 + a\zeta} \tag{192}$$

This has a pole at $\zeta = -1/a$, corresponding to a renormalon singularity.
Resummation: The Borel-Laplace integral:

$$\eta(\epsilon) = \int_0^\infty e^{-\zeta/\epsilon} \hat{\eta}(\zeta) d\zeta \tag{193}$$

is ambiguous because the pole lies on the integration contour for real $a < 0$ (alternating signs).
Physical prescription: Take the principal value or median resummation to get real physical predictions. The ambiguity is of order $e^{-1/(a\epsilon)}$, exponentially small for small ϵ.
For $\epsilon = 1$: The exponentially small ambiguity becomes order one! Full resurgent analysis is needed to make accurate predictions.

The Landscape of Fixed Points

The full picture includes all fixed points, both perturbative and non-perturbative, organized by their stability properties.

The RG "Phase Diagram"

In the extended parameter space including transseries parameters, fixed points form a landscape. The RG flow connects different fixed points,

and the stability structure determines which fixed points are "reached" from generic initial conditions.

Generic UV completions flow to IR fixed points. Which IR fixed point is reached depends on the relevant directions and how they are tuned. The irrelevant directions are forgotten.

The full fixed point landscape includes perturbative and non-perturbative fixed points, connected by RG flows in the extended parameter space.

Conformal Windows

In gauge theories, there can be ranges of parameter space ("conformal windows") where the theory flows to a non-trivial interacting fixed point rather than to a free theory. The boundaries of these windows are determined by when fixed points collide and disappear.

Non-perturbative fixed points can extend the conformal window beyond what perturbation theory predicts. This is an active area of research in strongly coupled gauge theories.

Emergent Symmetry at Fixed Points

Fixed points often have enhanced symmetry compared to generic points in theory space. Scale invariance is automatic, and under mild conditions scale invariance implies the full conformal symmetry in $d > 2$.

This emergent symmetry provides powerful constraints. Conformal field theory techniques can compute correlation functions exactly at fixed points, even in strongly coupled theories.

Looking Ahead

This chapter classified fixed points by stability and introduced anomalous dimensions. The three examples now cover complementary phenomena.

Oscillator: secular terms. ϕ^4: beta functions. PME: anomalous dimensions. Together they demonstrate the complete RG framework.

The oscillator demonstrated secular terms and running parameters with trivial fixed point structure. **The ϕ^4 theory** showed nontrivial beta functions and the Gaussian fixed point. **The PME** revealed anomalous dimensions and second-kind self-similarity.

The next two chapters develop the geometric structures underlying parameter space. **Chapter I** introduces metrics on theory space, relating RG to information geometry and gradient flow. **Chapter I** develops connections and parallel transport, leading to the unified picture of Stokes phenomena as monodromy.

Summary

Fixed points satisfy $\beta^i(g^*) = 0$. At fixed points, theories are scale-invariant.
Perturbative fixed points have $\beta_{\text{pert}}(g^*) = 0$. **Non-perturbative fixed points** have $\beta_{\text{full}}(g^*) = 0$ but $\beta_{\text{pert}}(g^*) \neq 0$.
Stability is determined by the eigenvalues of $B^i{}_j = \partial\beta^i/\partial g^j|_{g^*}$.
Classification:

- Relevant ($\Delta > 0$): grows under RG
- Irrelevant ($\Delta < 0$): shrinks under RG
- Marginal ($\Delta = 0$): fate depends on higher orders

Universality means different microscopic theories flow to the same fixed point and have identical IR behavior, including the same Stokes constants.
The porous medium equation $\partial_t\rho = D\nabla^2(\rho^m)$ exhibits **second-kind self-similarity** with anomalous exponents:

$$\alpha = \frac{d}{d(m-1)+2}, \qquad \beta = \frac{1}{d(m-1)+2} \tag{194}$$

Anomalous dimensions are corrections to engineering dimensions from interactions. They signal that dimensional analysis fails and scaling exponents must be computed dynamically.

Metric Structure on the Extended Theory Space

Chapters 1–4 developed the RG as a flow on parameter space. This chapter asks: does parameter space have more structure? The answer is yes, and the structure has profound physical meaning. The metric measures distinguishability between theories, and it extends naturally to the transseries-enlarged space.

Parameter space is not just a set of points. It has **geometry**. There is a natural notion of distance between theories, measured by a **metric**. This metric has deep physical meaning in statistical mechanics and information theory. The RG flow can often be written as **gradient flow** with respect to this metric, meaning theories flow "downhill" toward fixed points.

Even more remarkably, this geometric structure extends to the full theory space including transseries parameters. The metric acquires new components measuring distinguishability along non-perturbative directions. Near Stokes lines, these components become large, reflecting that theories differing in their transseries structure become highly distinguishable.

This chapter develops these ideas, connecting the RG to information geometry and establishing theorems about the irreversibility of the RG flow.

Why Metrics Matter

A metric on parameter space measures how "different" two nearby theories are.

The Question

Consider two theories with coupling constants g and $g + dg$. How different are their physical predictions?

The metric answers: how much do physical predictions change when we change parameters? Large metric means small changes in parameters cause large changes in physics.

If changing g by dg makes a huge difference, the metric $G_{ab}(g)$ should be large. If changing g barely affects anything, the metric should be small.

Formalizing "Distinguishability"

In statistical systems, we can make this precise. The output of a theory is a probability distribution $p(x; g)$ over configurations x. Two theories are "distinguishable" if their distributions are different.

The natural measure of distinguishability between probability distributions is the **Fisher information metric**, which quantifies how much the log-likelihood changes when parameters change.

Physical Significance

The metric has several physical interpretations.

For statistical inference, the metric determines how well we can estimate parameters from data. Large metric means parameters are easy to estimate because small changes produce noticeable effects.

For thermodynamics, the metric is related to fluctuations. Large metric means large fluctuations in the observables conjugate to the parameters.

For RG, the metric determines the "natural" speed of flow. And it enables gradient flow formulations where the RG becomes a descent toward minimum "potential."

The Fisher Information Metric

The Fisher information metric is the natural metric on a space of probability distributions.

Definition

Given a family of probability distributions $p(x; g)$ parameterized by $g = (g^1, \ldots, g^n)$, the **Fisher information metric** is:

$$G_{ab}(g) = \int dx\, p(x; g)\, \frac{\partial \log p}{\partial g^a}\, \frac{\partial \log p}{\partial g^b} \tag{195}$$

The Fisher metric measures the expected squared change in log-likelihood. It's positive semi-definite and symmetric.

This is the covariance matrix of the **score function** $s_a = \partial \log p / \partial g^a$.

Properties

The Fisher metric has several important properties.

It is **positive semi-definite** because $G_{ab} v^a v^b = \langle (v^a s_a)^2 \rangle \geq 0$.

It is **reparameterization covariant** because under $g^a \to g'^a(g)$, we have $G'_{a'b'} = (\partial g^a / \partial g'^{a'})(\partial g^b / \partial g'^{b'}) G_{ab}$, which is the transformation law for a tensor.

It is connected to the **Cramér-Rao bound**, and the inverse G^{-1} bounds the variance of any unbiased estimator for the parameters.

Box 5.1: Fisher Metric for a Gaussian

Setup: Consider a Gaussian distribution with mean μ and variance σ^2:

$$p(x; \mu, \sigma) = \frac{1}{\sqrt{2\pi\sigma^2}} \exp\left(-\frac{(x-\mu)^2}{2\sigma^2} \right) \tag{196}$$

The parameters are $g = (\mu, \sigma)$.

Step 1: Compute the log-likelihood.

$$\log p = -\frac{1}{2}\log(2\pi) - \log\sigma - \frac{(x-\mu)^2}{2\sigma^2} \tag{197}$$

Step 2: Compute the score functions.

$$\frac{\partial \log p}{\partial \mu} = \frac{x-\mu}{\sigma^2} \tag{198}$$

$$\frac{\partial \log p}{\partial \sigma} = -\frac{1}{\sigma} + \frac{(x-\mu)^2}{\sigma^3} \tag{199}$$

Step 3: Compute the expectations.

$$G_{\mu\mu} = \left\langle \frac{(x-\mu)^2}{\sigma^4} \right\rangle = \frac{1}{\sigma^2} \tag{200}$$

$$G_{\mu\sigma} = \left\langle \frac{(x-\mu)}{\sigma^2}\left(-\frac{1}{\sigma} + \frac{(x-\mu)^2}{\sigma^3}\right) \right\rangle = 0 \tag{201}$$

$$G_{\sigma\sigma} = \left\langle \left(-\frac{1}{\sigma} + \frac{(x-\mu)^2}{\sigma^3}\right)^2 \right\rangle = \frac{2}{\sigma^2} \tag{202}$$

Result: The Fisher metric is:

$$G = \frac{1}{\sigma^2}\begin{pmatrix} 1 & 0 \\ 0 & 2 \end{pmatrix} \tag{203}$$

Physical interpretation: At small σ, the metric is large because the distribution is sharply peaked. Small changes in μ or σ produce noticeable differences. At large σ, the metric is small because the distribution is spread out and changes are harder to detect.

The Zamolodchikov Metric

In quantum field theory, there is a natural metric on the space of theories that is closely related to the Fisher metric.

Definition

Consider a QFT with coupling constants g^a and corresponding operators $\mathcal{O}_a$ that appear in the action as $S = S_0 + \sum_a g^a \int d^d x\, \mathcal{O}_a(x)$.

The Zamolodchikov metric is the two-point function of the operators that "generate" deformations of the action.

The **Zamolodchikov metric** is:

$$G_{ab}(g) = \lim_{|x-y|\to 0} |x-y|^{2\Delta_a} \langle \mathcal{O}_a(x)\mathcal{O}_b(y)\rangle_g \tag{204}$$

where Δ_a is the scaling dimension of $\mathcal{O}_a$ and the limit extracts the coefficient of the leading singularity.

Relation to the Fisher Metric

In statistical mechanics, the partition function $Z[g] = \int \mathcal{D}\phi\, e^{-S[\phi;g]}$ defines a probability distribution. The Zamolodchikov metric is precisely the Fisher metric for this distribution.

The operators $\mathcal{O}_a$ generate changes in the action, and their two-point function measures how much the distribution changes under these deformations.

Properties at Fixed Points

At a conformal fixed point, the Zamolodchikov metric has special structure.

Operators organize into **conformal families**. Primary operators and their descendants have specific transformation properties. The metric is diagonal in the basis of primary operators (at the fixed point).

The metric coefficients are related to OPE coefficients, which are physical observables that can be measured experimentally or computed in conformal field theory.

Metric on the Extended Theory Space

The perturbative theory space $\mathcal{M}_{\text{pert}}$ is a submanifold of the full extended theory space $\mathcal{M}_{\text{ext}}$ that includes transseries parameters. The metric extends naturally to this larger space.

The Extended Coordinates

The extended theory space has coordinates $(g^1, \ldots, g^n, \sigma^1, \sigma^2, \ldots)$ where g^a are the perturbative couplings and σ^k are the transseries parameters weighting the k-instanton sectors.

The full theory space has coordinates (g^a, σ^n) combining perturbative couplings and transseries parameters.

The metric on the extended space has three types of components.

The first type is G_{ab} with purely perturbative indices. These are the standard Zamolodchikov metric components measuring distinguishability along perturbative directions.

The second type is $G_{\sigma^k\sigma^l}$ with purely transseries indices. These measure distinguishability between theories differing in their non-perturbative content.

The third type is $G_{a\sigma^k}$ with mixed indices. These measure cross-correlations between perturbative and non-perturbative directions.

Behavior Near Stokes Lines

The extended metric has interesting behavior near Stokes lines in the Borel plane.

Near Stokes lines, theories differing in σ become highly distinguishable. The metric component $G_{\sigma\sigma}$ diverges.

Far from Stokes lines, the exponentially suppressed sectors $e^{-nS/g}\sigma^n$ contribute negligibly to physical observables. Theories differing only in σ are almost indistinguishable, and $G_{\sigma\sigma}$ is small.

Near a Stokes line, the exponentially small terms become comparable to the error in the perturbative approximation. Different values of σ lead to noticeably different predictions, and $G_{\sigma\sigma}$ becomes large.

At a Stokes crossing, the ambiguity in the resummation becomes maximal. The metric component can diverge, signaling that the transseries parameter becomes a crucial degree of freedom.

Box 5.2: The Extended Metric Near a Stokes Line

Setup: Consider a toy model where the partition function is:

$$Z(g,\sigma) = Z_{\text{pert}}(g) + \sigma e^{-S/g} Z^{(1)}(g) + \cdots \tag{205}$$

The log-partition function:

$$W = \log Z \approx \log Z_{\text{pert}} + \sigma e^{-S/g} \frac{Z^{(1)}}{Z_{\text{pert}}} + O(\sigma^2) \tag{206}$$

The metric component $G_{\sigma\sigma}$:

$$G_{\sigma\sigma} = \frac{\partial^2 W}{\partial \sigma^2} - \left(\frac{\partial W}{\partial \sigma}\right)^2 \sim e^{-2S/g} \left(\frac{Z^{(1)}}{Z_{\text{pert}}}\right)^2 - \cdots \tag{207}$$

Far from Stokes lines: When g is real and positive, $e^{-S/g}$ is exponentially small. The metric $G_{\sigma\sigma}$ is negligible, and changing σ barely affects predictions.

Near a Stokes line: When $\text{Im}(g)$ approaches zero from a region where $\text{Re}(e^{-S/g})$ changes sign, the exponential terms become order one compared to the error. The metric $G_{\sigma\sigma}$ grows and indicates that σ matters.

Physical interpretation: The Stokes phenomenon is the transition from σ being "invisible" (small metric) to σ being "observable" (large metric).

Gradient Flow

A remarkable fact about many RG flows is that they can be written as **gradient flows**. This means the beta function is the gradient of some "potential" with respect to the metric.

Definition

A flow is **gradient** with respect to a metric G_{ab} and potential V if:

$$\beta^a = -G^{ab}\frac{\partial V}{\partial g^b} \tag{208}$$

where G^{ab} is the inverse metric.

Gradient flow: the RG "rolls downhill" on the potential landscape. Fixed points are stationary points of V.

In components with index raised:

$$\frac{dg^a}{d\ell} = -G^{ab}\partial_b V \tag{209}$$

Consequences of Gradient Structure

If the RG is gradient flow with V bounded below, then several important consequences follow.

The flow is **irreversible** in the sense that the potential decreases along trajectories:

$$\frac{dV}{d\ell} = \partial_a V \cdot \beta^a = -G_{ab}\beta^a\beta^b \leq 0 \tag{210}$$

because G is positive semi-definite.

Fixed points are **local minima** of V (or saddle points, but not maxima).

No **limit cycles** can exist because V keeps decreasing.

When Is the RG Gradient Flow?

Not all RG flows are gradient. The condition is:

$$\partial_a\beta_b = \partial_b\beta_a \tag{211}$$

where $\beta_a = G_{ab}\beta^b$.

A flow is gradient iff β_a is a closed 1-form. This can fail in theories with multiple couplings.

This says β_a must be a **closed 1-form**. Locally, it's then exact, meaning $\beta_a = -\partial_a V$ for some V.

In 2D CFT, Zamolodchikov proved this holds with $V = c$, the central charge. In higher dimensions, the situation is more subtle.

Zamolodchikov's c-Theorem

The most famous example of gradient flow structure is Zamolodchikov's c-theorem in two-dimensional quantum field theory.

The Central Charge

In 2D CFT, the **central charge** c is a fundamental quantity that counts degrees of freedom in a specific sense. It appears in the two-point

function of the stress tensor:

$$\langle T(z)T(w)\rangle = \frac{c/2}{(z-w)^4} \tag{212}$$

For free theories, c is the number of bosons plus half the number of fermions. For interacting theories, c takes non-integer values.

The central charge c counts "degrees of freedom" in 2D. Free scalars have $c = 1$, free fermions have $c = 1/2$.

The Theorem

Theorem 0.2 (Zamolodchikov, 1986)**.** *In any unitary 2D QFT, there exists a function $c(\ell)$ along RG trajectories such that:*

1. *c decreases monotonically: $dc/d\ell \leq 0$*
2. *At fixed points, c equals the central charge of the CFT*
3. *$dc/d\ell = 0$ only at fixed points*

The proof constructs the c-function explicitly from correlation functions of the stress tensor.

The c-theorem: the central charge decreases under RG. This is the "arrow of scale" in 2D.

Physical Interpretation

The c-theorem says that "degrees of freedom" decrease under coarse-graining. As we zoom out, we lose information about UV details, and the number of effective degrees of freedom decreases.

This makes intuitive sense. Integrating out short-wavelength modes should reduce the complexity of the effective description.

Box 5.3: The c-Function in Practice

Example: Free scalar to massive scalar.
A free massless scalar in 2D has $c_{\text{UV}} = 1$.
Add a mass term $m^2\phi^2$. At energies $E \gg m$, the theory looks massless. At energies $E \ll m$, the massive scalar decouples.
The flow:

$$c_{\text{UV}} = 1 \quad \xrightarrow{\text{RG}} \quad c_{\text{IR}} = 0 \tag{213}$$

The c-function interpolates smoothly between 1 and 0 as we flow from UV to IR.
What it measures: In the UV, one degree of freedom (the scalar). In the IR, zero degrees of freedom (the scalar has decoupled).
The gradient flow: The beta function satisfies:

$$\beta^a = -G^{ab}\frac{\partial c}{\partial g^b} \tag{214}$$

with c as the potential. Fixed points are extrema of c.

Higher-Dimensional Generalizations

The c-theorem is specific to 2D. In higher dimensions, similar but weaker results hold.

The F-Theorem in 3D

In 3D CFT, the analog of c is the **F-quantity**, defined as the free energy on a 3-sphere:

$$F = -\log Z_{S^3} \tag{215}$$

The F-theorem: in 3D, the S^3 free energy decreases under RG. Proved by Jafferis, Klebanov, Pufu, and Safdi (2011).

Jafferis and collaborators proved that F decreases under RG:

$$F_{\text{UV}} \geq F_{\text{IR}} \tag{216}$$

with equality only if the theories are the same.

The a-Theorem in 4D

In 4D, there are two central charges, a and c, appearing in the conformal anomaly:

$$\langle T^\mu_\mu \rangle = \frac{c}{16\pi^2}(\text{Weyl})^2 - \frac{a}{16\pi^2}(\text{Euler}) \tag{217}$$

Cardy conjectured that a decreases under RG. This was proved by Komargodski and Schwimmer in 2011:

$$a_{\text{UV}} \geq a_{\text{IR}} \tag{218}$$

This is the **a-theorem**, which is the 4D generalization of the c-theorem.

The General Pattern

In all known cases, there exists a quantity that decreases under RG:

Dimension	Quantity	Name
$d = 2$	c (central charge)	c-theorem
$d = 3$	F (S^3 free energy)	F-theorem
$d = 4$	a (Euler anomaly coeff.)	a-theorem

This supports the picture of RG as "information loss" and suggests a universal structure that transcends dimension.

The Resurgent c-Function

The monotonicity theorems apply to the full theory, not just the perturbative sector. This leads to constraints on the transseries structure.

Extension to the Full Theory Space

The c-function on the extended theory space $\mathcal{M}_{\text{ext}}$ includes dependence on transseries parameters:

$$c_{\text{full}}(g, \sigma) = c_{\text{pert}}(g) + \sum_{n=1}^{\infty} \sigma^n e^{-nS/g} c^{(n)}(g) \tag{219}$$

The full c-function is a transseries. Monotonicity applies to the complete object, including non-perturbative sectors.

The monotonicity theorem says c_{full} decreases along any RG trajectory, including trajectories that cross Stokes lines.

Constraints on Stokes Constants

The requirement that c_{full} decreases continuously across Stokes lines places constraints on the Stokes constants.

At a Stokes crossing, σ jumps by the Stokes constant S_1. The continuity of c_{full} requires:

$$c_{\text{full}}(g, \sigma + S_1) = c_{\text{full}}(g, \sigma) + O(\text{exponentially small}) \tag{220}$$

This is automatic if the c-function is correctly defined including all sectors, but it provides a non-trivial consistency check on the resurgent structure.

Irreversibility and Non-Perturbative Information

The c-theorem applies to both perturbative and non-perturbative information. Under coarse-graining, information is lost from both high-energy Feynman diagrams and high-action instanton configurations.

The RG loses both perturbative (short-distance) and non-perturbative (high-action) information as we coarse-grain.

This has a beautiful interpretation. In the UV, the theory has access to both high-energy perturbative physics and high-action non-perturbative configurations. As we flow to the IR, both types of information are integrated out.

The Porous Medium Equation as Gradient Flow

Our third example, the PME, has a beautiful gradient flow structure in a different geometry: the **Wasserstein metric** from optimal transport theory.

The Wasserstein Space

Consider probability densities $\rho(x)$ with $\int \rho \, dx = 1$ and $\rho \geq 0$. The **Wasserstein distance** $W_2(\rho_1, \rho_2)$ measures the minimum "cost" to transport mass from distribution ρ_1 to ρ_2.

The Wasserstein metric comes from optimal transport. It measures the cost of moving mass from one distribution to another.

Formally:

$$W_2(\rho_1, \rho_2)^2 = \inf_{\gamma} \int |x - y|^2 \, d\gamma(x, y) \tag{221}$$

where the infimum is over "transport plans" γ with marginals ρ_1 and ρ_2.

PME as Gradient Flow

Otto showed that the porous medium equation can be written as gradient flow in Wasserstein space:

$$\partial_t \rho = -\nabla_{W_2} E[\rho] \tag{222}$$

where $E[\rho]$ is an entropy-like functional.

The PME minimizes an "entropy" in the Wasserstein metric. This is a geometric reformulation of nonlinear diffusion.

For the PME with $m > 1$, the functional is:

$$E[\rho] = \frac{1}{m-1} \int \rho^m \, dx \tag{223}$$

The gradient is taken with respect to the Wasserstein metric, not the L^2 metric.

Box 5.4: Gradient Flow Structure of the PME

The standard PME:

$$\partial_t \rho = \nabla^2(\rho^m) = \nabla \cdot (\rho^{m-1} \nabla \rho) \tag{224}$$

The entropy functional:

$$E[\rho] = \frac{1}{m-1} \int \rho^m \, dx \tag{225}$$

The Wasserstein gradient: In Wasserstein geometry, the gradient of E at ρ is:

$$(\nabla_{W_2} E)[\rho] = -\nabla \cdot \left(\rho \nabla \frac{\delta E}{\delta \rho} \right) \tag{226}$$

where $\delta E / \delta \rho = \frac{m}{m-1} \rho^{m-1}$ is the functional derivative.

Computation:

$$(\nabla_{W_2} E)[\rho] = -\nabla \cdot \left(\rho \nabla \frac{m \rho^{m-1}}{m-1} \right) = -\nabla \cdot \left(\frac{m}{m-1} \rho^{m-1} \nabla \rho \right) \tag{227}$$

The PME:

$$\partial_t \rho = -(\nabla_{W_2} E) = \nabla \cdot \left(\frac{m}{m-1} \rho^{m-1} \nabla \rho \right) \propto \nabla^2(\rho^m) \tag{228}$$

Conclusion: The PME is gradient flow for the entropy E in the Wasserstein metric.

Physical meaning: The density evolves to minimize the "spread" measured by $\int \rho^m$. For $m > 1$, this penalizes concentration and favors spreading, which is diffusion.

Implications

The gradient flow structure implies entropy decreases along solutions:

$$\frac{dE}{dt} = -\int \rho \left| \nabla \frac{\delta E}{\delta \rho} \right|^2 dx \leq 0 \tag{229}$$

This is the analog of the c-theorem for the PME. The "degrees of freedom" (entropy) decrease as the density spreads.

Looking Ahead

This chapter established that parameter space has metric structure, and this metric extends to the full transseries-enlarged theory space.

The Fisher-Zamolodchikov metric measures distinguishability between theories. Gradient flow with respect to this metric underlies the c-theorem and related monotonicity results. The metric on the extended space has components measuring distinguishability along transseries directions, becoming large near Stokes lines.

Metrics tell us "how far apart" theories are. Connections tell us "how to compare" quantities at different theories.

The next chapter introduces a richer geometric structure, namely **connections** on parameter space. Connections tell us how to "parallel transport" quantities from one theory to another. This leads to the key insight unifying the geometric and resurgent viewpoints: Stokes phenomena are monodromy.

Summary

The Fisher information metric:

$$G_{ab}(g) = \int dx\, p(x;g)\, \frac{\partial \log p}{\partial g^a} \frac{\partial \log p}{\partial g^b} \tag{230}$$

measures distinguishability between nearby theories.

The Zamolodchikov metric in QFT is the two-point function of operators that generate deformations.

Extended theory space includes transseries parameters σ^n. The metric extends to components $G_{\sigma^k \sigma^l}$ that become large near Stokes lines.

Gradient flow: When $\beta^a = -G^{ab}\partial_b V$, the RG flows "downhill" on the potential V.

The c-theorem (2D): The central charge c decreases along RG trajectories. Analogous results hold in 3D (F-theorem) and 4D (a-theorem).

The resurgent c-function includes non-perturbative sectors. Monotonicity applies to the full transseries.

The PME as gradient flow: The porous medium equation minimizes an entropy functional in the Wasserstein metric, providing an alternative perspective on nonlinear diffusion.

Connections, Monodromy, and Stokes Phenomena

Chapter 5 introduced metrics on theory space. This chapter introduces **connections**, which tell us how to compare quantities at different points. The payoff is deep: Stokes phenomena in resurgent analysis are precisely monodromy in the geometric picture.

The metric tells us distances, but we need more structure to understand how quantities transform as we move through parameter space. A **connection** tells us how to "parallel transport" vectors, operators, and other objects from one theory to another.

This chapter develops connections on theory space and reveals the central unifying insight of this book. The **Stokes automorphism** that acts on transseries when we cross Stokes lines is mathematically identical to **monodromy** around singularities in coupling-constant space. What appears as a discrete jump in one picture is a smooth path-dependent transport in another. The alien derivative of alien calculus is a generalized covariant derivative that probes directions in the extended theory space.

This unification is not merely aesthetic. It provides powerful computational tools because monodromy matrices can be calculated from local data, and it explains why the Stokes constants are universal quantities independent of microscopic details.

Operator Mixing Under RG

When we change the scale, operators don't just rescale. They can **mix** with each other.

The Phenomenon

Consider a set of operators $\{\mathcal{O}_a\}$ in a QFT. Under an RG transformation from scale μ to $\mu + d\mu$, each operator can acquire contributions from others:

$$\mu \frac{d\mathcal{O}_a}{d\mu} = \gamma_a{}^b(g)\, \mathcal{O}_b \tag{231}$$

Operator mixing: under RG, $\mathcal{O}_1$ can become a superposition of $\mathcal{O}_1$ and $\mathcal{O}_2$. The mixing matrix $\gamma_a{}^b$ is the "anomalous dimension matrix."

The matrix $\gamma_a{}^b(g)$ is the **anomalous dimension matrix**. When γ is diagonal, each operator rescales independently. When γ has off-diagonal elements, operators mix.

Example: Mixing in ϕ^4 Theory

In ϕ^4 theory, consider the operators ϕ^2 (mass term) and ϕ^4 (interaction). Under RG, the ϕ^4 operator induces corrections to ϕ^2 through tadpole diagrams. The mixing is encoded in the anomalous dimension matrix:

$$\gamma = \begin{pmatrix} \gamma_{\phi^2} & \gamma_{\phi^2 \leftarrow \phi^4} \\ 0 & \gamma_{\phi^4} \end{pmatrix} \tag{232}$$

The off-diagonal element $\gamma_{\phi^2 \leftarrow \phi^4}$ is nonzero when ϕ^4 corrections generate ϕ^2 terms.

The Anomalous Dimension Matrix as Connection

The mixing equation (231) has the form of **parallel transport**. The operators form a vector bundle over parameter space, and $\gamma_a{}^b$ is a connection on this bundle.

The anomalous dimension matrix $\gamma_a{}^b$ is a **connection** on the bundle of operators over theory space.

This is not just a formal analogy. The mathematical structure is exactly that of a connection, and all the machinery of differential geometry applies.

Connections on Parameter Space

Let's develop the geometry properly.

What Is a Connection?

A connection tells us how to "parallel transport" objects along paths. If we have a vector V^a at a point g in parameter space, a connection $\Gamma^a{}_{bc}$ specifies how V^a changes as we move in direction dg^b:

$$DV^a = dV^a + \Gamma^a{}_{bc}\, dg^b\, V^c \tag{233}$$

The **covariant derivative** along a direction $\partial/\partial g^b$ is:

$$\nabla_b V^a = \partial_b V^a + \Gamma^a{}_{bc}\, V^c \tag{234}$$

The covariant derivative D generalizes the ordinary derivative to account for how the "basis" changes from point to point.

Parallel Transport

A vector is **parallel transported** along a curve $g(\ell)$ if:

$$\frac{DV^a}{d\ell} = \frac{dV^a}{d\ell} + \Gamma^a{}_{bc}\, \frac{dg^b}{d\ell}\, V^c = 0 \tag{235}$$

Given initial conditions, this ODE uniquely determines $V^a(\ell)$ along the curve.

Parallel transport: the vector "doesn't change" along the path, but what "doesn't change" means depends on the connection.

The RG Connection

In the RG context, the relevant connection is the **anomalous dimension matrix**:

$$\Gamma^a{}_{bc} = \gamma^a{}_c \cdot \delta^\ell_b \tag{236}$$

where δ^ℓ_b projects onto the RG direction and $\gamma^a{}_c$ is the anomalous dimension matrix.

The parallel transport equation (235) becomes the operator mixing equation (231). The RG flow parallel transports operators from one scale to another.

Box 6.1: Parallel Transport of Operators

Setup: Two operators $\mathcal{O}_1$ and $\mathcal{O}_2$ with anomalous dimension matrix:

$$\gamma = \begin{pmatrix} \gamma_{11} & \gamma_{12} \\ \gamma_{21} & \gamma_{22} \end{pmatrix} \tag{237}$$

The evolution:

$$\mu \frac{d}{d\mu} \begin{pmatrix} \mathcal{O}_1 \\ \mathcal{O}_2 \end{pmatrix} = \gamma \begin{pmatrix} \mathcal{O}_1 \\ \mathcal{O}_2 \end{pmatrix} \tag{238}$$

Solution: If γ is constant (leading order):

$$\begin{pmatrix} \mathcal{O}_1(\mu) \\ \mathcal{O}_2(\mu) \end{pmatrix} = \left(\frac{\mu}{\mu_0}\right)^\gamma \begin{pmatrix} \mathcal{O}_1(\mu_0) \\ \mathcal{O}_2(\mu_0) \end{pmatrix} \tag{239}$$

where $(\mu/\mu_0)^\gamma = \exp(\gamma \log(\mu/\mu_0))$ is a matrix exponential.

Diagonalization: If γ has eigenvalues Δ_+ and Δ_-, the eigenvectors are "scaling operators" with definite dimension:

$$\mathcal{O}_\pm(\mu) = \left(\frac{\mu}{\mu_0}\right)^{\Delta_\pm} \mathcal{O}_\pm(\mu_0) \tag{240}$$

Physical interpretation: The "natural" operators are the scaling operators, not the original $\mathcal{O}_1$ and $\mathcal{O}_2$. These are the principal directions of the connection.

Curvature and Path Dependence

A connection may or may not be "flat." Curvature measures the failure of parallel transport to be path-independent.

The Curvature Tensor

The **curvature tensor** is:

$$R^a{}_{bcd} = \partial_c \Gamma^a{}_{bd} - \partial_d \Gamma^a{}_{bc} + \Gamma^a{}_{ec}\Gamma^e{}_{bd} - \Gamma^a{}_{ed}\Gamma^e{}_{bc} \tag{241}$$

If $R^a{}_{bcd} = 0$, the connection is flat and parallel transport depends only on the endpoints, not the path.

If $R \neq 0$, different paths from A to B give different results. This path dependence is called **holonomy**.

Curvature measures the failure of parallel transport to be path-independent. If $R = 0$, the connection is "flat."

Monodromy

A special case of holonomy is **monodromy**: the transformation acquired by parallel transporting around a closed loop.

If we transport a vector V around a loop $\mathcal{C}$ starting and ending at g, we get:

$$V^a_{\text{final}} = M^a{}_b(\mathcal{C})\, V^b_{\text{initial}} \tag{242}$$

where $M(\mathcal{C})$ is the **monodromy matrix**.

Monodromy: transport around a closed loop may not return to the starting point. The failure is encoded in the monodromy matrix.

For a flat connection, $M = \mathbf{1}$ (no monodromy). For a curved connection, $M \neq \mathbf{1}$.

Monodromy from Singularities

In many physical situations, the connection is flat almost everywhere but has singularities at special points. The monodromy around these singularities is non-trivial.

Consider a singularity at $g = g_*$. Parallel transport around a small loop encircling g_* gives monodromy:

$$M = \mathcal{P} \exp\left(\oint_{\mathcal{C}} \Gamma^a{}_{bc}\, dg^b \right) \tag{243}$$

where $\mathcal{P}$ denotes path ordering.

The OPE Connection

In conformal field theory, there is a natural connection related to the operator product expansion.

The Operator Product Expansion

When two operators approach each other, their product can be expanded:

$$\mathcal{O}_a(x)\mathcal{O}_b(0) = \sum_c C^c_{ab}(g)\, |x|^{\Delta_c - \Delta_a - \Delta_b}\, \mathcal{O}_c(0) + \cdots \tag{244}$$

The **OPE coefficients** $C^c_{ab}(g)$ depend on the couplings and encode the "algebra" of operators.

The OPE coefficients C^c_{ab} encode how operators "multiply." They define a ring structure on operators.

The OPE Connection

The OPE coefficients define a connection:

$$\Gamma^c_{ab}(g) = \frac{\partial C^c_{de}(g)}{\partial g^f} \cdot (\text{structure constants}) \tag{245}$$

The precise formula involves the structure of the CFT, but the key point is that the OPE provides a natural connection on the space of operators.

Parallel Transport and Conformal Perturbation Theory

Conformal perturbation theory studies how CFTs change when we deform by adding terms $\delta g^a \int \mathcal{O}_a$ to the action. The OPE connection tells us how operators in the original CFT relate to operators in the deformed theory.

Box 6.2: Conformal Perturbation Theory

Setup: Start with CFT_0 and perturb by $\delta S = \lambda \int d^d x\, \phi^4$.
The deformed theory: For small λ, the deformed theory is still approximately conformal with modified OPE coefficients:

$$C^c_{ab}(\lambda) = C^c_{ab}(0) + \lambda\, \delta C^c_{ab} + O(\lambda^2) \tag{246}$$

The connection: The change δC^c_{ab} can be computed from three-point functions in CFT_0:

$$\delta C^c_{ab} \sim \int d^d z\, \langle \mathcal{O}_a(x) \mathcal{O}_b(y) \phi^4(z) \mathcal{O}_c(w) \rangle_0 \tag{247}$$

Path dependence: If we deform by $\lambda_1 \mathcal{O}_1 + \lambda_2 \mathcal{O}_2$, the result depends on the order of deformations (path in coupling space). This is curvature.

Stokes Phenomena as Monodromy

We now arrive at the central insight: Stokes phenomena in resurgent analysis are monodromy in the extended theory space.

Review of Stokes Phenomena

Recall from Chapter I that when we resum a divergent series using Borel-Laplace, the result depends on the direction of integration. When the coupling g crosses a **Stokes line**, the resummation prescription changes discontinuously.

The transseries

$$\tilde{f}(g, \sigma) = f_0(g) + \sigma e^{-S/g} f_1(g) + \sigma^2 e^{-2S/g} f_2(g) + \cdots \tag{248}$$

Stokes phenomenon: the transseries parameter σ jumps discontinuously when crossing a Stokes line in coupling space.

undergoes a transformation $\sigma \to \sigma + S_1$ when g crosses a Stokes line, where S_1 is the Stokes constant.

The Geometric Picture

Now view this from the perspective of the extended theory space with coordinates (g, σ).

The Stokes line in the g-plane becomes a codimension-one surface in (g, σ) space. As g moves continuously, σ must jump to maintain the same physical answer.

But this "jump" is really **monodromy**! The extended parameter space has a non-trivial connection, and parallel transport around the Stokes line produces the transformation $\sigma \to \sigma + S_1$.

The Stokes automorphism is monodromy in the extended theory space. The "jump" in σ is path-dependent parallel transport.

The Mathematical Equivalence

Let's make this precise. Consider the extended space $\mathcal{M}_{\text{ext}}$ with coordinates (g, σ). Define a connection with:

$$\Gamma^{\sigma}{}_{\sigma g} = \frac{S_1}{2\pi i} \cdot \delta(\arg(g) - \theta_{\text{Stokes}}) \tag{249}$$

where the delta function is supported on the Stokes line.

Parallel transport of σ around a loop encircling the Stokes line gives:

$$\Delta\sigma = \oint \Gamma^{\sigma}{}_{\sigma g}\, dg = S_1 \tag{250}$$

The Stokes automorphism $\mathfrak{S} : \sigma \mapsto \sigma + S_1$ is precisely the monodromy matrix.

Box 6.3: Stokes Phenomena as Monodromy

Setup: Consider the transseries $\tilde{f}(g, \sigma) = f_0(g) + \sigma e^{-S/g} f_1(g) + \cdots$ with Stokes line at $\arg(g) = 0$.

The Stokes automorphism: Crossing the Stokes line clockwise:

$$\mathfrak{S} : \sigma \mapsto \sigma + S_1 \tag{251}$$

The monodromy interpretation:
Define a flat connection on $\mathcal{M}_{\text{ext}}$ with a "singularity" at the Stokes line. The connection 1-form is:

$$A = S_1 \cdot \frac{dg}{g} \cdot \Theta(\text{Stokes}) \tag{252}$$

where Θ is a distributional form supported on the Stokes line.
Integrating around a small loop encircling the origin:

$$M = \exp\left(\oint A\right) = \exp(S_1 \cdot 2\pi i \cdot \frac{1}{2\pi i}) = e^{S_1} \tag{253}$$

For the linear action on σ, this gives $\sigma \to \sigma + S_1$.
Key insight: The monodromy is computed from *local* data near the Stokes line. But it determines the *global* transformation. This is why Stokes constants are universal.

Alien Calculus as Covariant Differentiation

The tools of alien calculus have natural interpretations in the geometric framework.

The Alien Derivative

The **alien derivative** Δ_ω is an operator that "probes" the singularity at $\zeta = \omega$ in the Borel plane. It extracts the coefficient of the singularity and relates the perturbative sector to non-perturbative sectors.

The alien derivative probes singularities in the Borel plane. It relates different sectors of the transseries.

Formally, if $\hat{f}_B(\zeta)$ has a singularity at $\zeta = \omega$:

$$\hat{f}_B(\zeta) \sim \frac{c}{(\zeta - \omega)^\alpha} + \cdots \tag{254}$$

then $\Delta_\omega f$ extracts c (roughly speaking).

The Bridge Equation

The **bridge equation** relates alien derivatives to ordinary derivatives:

$$\Delta_\omega \tilde{f} = S_\omega \cdot \partial_\sigma \tilde{f} \tag{255}$$

where S_ω is the Stokes constant at ω.

This says: the alien derivative in the Borel plane is equivalent to differentiation along the transseries direction in parameter space.

Alien Derivative as Covariant Derivative

In the geometric picture, the alien derivative extends the covariant derivative to include "non-local" directions:

$$D_{\text{ext}} = \nabla_g + \sum_\omega e^{-\omega/g} \Delta_\omega \tag{256}$$

The alien derivative extends the covariant derivative. Just as ∇_a probes coupling directions, Δ_ω probes instanton directions.

The ordinary covariant derivative ∇_g differentiates along perturbative coupling directions. The alien derivatives Δ_ω differentiate along "instanton directions" in the extended space.

The full covariant derivative D_{ext} on the extended space includes both:

$$D_{\text{ext}} V = \nabla V + \Gamma_{\text{Stokes}} V \tag{257}$$

where Γ_{Stokes} is the connection encoding Stokes jumps.

Box 6.4: The Bridge Equation as Parallel Transport

The bridge equation:

$$\Delta_\omega f = S_\omega \cdot \partial_\sigma f \tag{258}$$

Geometric interpretation: The alien derivative Δ_ω probes the singularity at $\zeta = \omega$ in the Borel plane.
The derivative ∂_σ differentiates along the transseries direction.
The bridge equation says these are related by the connection coefficient S_ω.
In covariant derivative language:

$$\nabla_\omega f \equiv \partial_\omega f + \Gamma^\sigma_\omega \partial_\sigma f = 0 \tag{259}$$

with $\Gamma^\sigma_\omega = -S_\omega$.
This is a **flatness condition**! The transseries f is "parallel" (covariantly constant) in the direction ω.
Physical meaning: The physical content is independent of how we distribute information between perturbative and non-perturbative sectors. The bridge equation is the consistency condition enforcing this.

Scheme Independence and Gauge Transformations

Different renormalization schemes give different parameterizations of the same physics. Scheme changes are "gauge transformations" of the connection.

Renormalization Scheme Dependence

The beta function and anomalous dimensions depend on the renormalization scheme. In scheme A:

$$\beta^i_A(g_A), \quad \gamma_{A,a}{}^b(g_A) \tag{260}$$

In scheme B, related by $g_B = g_B(g_A)$:

$$\beta^i_B(g_B), \quad \gamma_{B,a}{}^b(g_B) \tag{261}$$

Scheme changes are coordinate transformations on theory space. Physical quantities are scheme-independent.

These are related by coordinate transformations, which is exactly how connection components transform under diffeomorphisms.

Gauge Transformations

Under a scheme change $g \to g'(g)$, the connection transforms as:

$$\Gamma'^a{}_{bc} = \frac{\partial g'^a}{\partial g^d}\frac{\partial g^e}{\partial g'^b}\frac{\partial g^f}{\partial g'^c}\Gamma^d{}_{ef} + \frac{\partial g'^a}{\partial g^d}\frac{\partial^2 g^d}{\partial g'^b \partial g'^c} \tag{262}$$

This is the standard transformation law for connections. The curvature (and hence monodromy) is invariant.

Scheme Independence of Stokes Constants

The Stokes constants are **scheme-independent** because they are monodromy data. Monodromy depends only on the intrinsic geometry, not on the coordinate system.

Stokes constants are universal because they are monodromy data, which is coordinate-independent geometric information.

This explains the remarkable universality of Stokes constants. Different microscopic theories flowing to the same fixed point have the same Stokes constants because they have the same geometry near the fixed point.

The Extended Connection in Practice

Let's see how the extended connection works in our three examples.

The Anharmonic Oscillator

The oscillator's parameter space (A, ϕ) extends to (A, ϕ, σ) including the transseries parameter.

The perturbative connection is trivial because there's no operator mixing in this one-particle problem.

The Stokes connection is non-trivial. When λ continues to negative values (or equivalently when we consider complex time), a Stokes line is crossed. The transseries parameter jumps by:

$$\Delta\sigma = S_{\text{osc}} \tag{263}$$

where S_{osc} is related to the tunneling amplitude in the inverted potential.

The 1D ϕ^4 Theory

The parameter space (r, λ) extends to $(r, \lambda, \sigma_{\text{ren}})$ where σ_{ren} weights the renormalon sector.

The perturbative connection is the anomalous dimension matrix from Chapter I.

The Stokes connection encodes how the renormalon sector turns on. The Stokes constant is:

$$S_{\text{ren}} = \frac{1}{\beta_1} + O(1) \tag{264}$$

where $\beta_1 = 2$ is the one-loop beta function coefficient.

The Porous Medium Equation

For the PME, the parameter is essentially m, and the transseries extension includes parameters σ_k weighting sub-leading self-similar modes.

The selection of the Barenblatt exponent corresponds to setting the transseries parameters to specific values. The "physical" resummation prescription that gives real exponents for real m is median resummation, which corresponds to a specific value of σ.

The Complete Geometric Picture

We can now state the unified geometric framework.

The Full Structure

The theory space $\mathcal{M}_{\text{ext}}$ is a manifold with coordinates (g^a, σ^n) that combine perturbative couplings with transseries parameters.

The full picture: theory space is a fiber bundle with connection. RG is parallel transport. Stokes phenomena are monodromy.

There is a **metric** G measuring distinguishability between theories. The metric extends to include components $G_{\sigma\sigma}$ that become large near Stokes lines.

There is a **connection** Γ encoding how quantities transform under RG. The connection has two parts. The first is the perturbative anomalous dimensions $\gamma_a{}^b$ governing operator mixing. The second is the Stokes connection Γ^σ_g encoding jumps in transseries parameters.

The **curvature** is concentrated at Stokes lines. Away from Stokes lines, the connection is flat. The **monodromy** around Stokes lines is the Stokes automorphism.

The Alien Derivative in Context

The alien derivative Δ_ω is the "covariant derivative in the direction of the ω-singularity." The bridge equation $\Delta_\omega f = S_\omega \partial_\sigma f$ says this is proportional to the ordinary derivative along σ.

The collection $\{\nabla_a, \Delta_\omega\}$ forms a complete basis of "directions" in the extended theory space. The former probe perturbative directions, and the latter probe non-perturbative directions.

Universality Revisited

The universality of critical behavior now has a geometric explanation. Systems in the same universality class have the same geometry near the fixed point, including the same connection, curvature, metric, and monodromy. All physical quantities derived from these geometric structures are therefore identical.

Looking Ahead

This chapter unified the geometric and resurgent perspectives on the RG. The Stokes automorphism is monodromy, the alien derivative is a covariant derivative, and scheme independence is coordinate invariance.

The unified picture shows that perturbative and non-perturbative physics are two aspects of a single geometric structure.

The next chapter, the final chapter of Part I, synthesizes everything into a practical methodology. The "RG Recipe" will show how to apply the unified framework to new problems, with full awareness of both perturbative and non-perturbative aspects from the beginning.

Summary

Operator mixing: Under RG, operators transform via

$$\mu \frac{d\mathcal{O}_a}{d\mu} = \gamma_a{}^b \, \mathcal{O}_b \tag{265}$$

The matrix $\gamma_a{}^b$ is a **connection** on the bundle of operators.
Parallel transport: Operators are parallel transported along RG trajectories. The result depends on the path (curvature) and can acquire non-trivial transformations around loops (monodromy).
Stokes phenomena = monodromy: The Stokes automorphism $\sigma \to \sigma + S_\omega$ is monodromy around the Stokes line in the extended parameter space.
Alien derivative = covariant derivative: The alien derivative Δ_ω probes non-perturbative directions. The bridge equation

$$\Delta_\omega f = S_\omega \, \partial_\sigma f \tag{266}$$

relates it to ordinary differentiation along transseries coordinates.
Scheme independence: Renormalization schemes are coordinates. Physical quantities (monodromy, Stokes constants) are coordinate-independent.
Universality explained: Systems in the same universality class share the same geometry near the fixed point, including all monodromy and Stokes data.

The Unified Recipe

This chapter distills the unified framework into a practical methodology. There is no separate "resurgence step" because resurgent thinking has been present from the beginning. The recipe shows how perturbative and non-perturbative analysis are inseparable aspects of one approach.

The preceding chapters developed the unified geometric-resurgent framework for the renormalization group. Parameter space is a manifold with metric and connection structure. Perturbation series are asymptotic with Gevrey-1 divergence encoding non-perturbative physics through the Borel plane. Stokes phenomena are monodromy in the extended theory space. Fixed points can be perturbative or non-perturbative.

This final chapter of Part I synthesizes everything into a practical **methodology** that can be applied to new problems. The recipe has six steps, but unlike traditional treatments, there is no separate "resurgence step" tacked on at the end. The transseries structure and Borel analysis appear naturally throughout.

The Six Steps

The unified RG analysis proceeds as follows.

Step 1: Identify Scales and Recognize Divergence Structure

Step 1: Find the scales, the small parameter, and where naive perturbation theory breaks down. Recognize that the perturbative series will diverge with Gevrey-1 structure.

Every RG problem begins with a hierarchy of scales. Identify the UV and IR scales, the small parameter ϵ connecting them, and the regime where naive analysis fails.

Simultaneously, recognize that the perturbative expansion in ϵ will diverge. Perturbation series in physical problems generically have factorially growing coefficients, which is Gevrey-1 structure. This is not a failure but a feature because the pattern of divergence encodes non-perturbative physics.

Questions to ask: What are the separated scales? What small parameter relates them? Where does naive perturbation theory fail (secular terms, UV divergences, boundary mismatches)? What is the expected source of non-perturbative effects (instantons, tunneling, renormalons)?

For the oscillator: The scales are the oscillation period $1/\omega_0$ and the amplitude-drift time $\omega_0/(\lambda A^2)$. The small parameter is $\lambda A^2/\omega_0^2$. Naive perturbation theory fails at $t \sim 1/(\lambda A^2)$ with secular terms.

Non-perturbative effects come from complex-time instantons.

For 1D ϕ^4: The scales are the UV cutoff Λ and the mass scale $\sqrt{r}$. The small parameter is λ/Λ^2. Loop integrals are finite in 1D, but the perturbative series still diverges. Non-perturbative effects are renormalons from RG running.

For the PME: The scales are the initial localization width and the time-evolved width. The small parameter is $(m-1)$ measuring deviation from linear diffusion. The perturbative expansion in $(m-1)$ is asymptotic. The selection of the physical exponent involves resummation.

Step 2: Set Up Perturbation Theory and Borel Transform

Construct the formal perturbative expansion. Compute the first few orders and identify the structure of divergence (alternating signs, specific factorial growth rate). Immediately construct the Borel transform to see the singularity structure.

Step 2: Compute the perturbative series, take its Borel transform, and identify the singularities. The singularities correspond to non-perturbative sectors.

Questions to ask: What is the perturbative series? What is the pattern of coefficients? Where are the singularities in the Borel plane? What physical effects do these singularities correspond to (instantons, renormalons, etc.)?

For the oscillator: The perturbative frequency correction is $\omega = \omega_0(1 + \frac{3}{8}\Pi + c_2\Pi^2 + \cdots)$ where $\Pi = \lambda A^2/\omega_0^2$. The Borel transform has singularities related to the complex-time instanton action $S = \omega_0^3/(3\lambda)$.

For 1D ϕ^4: The perturbative beta functions are asymptotic series. The Borel transform of β_λ has renormalon singularities at $\zeta_k = k/\beta_1 = k/2$ for positive integer k.

For the PME: The exponent $\beta(m)$ expanded around $m = 1$ is an asymptotic series. The Borel transform has singularities corresponding to sub-leading self-similar modes that were discarded in selecting the Barenblatt solution.

Step 3: Identify Running Parameters Including Transseries

Determine which quantities must become scale-dependent to absorb the divergence. These are the "running parameters." Include not only the perturbative couplings but also the transseries parameters that weight non-perturbative sectors.

Step 3: Identify which parameters run, including the transseries weights. The full parameter space is the extended space (g^a, σ^n).

Questions to ask: Which parameters absorb secular terms or divergences? What are the transseries parameters σ^n? What is the full extended parameter space?

For the oscillator: The running parameters are $A(t)$ and $\phi(t)$. The extended space adds σ weighting the instanton sector: (A, ϕ, σ).

For 1D ϕ^4: The running parameters are $r(\mu)$ and $\lambda(\mu)$. The extended space adds renormalon transseries parameters: $(r, \lambda, \sigma_{\text{ren}})$.

For the PME: The running parameter is the effective scaling exponent. The extended space includes parameters selecting among possible self-similar modes.

Step 4: Derive Full Transseries Beta Functions

Derive the RG equations for all parameters, including transseries coordinates. Use the envelope method or Callan-Symanzik approach. The consistency requirement across Stokes lines automatically produces the bridge equations.

Step 4: Derive RG equations for all coordinates in extended space. Consistency at Stokes crossings produces the bridge equations of alien calculus.

Questions to ask: What are the beta functions for perturbative couplings? What are the beta functions for transseries parameters? Where are the Stokes lines? What are the Stokes constants (monodromy data)?

For the oscillator:

$$\beta_A = 0 + O(\sigma e^{-S/\lambda}) \tag{267}$$

$$\beta_\phi = \frac{3\lambda A^2}{8\omega_0} + O(\sigma e^{-S/\lambda}) \tag{268}$$

The transseries corrections are exponentially small. The Stokes constant S_1 is determined by the instanton calculation.

For 1D ϕ^4:

$$\beta_r = 2r + \frac{3\lambda\Lambda}{\pi(\Lambda^2 + r)} + O(\sigma_{\text{ren}} e^{-\zeta_1/\lambda}) \tag{269}$$

$$\beta_\lambda = 2\lambda + O(\sigma_{\text{ren}} e^{-\zeta_1/\lambda}) \tag{270}$$

The renormalon Stokes constant is related to the one-loop beta function.

For the PME: The beta function for the exponent is trivial (exponents don't run once determined), but the selection involves the resummation prescription.

Step 5: Analyze Flow Structure in Extended Space

Find all fixed points, including perturbative and non-perturbative ones. Classify stability using the eigenvalues of the full stability matrix on extended space. Identify universality classes.

Step 5: Find fixed points, classify stability, and identify universality. Include non-perturbative fixed points where $\beta_{\text{pert}} \neq 0$ but $\beta_{\text{full}} = 0$.

Questions to ask: Where are the fixed points of β_{pert}? Are there non-perturbative fixed points where $\beta_{\text{pert}} \neq 0$ but $\beta_{\text{full}} = 0$? What is the stability matrix? Which directions are relevant, irrelevant, marginal? What is the basin of attraction?

For the oscillator: The only fixed point is $A = 0$ (trivial). All trajectories with $A > 0$ flow forever without reaching a non-trivial fixed point.

For 1D ϕ^4: The Gaussian fixed point $(0, 0)$ is the only perturbative fixed point. Both directions are relevant (unstable). No non-perturbative fixed points are known in 1D.

For the PME: The Barenblatt profile is a stable attractor in the space of self-similar solutions. The exponents are uniquely determined for $m > 1$.

Step 6: Extract Physics Using Median Resummation

Physical predictions come from correctly resummed transseries, not from naive perturbative truncation. Use median resummation or related prescriptions to obtain real, unambiguous answers.

Step 6: Extract physical predictions by resumming the full transseries. Median resummation gives real, unambiguous results.

Questions to ask: What physical observable are we computing? How does it depend on the resummation prescription? What is the median resummation? Are there ambiguities, and how do they cancel?

For the oscillator: The physical frequency is

$$\omega_{\text{eff}} = \omega_0 + \frac{3\lambda A^2}{8\omega_0} + O(\lambda^2) \tag{271}$$

Higher-order corrections require resummation for quantitative accuracy at large λ.

For 1D ϕ^4: Physical quantities like the correlation length are computed from the resummed running couplings. Renormalon ambiguities cancel in physical observables.

For the PME: The physical Barenblatt exponent

$$\beta = \frac{1}{d(m-1)+2} \tag{272}$$

is exact (the PME is special). For more general problems, the exponent would require resummation.

The Recipe Applied: Anharmonic Oscillator

Let's walk through the complete recipe for the anharmonic oscillator.

Box 7.1: Complete Analysis of the Anharmonic Oscillator

Step 1: Scales and divergence. UV scale: oscillation period $\tau_{\text{fast}} \sim 1/\omega_0$. IR scale: amplitude-drift time $\tau_{\text{slow}} \sim \omega_0/(\lambda A^2)$. Small parameter: $\epsilon = \lambda A^2/\omega_0^2 \ll 1$. Breakdown: secular terms at $t \sim \tau_{\text{slow}}$. Non-perturbative: complex-time instantons.

Step 2: Perturbation theory and Borel. The perturbative solution $x(t) = A\cos(\omega_0 t) + O(\lambda)$ develops secular terms. The frequency series $\omega = \omega_0(1 + \frac{3}{8}\epsilon + c_2\epsilon^2 + \cdots)$ diverges with $|c_n| \sim n!$. The Borel transform $\hat{\omega}(\zeta)$ has singularities at $\zeta = \omega_0^3/(3\lambda)$ (instanton action).
Step 3: Running parameters. Perturbative: (A, ϕ). Extended: (A, ϕ, σ) with σ weighting instanton sector.
Step 4: Beta functions.

$$\frac{dA}{dt} = 0 \tag{273}$$

$$\frac{d\phi}{dt} = \frac{3\lambda A^2}{8\omega_0} \tag{274}$$

Transseries corrections: $O(\sigma e^{-S/\lambda})$. The Stokes constant S_1 relates perturbative and instanton sectors.
Step 5: Fixed points and stability. Perturbative fixed point: $A = 0$ (trivial). No non-perturbative fixed points. All $A > 0$ trajectories flow forever.
Step 6: Physical prediction. The effective frequency is:

$$\omega_{\text{eff}} = \omega_0\left(1 + \frac{3\lambda A^2}{8\omega_0^2}\right) + O(\lambda^2) \tag{275}$$

For quantitative accuracy at larger λ, resum using median prescription.

The Recipe Applied: 1D ϕ^4 Theory

The field theory example demonstrates statistical RG with non-trivial flow.

Box 7.2: Complete Analysis of 1D ϕ^4 Theory

Step 1: Scales and divergence. UV scale: cutoff Λ (lattice spacing). IR scale: correlation length $\xi \sim 1/\sqrt{r}$. Small parameter: $\lambda/\Lambda^2 \ll 1$. Breakdown: tadpole corrections grow with Λ. Non-perturbative: renormalons from RG running.
Step 2: Perturbation theory and Borel. The beta functions $\beta_r = 2r + 3\lambda\Lambda/\pi(\Lambda^2 + r)$ and $\beta_\lambda = 2\lambda$ are perturbative leading terms. Higher-order coefficients grow factorially. The Borel transform has renormalon singularities at $\zeta_k = k/2$.
Step 3: Running parameters. Perturbative: (r, λ). Extended: $(r, \lambda, \sigma_{\text{ren}})$.

Step 4: Beta functions.

$$\beta_r = 2r + \frac{3\lambda\Lambda}{\pi(\Lambda^2 + r)} + O(\sigma_{\text{ren}} e^{-1/(2\lambda)}) \tag{276}$$

$$\beta_\lambda = 2\lambda + O(\sigma_{\text{ren}} e^{-1/(2\lambda)}) \tag{277}$$

The renormalon Stokes constant: $S_{\text{ren}} = 1/\beta_1 + O(1) = 1/2 + O(1)$.

Step 5: Fixed points and stability. Perturbative: Gaussian fixed point $(0, 0)$. Stability matrix eigenvalues: both $= 2$ (relevant, unstable). No non-perturbative fixed points in 1D. In $d = 4 - \epsilon$, the Wilson-Fisher fixed point appears.

Step 6: Physical prediction. Running couplings:

$$\lambda(\mu) = \lambda_0 \left(\frac{\mu}{\mu_0}\right)^2 \tag{278}$$

Physical correlation functions computed from resummed expressions.

The Recipe Applied: Porous Medium Equation

The PME demonstrates anomalous dimensions and second-kind self-similarity.

Box 7.3: Complete Analysis of the Porous Medium Equation

Step 1: Scales and divergence. UV scale: initial localization width. IR scale: late-time spread $L(t) \sim t^\beta$. Small parameter: $(m - 1)$ (deviation from linear diffusion). Breakdown: anomalous exponent $\beta \neq 1/2$ for $m \neq 1$. Non-perturbative: sub-leading self-similar modes.

Step 2: Perturbation theory and Borel. Expand $\beta(m)$ around $m = 1$:

$$\beta = \frac{1}{2} - \frac{d}{4}(m - 1) + O((m - 1)^2) \tag{279}$$

This is asymptotic with singularities corresponding to competing modes.

Step 3: Running parameters. The exponent β is determined by the self-similar ansatz. Extended space includes mode weights selecting among solutions.

Step 4: Selection principle. Mass conservation: $\alpha = d\beta$. Self-consistency: $\beta(md + 2 - d) = 1$. Result:

$$\beta = \frac{1}{d(m - 1) + 2} \tag{280}$$

The physical mode is selected by boundary conditions (finite mass, compact support).

Step 5: Fixed points and stability. The Barenblatt profile is the unique stable self-similar attractor. Other self-similar modes exist but are unstable.

Step 6: Physical prediction. The late-time density profile:

$$\rho(x,t) = \frac{1}{t^\alpha}\left[C - \frac{(m-1)}{4md}\frac{|x|^2}{(Dt)^{2\beta}}\right]_+^{1/(m-1)} \tag{281}$$

This is exact for the PME. More general nonlinear diffusion would require resummation.

When to Trust Perturbation Theory

The unified framework includes both perturbative and non-perturbative physics, but in many practical situations perturbation theory alone is sufficient.

Conditions for Perturbative Accuracy

Perturbation theory gives accurate answers when the coupling is small ($\epsilon \ll 1$), no Stokes lines are crossed in the physical region, and we stay near a perturbative fixed point.

Perturbation theory works when you're far from Stokes lines and close to a perturbative fixed point with small coupling.

Under these conditions, the exponentially suppressed transseries corrections $e^{-S/\epsilon}$ are genuinely negligible. Computing to order ϵ^n gives accuracy $O(\epsilon^{n+1})$ as expected.

When Full Analysis Is Required

The full resurgent analysis becomes necessary when the coupling is not small, Stokes lines are crossed (e.g., analytic continuation in parameters), we approach non-perturbative fixed points, or ambiguities must cancel for physical predictions.

In these situations, truncating the perturbative series can give qualitatively wrong answers. The transseries structure is essential.

The Oscillator at Strong Coupling

For the anharmonic oscillator at large $\lambda A^2/\omega_0^2$, perturbation theory breaks down. The frequency correction is no longer well-approximated by the leading term. Resummation of the full series, including proper treatment of Stokes phenomena, is required for accurate predictions.

Critical Phenomena

Near critical points (phase transitions), fluctuations are large and perturbation theory in the original couplings fails. However, the epsilon expansion around $d = 4$ can be perturbative in ϵ. Even then, accurate exponents at $\epsilon = 1$ (3D) require resummation.

Common Pitfalls

Several common errors can derail an RG analysis.

Ignoring Divergence Structure

Treating perturbative series as convergent and simply truncating at some order ignores the information encoded in the divergence pattern. For asymptotic series, optimal truncation (stopping at the smallest term) gives exponentially small error, but not the full answer.

Ignoring divergence structure throws away non-perturbative information encoded in the pattern of coefficients.

Missing Stokes Lines

When continuing analytically in parameters (complex coupling, etc.), Stokes lines may be crossed. Ignoring the resulting jumps in transseries parameters leads to wrong answers in the new region.

Confusing Scheme Dependence with Physics

Beta functions and anomalous dimensions are scheme-dependent. Only scheme-independent quantities (critical exponents, Stokes constants, physical observables) are meaningful. Comparing beta functions in different schemes without accounting for the scheme transformation is a common error.

Overlooking Non-Perturbative Fixed Points

If only perturbative fixed points are sought, non-perturbative ones are missed. For some problems, the physically relevant fixed point may be non-perturbative.

The Three Examples in Perspective

The three canonical examples were chosen to illustrate different aspects of the unified framework.

The anharmonic oscillator is the simplest example and suffices to demonstrate secular terms and running parameters, the resolution via RG equations, Gevrey-1 divergence and the Borel plane, and the basic transseries structure.

It is too simple for non-trivial fixed points, operator mixing or anomalous dimensions, and statistical RG with coarse-graining.

The three examples form a ladder: oscillator → field theory → PDE. Each adds capabilities the previous lacked.

The 1D ϕ^4 theory adds non-trivial beta functions with multiple couplings, the Gaussian fixed point and its stability, renormalon singularities from RG running, and statistical mechanics interpretation.

It is still too simple for non-trivial interacting fixed points (which require $d < 4$) and anomalous dimensions.

The porous medium equation adds anomalous dimensions (second-kind self-similarity), non-trivial scaling exponents from dynamics, Wasserstein gradient flow structure, and selection principles for physical solutions.

Together, the three examples demonstrate the complete framework. Any new problem will share features with one or more of these examples, and the techniques transfer accordingly.

Transition to Part II

Part I has developed the theoretical framework. Part II applies it to specific physical systems.

Each application chapter will use the six-step recipe and identify scales, set up perturbation theory with Borel analysis, find running parameters including transseries, derive beta functions and flow equations, analyze fixed points and universality, and extract physical predictions with proper resummation.

Part II applications: each physical system analyzed using the unified recipe developed in Part I.

The applications span diverse areas including chaotic dynamics (Lorenz system), fluid mechanics (Navier-Stokes), solid mechanics (fracture), statistical mechanics (Ising, O(N) models), quantum field theory (QED), and condensed matter (Hubbard model).

In each case, the unified geometric-resurgent perspective reveals structure that would be invisible to purely perturbative analysis.

Summary of Part I

The renormalization group is a framework for analyzing systems with scale hierarchy. Parameters that appear constant become scale-dependent when we properly handle secular terms, divergences, or boundary mismatches.

Perturbation series diverge with Gevrey-1 structure. The Borel transform converts factorial growth to geometric, revealing singularities that encode non-perturbative physics (instantons, renormalons).

The transseries $\tilde{f}(g,\sigma) = f_0(g) + \sum_n \sigma^n e^{-nS/g} f_n(g)$ is the complete solution including all non-perturbative sectors.

Parameter space is a manifold with coordinates (g^a, σ^n) combining perturbative couplings and transseries parameters. It has metric and connection structure.

The beta function $\boldsymbol{\beta}$ is the generator of scale transformations. Fixed points satisfy $\beta = 0$ and can be perturbative or non-perturbative.

Stokes phenomena are monodromy in the extended parameter space. The alien derivative is a covariant derivative probing non-perturbative directions.

The unified recipe:

1. Identify scales and divergence structure
2. Set up perturbation theory and Borel transform
3. Identify running parameters including transseries
4. Derive full beta functions with Stokes consistency
5. Analyze flow in extended space
6. Extract physics via median resummation

The three examples demonstrate the framework: The oscillator shows secular terms and running parameters. The ϕ^4 theory shows beta functions and fixed points. The PME shows anomalous dimensions.

Part II

Applications

Chaotic Dynamics: The Lorenz System

The Lorenz system provides our first extended application of the RG framework developed in Part I. This chapter demonstrates how the five-step recipe of Chapter I applies to chaotic dynamical systems. Originally derived as a simplified model of atmospheric convection, the Lorenz equations exhibit multi-scale behavior that makes them a natural testing ground for RG methods.

We will proceed through the recipe systematically. Step 1 identifies the temporal scale hierarchy created by the parameter σ, which separates fast velocity relaxation from slow temperature evolution. Step 2 defines coarse-graining through the slow manifold reduction. Step 3 constructs a theory space parametrized by the control parameters σ, ρ, and β. Step 4 derives the beta functions for slowly varying amplitudes near bifurcation points. Step 5 analyzes the fixed-point landscape, including both the simple fixed points of the flow and the strange attractor viewed as a "fixed set."

The Lorenz system was one of the first examples of deterministic chaos, demonstrating that simple equations can produce infinitely complex behavior.

The Lorenz Equations

The Lorenz system consists of three coupled ordinary differential equations:

$$\dot{x} = \sigma(y - x), \tag{282}$$

$$\dot{y} = x(\rho - z) - y, \tag{283}$$

$$\dot{z} = xy - \beta z. \tag{284}$$

Here x represents the intensity of convective motion, y the temperature difference between ascending and descending currents, and z the deviation of the vertical temperature profile from linearity. The parameters are the Prandtl number σ, the reduced Rayleigh number ρ, and a geometric factor β.

The classic Lorenz values $\sigma = 10$, $\rho = 28$, $\beta = 8/3$ produce the famous butterfly-shaped strange attractor.

Scale Identification

Following Step 1 of the recipe, we identify the scales in the Lorenz system. The system contains multiple time scales whose separation

is controlled by the parameter σ. This ratio compares the relaxation rates of velocity and temperature: when $\sigma \gg 1$, the variable x adjusts rapidly to y, creating a slow manifold on which the effective dynamics is lower-dimensional.

The parameter ρ sets the driving strength and determines the amplitude scales of the motion. Near $\rho = 1$, convection just begins and the motion has small amplitude. As ρ increases, the amplitude of motion grows, and qualitative changes in dynamics occur through bifurcations.

We take $s = \ln t$ as our scale parameter, examining how the effective dynamics changes when we coarse-grain over different time windows. The separation of scales required for RG analysis is present when $\sigma \gg 1$, allowing us to average over the fast relaxation of x to obtain effective equations for the slow variables.

Fixed Points and Their Stability

The fixed points of the Lorenz system, where $\dot{x} = \dot{y} = \dot{z} = 0$, correspond to steady states of convection.

The Origin

The trivial fixed point $(x^*, y^*, z^*) = (0, 0, 0)$ represents the conductive state with no fluid motion. The stability matrix (equation **??**) at the origin is

$$B = \begin{pmatrix} -\sigma & \sigma & 0 \\ \rho & -1 & 0 \\ 0 & 0 & -\beta \end{pmatrix}. \tag{285}$$

The eigenvalues are $\lambda_1 = -\beta$ and

$$\lambda_{2,3} = \frac{-(\sigma+1) \pm \sqrt{(\sigma+1)^2 + 4\sigma(\rho-1)}}{2}. \tag{286}$$

The onset of convection at $\rho = 1$ is a pitchfork bifurcation, the fluid analog of a ferromagnetic phase transition.

For $\rho < 1$, all eigenvalues are negative, and the origin is stable. At $\rho = 1$, one eigenvalue crosses zero, signaling the onset of convection. This is precisely analogous to the relevant operator crossing zero at the Gaussian fixed point in ϕ^4 theory (Chapter I).

The Convective Fixed Points

For $\rho > 1$, two symmetric fixed points appear:

$$C^{\pm} = (\pm\sqrt{\beta(\rho-1)}, \pm\sqrt{\beta(\rho-1)}, \rho - 1). \tag{287}$$

These represent steady convection rolls rotating in opposite directions.

The stability analysis at $C^{\pm}$ gives eigenvalues that become complex for large enough σ, indicating oscillatory approach to the fixed point. At the critical value

$$\rho_c = \sigma \frac{\sigma + \beta + 3}{\sigma - \beta - 1} \tag{288}$$

a Hopf bifurcation occurs, and the fixed points become unstable.

The Strange Attractor as a "Fixed Set"

For $\rho > \rho_c$, the system exhibits chaotic motion on a strange attractor. While not a fixed point in the traditional sense, the attractor can be viewed as a "fixed set" under the RG in an appropriate sense.

Invariant Measure

The strange attractor supports an invariant probability measure μ that describes the statistical distribution of trajectories in the long-time limit. This measure is the analog of the fixed-point theory in QFT.

The invariant measure on the attractor plays the role of the fixed-point correlation functions in field theory.

Physical quantities computed with respect to μ are independent of initial conditions and represent the "universal" properties of the chaotic state. The Lyapunov exponents, fractal dimension, and correlation functions are all defined with respect to this measure.

Lyapunov Exponents as Scaling Dimensions

The Lyapunov exponents λ_i characterize the rate of separation of nearby trajectories:

$$|\delta \mathbf{x}(t)| \sim e^{\lambda_{\max} t} |\delta \mathbf{x}(0)|. \tag{289}$$

These exponents play a role analogous to scaling dimensions at a fixed point. Just as the eigenvalues of the stability matrix classify operators as relevant or irrelevant, the Lyapunov exponents classify perturbations to trajectories. A positive exponent indicates an exponentially growing perturbation, analogous to a relevant operator that drives the system away from a fixed point. A negative exponent indicates an exponentially decaying perturbation, analogous to an irrelevant operator whose effects wash out at long times. A zero exponent is marginal and corresponds to motion along the trajectory itself.

For the Lorenz attractor, there is one positive, one zero, and one negative Lyapunov exponent. The positive exponent is responsible for sensitive dependence on initial conditions—the hallmark of chaos. The zero exponent reflects the continuous time translation symmetry. The negative exponent corresponds to the contraction of phase space volume that makes the attractor a set of measure zero.

RG for Slow Variables

The RG approach to the Lorenz system focuses on the slow variables that emerge when there is a separation of time scales.

The Slow Manifold

When $\sigma \gg 1$, the variable x rapidly equilibrates to y. On time scales long compared to $1/\sigma$, the dynamics effectively reduces to the slow manifold defined by $x = y$.

The slow manifold is the invariant manifold that survives coarse-graining over fast time scales.

To derive the reduced dynamics, we use the multiple scales method. We write

$$x = y + \epsilon x_1 + \epsilon^2 x_2 + \cdots \tag{290}$$

where $\epsilon = 1/\sigma$, and require that secular terms vanish.

At leading order, the slow dynamics on the manifold is

$$\dot{y} = y(\rho - 1 - z), \tag{291}$$

$$\dot{z} = y^2 - \beta z. \tag{292}$$

Beta Functions for Amplitude

Following the analysis of the anharmonic oscillator in Chapter I, we can derive beta functions for slowly varying amplitudes. Near the onset of chaos, the amplitude A of oscillations around the unstable fixed points evolves according to

$$\frac{\mathrm{d}A}{\mathrm{d}s} = \lambda A - \kappa A^3 + \cdots \tag{293}$$

where $\lambda > 0$ near the Hopf bifurcation and $\kappa > 0$ is a nonlinear saturation coefficient.

This amplitude equation has the same structure as the RG flow for ϕ^4 theory, where the coupling runs as $\mathrm{d}g/\mathrm{d}s = -\epsilon g + cg^2$. The fixed point $A^* = \sqrt{\lambda/\kappa}$ corresponds to the limit cycle amplitude.

Universality and Critical Phenomena

The Lorenz system exhibits features analogous to critical phenomena in equilibrium statistical mechanics.

Routes to Chaos

Several universal routes to chaos have been identified, each with its own characteristic scaling behavior. The period-doubling cascade, discovered independently by Feigenbaum and Coullet-Tresser, exhibits

universal scaling ratios as successive bifurcations accumulate. Intermittency routes involve alternation between regular and chaotic behavior, with power-law statistics for the duration of regular episodes. The quasiperiodicity route, analyzed by Ruelle, Takens, and Newhouse, shows how three incommensurate frequencies can produce strange attractors.

Each route has universal scaling exponents independent of the specific equations. This universality arises because different systems can flow to the same "strange attractor fixed point" under coarse-graining. The specific route determines which fixed point is relevant, but within each universality class the scaling behavior is identical.

Feigenbaum's discovery of universal scaling in period-doubling cascades was one of the great triumphs of the RG approach to dynamical systems.

Feigenbaum Universality

In the period-doubling route, the parameter values ρ_n where the nth period-doubling occurs satisfy

$$\lim_{n\to\infty} \frac{\rho_n - \rho_{n-1}}{\rho_{n+1} - \rho_n} = \delta = 4.669\ldots \tag{294}$$

where δ is the Feigenbaum constant. This number is universal across all unimodal maps undergoing period-doubling.

The RG explanation is that the period-doubling accumulation point is a fixed point of a functional RG transformation, and δ is determined by the relevant eigenvalue of the linearization around this fixed point.

The Chaos–Phase Transition Analogy

The analogy between the onset of chaos and equilibrium phase transitions runs deep. Table 1 summarizes the correspondence:

Statistical Mechanics	**Dynamical Systems**
Spatial position $z_j = ja$	Time $t_j = j\tau$
Spin configuration $[s]$	Trajectory $[x]$
Boltzmann–Gibbs distribution	Invariant measure m_μ
Dimensionless Hamiltonian $\mathcal{H}$	Evolution map f_μ
Control parameter $K = \beta J$	Nonlinearity parameter μ
Correlation length ξ	Characteristic time τ
Thermodynamic limit $N \to \infty$	Asymptotic dynamics $T \to \infty$
Order parameter $\langle s \rangle$	Lyapunov exponent $L(\mu)$
Critical point K_c	Onset of chaos μ_c

Table 1: Correspondence between equilibrium statistical mechanics and the transition to chaos.

The Lyapunov exponent $L(\mu)$ plays the role of an order parameter for the transition to chaos. In the regular phase ($\mu < \mu_c$), $L \leq 0$ and nearby trajectories converge or stay bounded. In the chaotic phase

The Lyapunov exponent $L(\mu)$ serves as the order parameter for chaos: $L > 0$ in the chaotic phase, $L \leq 0$ in the regular phase.

($\mu > \mu_c$), $L > 0$ and trajectories diverge exponentially. Near the transition, the smoothed Lyapunov exponent exhibits power-law scaling:

$$\bar{L}(\mu) \sim (\mu - \mu_c)^{\beta} \quad \text{for } \mu > \mu_c \tag{295}$$

with a universal exponent β determined by the specific route to chaos.

Critical slowing down in chaos: the characteristic time $\tau(\mu) \sim |\mu - \mu_c|^{-\nu}$ diverges as the system approaches the transition.

Just as the correlation length ξ diverges at a thermodynamic critical point, the characteristic time $\tau(\mu)$ diverges at the onset of chaos:

$$\tau(\mu) \sim |\mu - \mu_c|^{-\nu} \tag{296}$$

This is the dynamical analog of critical slowing down. Near the transition, the system takes longer and longer to settle into its asymptotic behavior, whether that behavior is periodic or chaotic. The exponent ν is related to the Feigenbaum constant by $\nu = \ln 2 / \ln \delta$.

This correspondence extends to the RG structure itself. Just as the Ising model's RG acts on spin-block Hamiltonians, the period-doubling RG acts on the space of unimodal maps. The fixed-point map φ^* satisfying $R\varphi^* = \varphi^*$ (where R is the doubling transformation) is the analog of the Ising critical Hamiltonian. The universal exponent δ emerges from the relevant eigenvalue of $DR(\varphi^*)$, exactly paralleling how critical exponents emerge from eigenvalues at the Wilson–Fisher fixed point.

Connection to the Geometric Framework

We now explicitly connect the Lorenz dynamics to the geometric framework of Part I.

Theory Space for Lorenz

The "theory space" for the Lorenz system is the three-dimensional parameter space (σ, ρ, β). Points in this space correspond to different physical systems (different fluid properties or geometries).

The RG flow on this space describes how the effective parameters change as we coarse-grain. For the amplitude equation (293), the flow is

$$\frac{\mathrm{d}\lambda}{\mathrm{d}s} = 2\lambda - \text{nonlinear corrections} \tag{297}$$

indicating that λ is a relevant parameter near the trivial fixed point.

Metric from Fluctuations

By analogy with the Zamolodchikov metric (equation **??**), we can define a metric on parameter space from the fluctuations in physical observables:

$$G_{\mu\nu} = \langle \delta O_\mu \, \delta O_\nu \rangle \tag{298}$$

where O_μ is the observable conjugate to parameter μ and the average is over the invariant measure.

This metric encodes the sensitivity of the chaotic dynamics to parameter changes and provides a natural distance function on the space of Lorenz systems.

Summary

The Lorenz system demonstrates how the five-step RG recipe applies to chaotic dynamics. We identified the temporal scale hierarchy created by large σ (Step 1) and defined coarse-graining through slow manifold reduction (Step 2). The theory space is parametrized by the control parameters σ, ρ, and β (Step 3). The beta functions for slowly varying amplitudes, equation (293), describe the evolution near bifurcation points (Step 4). The fixed-point analysis (Step 5) revealed both simple fixed points of the flow and the strange attractor as a "fixed set" with invariant measure.

The correspondence between dynamical systems and the RG is systematic. Fixed points of the ODE map to fixed points of the RG flow. The strange attractor supports an invariant measure analogous to a fixed-point theory. Lyapunov exponents play the role of scaling dimensions, classifying perturbations as relevant, irrelevant, or marginal. Slow manifold reduction is the dynamical analog of integrating out irrelevant operators, producing effective equations for the slow variables alone.

The key equations from Part I that we invoked include the stability matrix for fixed point analysis, the envelope method for slow manifold reduction, and the amplitude equation (293) which takes the same form as the beta function for ϕ^4 theory. Universal routes to chaos arise from RG fixed points with universal eigenvalues, explaining why systems as different as the Lorenz equations and the logistic map share the same Feigenbaum scaling constants. This application demonstrates that the geometric RG framework extends naturally beyond equilibrium statistical mechanics to dissipative dynamical systems.

Turbulence and Fluid Dynamics

Fluid turbulence represents one of the most spectacular manifestations of scale hierarchy in physics. Energy injected at large scales cascades through an inertial range before being dissipated at small scales. The RG provides the natural language for describing this multi-scale structure, and this chapter applies the five-step recipe of Chapter I to the Navier-Stokes and Burgers equations.

The scale hierarchy (Step 1) ranges from the integral scale L of energy injection down to the Kolmogorov scale η of viscous dissipation, with the Reynolds number measuring the separation. Coarse-graining (Step 2) integrates out velocity fluctuations at successively smaller scales while adjusting the effective viscosity. Theory space (Step 3) is parametrized by the effective viscosity and forcing spectrum. The beta functions (Step 4) describe the scale dependence of these effective parameters. Fixed-point analysis (Step 5) identifies the Kolmogorov scaling as a fixed point, with intermittency corrections arising from anomalous dimensions. Throughout, we make essential contact with Barenblatt's theory of intermediate asymptotics.

Turbulence involves fluctuations over a vast range of scales, making it a perfect arena for RG methods.

The Navier-Stokes Equations

The incompressible Navier-Stokes equations describe the motion of a viscous fluid:

$$\frac{\partial \mathbf{u}}{\partial t} + (\mathbf{u} \cdot \nabla)\mathbf{u} = -\frac{1}{\rho}\nabla p + \nu \nabla^2 \mathbf{u} + \mathbf{f}, \tag{299}$$

$$\nabla \cdot \mathbf{u} = 0. \tag{300}$$

Here $\mathbf{u}(\mathbf{x}, t)$ is the velocity field, p the pressure, ρ the density, ν the kinematic viscosity, and $\mathbf{f}$ an external forcing.

Scale Identification

Following Step 1 of the recipe, we identify the key scales. The integral scale L characterizes the largest eddies where energy is injected, typically set by the geometry of the flow or the forcing mechanism.

The Kolmogorov scale $\eta = (\nu^3/\varepsilon)^{1/4}$ characterizes the smallest eddies where viscous dissipation dominates, with ε the energy dissipation rate per unit mass.

The corresponding velocity scales are the large-scale velocity U at the integral scale and the Kolmogorov velocity $u_\eta = (\nu\varepsilon)^{1/4}$ at the dissipation scale. The Reynolds number $Re = UL/\nu$ measures the scale separation: for $Re \gg 1$, there is a wide inertial range $\eta \ll r \ll L$ where neither injection nor dissipation dominates. It is in this inertial range that universal scaling behavior emerges.

The Reynolds number is the control parameter analogous to ρ in the Lorenz system or inverse temperature in statistical mechanics.

Kolmogorov Theory as an RG Fixed Point

Kolmogorov's 1941 theory posits that in the inertial range, the statistics of turbulence are universal and determined only by the energy dissipation rate ε.

Dimensional Analysis

By dimensional analysis, the structure function (velocity increment moments) must scale as

$$S_n(r) = \langle |\mathbf{u}(\mathbf{x}+\mathbf{r}) - \mathbf{u}(\mathbf{x})|^n \rangle \sim (\varepsilon r)^{n/3}. \tag{301}$$

This is a prediction of scale-invariant behavior, precisely what we expect at an RG fixed point (Chapter I).

Fixed Point Interpretation

In the RG language, the Kolmogorov scaling (301) corresponds to a fixed point where the effective parameters of the theory remain constant under scale change. The scaling exponent $\zeta_n = n/3$ is the analog of the scaling dimension at a CFT fixed point.

Deviations from K41 scaling, called intermittency corrections, indicate that the Kolmogorov fixed point is not exact.

The RG transformation for turbulence proceeds in three stages. First, we integrate out velocity fluctuations at scales below some cutoff ℓ, eliminating the small-scale eddies from the explicit description. Second, we rescale space by $\mathbf{x} \to s\mathbf{x}$ and velocity by $\mathbf{u} \to s^h\mathbf{u}$ where the exponent h must be determined. Third, we adjust the effective viscosity to maintain the dynamical equations in their original form. At the fixed point, the effective viscosity reaches a scale-invariant value, and the scaling exponent $h = 1/3$ follows from dimensional analysis with constant ε.

The Burgers Equation

The Burgers equation provides a simpler model that captures essential features of turbulence:

$$\frac{\partial u}{\partial t} + u\frac{\partial u}{\partial x} = \nu\frac{\partial^2 u}{\partial x^2}. \tag{302}$$

Self-Similar Solutions

The Burgers equation admits self-similar solutions of the form

$$u(x,t) = t^{-\alpha} f(\xi), \quad \xi = x/t^{\beta} \tag{303}$$

where α and β are scaling exponents determined by requiring that the similarity ansatz solve the equation.

Self-similar solutions are the hallmark of intermediate asymptotics, describing behavior far from both initial conditions and final equilibrium.

Substituting into (302) gives constraints on the exponents. For the inviscid limit $\nu \to 0$, we find $\alpha = \beta = 1/2$ (first kind self-similarity). With viscosity, anomalous dimensions can appear.

Connection to Intermediate Asymptotics

Following Barenblatt [1], self-similar solutions arise in the "intermediate asymptotic" regime where the solution has forgotten initial conditions but has not yet reached final equilibrium.

[1] G. I. Barenblatt. *Similarity, Self-Similarity, and Intermediate Asymptotics*. Consultants Bureau, New York, 1979

The RG interpretation is direct: intermediate asymptotics corresponds to the RG flow approaching a fixed point. The self-similar exponents are scaling dimensions at this fixed point. First-kind similarity (where exponents follow from dimensional analysis) corresponds to a classical fixed point, while second-kind similarity (with anomalous exponents) corresponds to a nontrivial quantum/fluctuation-corrected fixed point.

RG for Navier-Stokes

Several approaches apply RG to the Navier-Stokes equations.

Yakhot-Orszag ε-Expansion

Inspired by the Wilson-Fisher ε-expansion for critical phenomena (Chapter II), Yakhot and Orszag developed an RG approach to forced Navier-Stokes turbulence. Their key insight was that the forcing power spectrum provides a tunable parameter analogous to $\varepsilon = 4 - d$ in scalar field theory.

The forcing is taken to have power-law spectrum $\sim k^y$ where y is varied as a control parameter (analogous to $\varepsilon = 4 - D$ in ϕ^4 theory).

The RG flow equations for the effective viscosity ν and forcing amplitude D_0 are:

$$\frac{\mathrm{d}\nu}{\mathrm{d}s} = \nu\left[z - 2 + \frac{AD_0}{\nu^3} + \cdots\right], \tag{304}$$

$$\frac{\mathrm{d}D_0}{\mathrm{d}s} = D_0\left[y + 4 - 2z + \cdots\right], \tag{305}$$

where z is the dynamic exponent and A is a calculable constant.

At the fixed point, these equations give Kolmogorov-like scaling with computable corrections.

Box 10.1: Derivation of the Yakhot-Orszag Beta Functions

Setup: The Navier-Stokes equation in Fourier space with random forcing $\mathbf{f}$ having correlation $\langle f_i(\mathbf{k}) f_j(\mathbf{k}')\rangle = D_0 k^y P_{ij}(\mathbf{k})\delta(\mathbf{k}+\mathbf{k}')$, where P_{ij} is the transverse projector.

Step 1 (Dimensional analysis): The viscosity has dimensions $[\nu] = L^2/T$, so ν scales as ℓ^{2-z} under $x \to \ell x$, $t \to \ell^z t$. The forcing amplitude has $[D_0] = L^{4-y}/T^3$, so $D_0 \to \ell^{4-y-2z} D_0$.

Step 2 (Coarse-graining): Integrate out velocity modes with $|\mathbf{k}| > \Lambda/b$ where $b > 1$. The key one-loop diagram is:

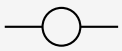

(tadpole) (306)

Step 3 (Loop integral): The one-loop correction to the effective viscosity is:

$$\delta\nu = -A\int_{\Lambda/b}^{\Lambda} \frac{d^d k}{(2\pi)^d} \frac{D_0 k^y}{k^2 \cdot (k^2+\nu k^2)^2} \approx \frac{AD_0\Lambda^{y-2}}{\nu^2}\ln b \tag{307}$$

where A is a geometric factor from the angular integration.

Step 4 (Beta functions): Taking $b = e^{ds}$ and combining with dimensional scaling:

$$\beta_\nu = (z-2)\nu + \frac{AD_0}{\nu^2\Lambda^{2-y}} \tag{308}$$

$$\beta_{D_0} = (y+4-2z)D_0 \tag{309}$$

Fixed point: Setting $\beta_{D_0} = 0$ determines $z = (y+4)/2$. For Kolmogorov turbulence with constant energy flux, $y = 4$ gives $z = 4$, which is modified by the viscosity correction to yield $z \approx 2$ (the Kolmogorov result $u \sim r^{1/3}$ comes from $h = 1/z$).

Physical interpretation: The fixed point represents the balance between energy injection at large scales and dissipation at small scales. The anomalous corrections come from the nonlinear mode coupling.

Functional RG

The functional RG approach can also be applied to turbulence. This nonperturbative method defines an effective action $\Gamma_k[\mathbf{u}]$ that incorporates fluctuations at scales larger than $1/k$. The Wetterich equation describes its flow:

$$\frac{\partial \Gamma_k}{\partial s} = \frac{1}{2}\mathrm{Tr}\left[\left(\Gamma_k^{(2)} + R_k\right)^{-1}\frac{\partial R_k}{\partial s}\right] \tag{310}$$

where $s = \ln(k_0/k)$ and R_k is the regulator.

The functional RG provides a nonperturbative approach that can handle strong fluctuations.

Energy Cascade and Irreversibility

Turbulence exhibits a characteristic irreversible flow of energy from large to small scales.

Energy Flux

In the inertial range, energy is transferred from scale to scale at a constant rate ε. This cascade is described by the Kármán-Howarth equation:

$$\frac{\partial}{\partial t}\langle u^2\rangle = -\frac{2}{r}\frac{\partial}{\partial r}(r^2\varepsilon_r) + 2\nu\nabla^2\langle u^2\rangle \tag{311}$$

where ε_r is the energy flux at scale r.

Connection to the c-Theorem

The monotonic decrease of energy to small scales is analogous to the c-theorem in conformal field theory. We can define an "enstrophy" (mean-square vorticity in 2D) or other quantities that decrease monotonically along the RG flow.

In 2D turbulence, there is additionally an inverse cascade of energy to large scales, while enstrophy cascades to small scales. This dual cascade structure reflects the additional conserved quantity in 2D.

The energy cascade implements irreversibility in turbulence, just as the c-function decrease implements irreversibility in QFT.

Intermittency and Anomalous Dimensions

Experimental measurements show systematic deviations from K41 scaling:

$$S_n(r) \sim r^{\zeta_n}, \quad \zeta_n \neq n/3. \tag{312}$$

These deviations, called intermittency, indicate that the simple Kolmogorov fixed point does not capture the full physics.

Multifractal Models

The deviation $\Delta_n = \zeta_n - n/3$ represents anomalous dimensions arising from the multi-scale structure of dissipation. Various phenomenological models (log-normal, She-Leveque, etc.) parameterize these corrections.

Intermittency corrections are the turbulent analog of anomalous dimensions in critical phenomena.

RG Interpretation

From the RG viewpoint, intermittency arises because the Kolmogorov fixed point has relevant or marginally relevant perturbations. The flow does not exactly reach the fixed point, and corrections to scaling appear.

This is analogous to the situation in ϕ^4 theory where the Wilson-Fisher fixed point has corrections from irrelevant operators that give subleading scaling behavior.

Application: Shock Waves in Burgers

As a concrete application, consider shock formation in the inviscid Burgers equation.

Method of Characteristics

The inviscid Burgers equation $u_t + uu_x = 0$ can be solved by characteristics. For smooth initial data $u(x, 0) = u_0(x)$, the solution develops shocks in finite time when characteristics cross.

Intermediate Asymptotics

After shock formation, the solution enters an intermediate asymptotic regime where the specific initial conditions are forgotten but the overall structure of shocks persists.

The similarity solution for a single shock is

$$u(x, t) = \frac{x}{t} \tag{313}$$

for $|x| < s(t)$ where $s(t)$ is the shock position. This is a self-similar solution of the first kind.

Viscous Corrections

With small viscosity $\nu > 0$, the shock has finite width $\sim \nu/\Delta u$ where Δu is the velocity jump. The shock structure is

$$u(x, t) = \frac{u_L + u_R}{2} - \frac{\Delta u}{2} \tanh\left(\frac{\Delta u (x - st)}{4\nu}\right) \tag{314}$$

where u_L, u_R are the velocities on either side and $s = (u_L + u_R)/2$ is the shock speed.

The shock width $\sim \nu$ is the dissipation scale, analogous to the Kolmogorov scale η in turbulence.

This solution illustrates how small-scale physics (viscosity) regularizes the large-scale dynamics (shock), precisely the multi-scale structure that the RG is designed to handle.

Connection to the Geometric Framework

We now make explicit the connection to Part I.

Theory Space for Fluids

The couplings that parametrize theory space for fluid dynamics include the viscosity ν (or equivalently the Reynolds number Re), parameters characterizing the forcing spectrum such as its amplitude and spatial structure, and any additional dimensionless parameters that enter the problem. For homogeneous isotropic turbulence with power-law forcing, the essential parameters reduce to the effective viscosity and the forcing exponent.

The RG flow describes how the effective viscosity changes as we coarse-grain:

$$\frac{d\nu_{\text{eff}}}{ds} = \beta_\nu(\nu_{\text{eff}}, \ldots). \tag{315}$$

At the Kolmogorov fixed point, $\beta_\nu = 0$ and the effective viscosity has reached a scale-invariant value. The fixed-point theory describes the universal scaling behavior in the inertial range.

Self-Similarity from Equivariance

The self-similar solutions of Section II arise from the scale covariance requirement discussed in Chapter I. If the solution is to be independent of the arbitrary choice of length scale, it must take the self-similar form.

The scaling exponents emerge as eigenvalues of the RG transformation, exactly as in Chapter I.

Summary

This chapter has applied the five-step RG recipe to turbulence and fluid dynamics. The scale hierarchy (Step 1) spans from the integral scale L to the Kolmogorov scale η, with the Reynolds number measuring the separation. Coarse-graining (Step 2) integrates out velocity fluctuations while rescaling space and adjusting the effective viscosity. Theory space (Step 3) is parametrized by the effective viscosity and forcing spectrum. The beta functions (Step 4) from the Yakhot-Orszag analysis describe the scale dependence of these effective parameters.

Fixed-point analysis (Step 5) identifies Kolmogorov scaling as a fixed point.

The RG perspective reveals Kolmogorov scaling as fixed-point behavior, with structure function exponents playing the role of scaling dimensions. Intermittency corrections are anomalous dimensions arising from the multi-scale structure of dissipation. Self-similar solutions of the Burgers equation exemplify fixed-point structure in its simplest form. The energy cascade, transferring energy monotonically from large to small scales, is an irreversible RG flow analogous to the c-theorem in two-dimensional field theory. Barenblatt's intermediate asymptotics provides the physical interpretation of approach to a fixed point.

This chapter demonstrates that the geometric RG framework unifies the treatment of turbulence with critical phenomena, revealing the deep mathematical connections between fluid dynamics and statistical physics. The same five-step recipe that organized the anharmonic oscillator and Lorenz equations applies equally well to the Navier-Stokes equations, despite the enormous increase in complexity.

Scaling in Solid Mechanics

Continuum mechanics provides a rich arena for the renormalization group, with phenomena ranging from the stress singularities at crack tips to the scaling laws governing fatigue failure. This chapter applies the RG recipe to solid mechanics, focusing on two examples that exemplify self-similar solutions of the second kind: the elastic wedge under concentrated loading and fatigue crack growth under cyclic loading. In both cases, dimensional analysis alone cannot determine the critical exponents, which must instead emerge from the dynamics through an eigenvalue problem analogous to computing anomalous dimensions in field theory.

The connection between fracture mechanics and the RG was anticipated by Barenblatt's work on intermediate asymptotics, though the geometric interpretation developed here is more recent.

Step 1: Scale Hierarchy in Elastic Bodies

The mechanical behavior of solids exhibits multiple characteristic scales that interact in ways amenable to RG analysis. These scales emerge from the geometry of the body, the applied loading, and the material properties.

Geometric and Material Scales

An elastic body under load exhibits behavior that depends on several length scales. The overall dimensions of the body set a macroscopic scale L. Geometric features such as cracks, notches, or corners introduce intermediate scales. At the microscopic level, the material itself has a characteristic scale a related to grain size, dislocation spacing, or atomic structure.

The separation between macroscopic and microscopic scales is what makes continuum mechanics possible. The RG connects these scales systematically.

When a sharp crack of length c exists in a body, the crack tip introduces a stress singularity. The region very close to the tip, at distances $r \ll c$, sees only the local geometry and loading. The region far from the tip, at distances $r \gg c$, responds to the overall elastic field. The ratio c/a measures how many decades separate the continuum description from the atomic scale where the singularity must be cut off.

The Elastic Wedge Problem

Consider an elastic body in the shape of a wedge with internal angle 2α, subject to a concentrated force at the apex. The distance r from the apex serves as the scale parameter. Very close to the apex ($r \to 0$), the stress field exhibits a power-law singularity whose exponent depends on the wedge angle and the type of loading.

Dimensional analysis suggests that the stress components should scale as $\sigma_{ij} \sim Fr^{-\lambda}$ where F is the applied force and λ is an exponent. For a half-space ($\alpha = \pi$), the classical solution gives $\lambda = 1$. But for general wedge angles, dimensional analysis cannot determine λ; it must be computed from the equations of elasticity. This is the signature of a self-similar solution of the second kind.

The Fatigue Crack Problem

A different scale hierarchy appears in fatigue crack growth. Under cyclic loading, a crack advances incrementally with each load cycle. The crack growth rate $\mathrm{d}c/\mathrm{d}N$ (where N is the number of cycles) depends on the stress intensity factor range ΔK, which measures the amplitude of the singular stress field at the crack tip.

Fatigue failure is responsible for the majority of mechanical failures in engineering practice. Understanding its scaling is of considerable practical importance.

The characteristic scales are the crack length c, the specimen dimension L, the material's microstructural scale a, and the cyclic loading amplitude. In the intermediate asymptotic regime where $a \ll c \ll L$, the crack growth rate follows a power law independent of the specific details of the loading geometry. This universality is the hallmark of RG fixed-point behavior.

Step 2: Coarse-Graining in Elasticity

The coarse-graining procedure in solid mechanics differs from that in field theory but serves the same purpose: eliminating short-distance structure to obtain an effective description at longer scales.

Similarity Transformations

For self-similar problems, coarse-graining takes the form of a similarity transformation. We rescale distances by a factor b and ask how the fields must transform to preserve the governing equations. In elasticity, under $r \to br$ and $\theta \to \theta$, the displacement field transforms as

$$u_i(r, \theta) \to b^{\nu} u_i(r, \theta) \tag{316}$$

where the exponent ν must be determined.

The similarity exponent ν is the analogue of the scaling dimension in field theory. It must satisfy consistency conditions derived from the equations.

The stress and strain fields, being derivatives of displacement, transform as $\sigma_{ij} \to b^{\nu-1}\sigma_{ij}$. For the problem to admit a self-similar solution,

these transformation laws must be consistent with the equations of equilibrium, compatibility, and the boundary conditions.

The Elastic Wedge Analysis

For the elastic wedge, we seek solutions of the form

$$u_r(r,\theta) = r^\nu f(\theta), \qquad u_\theta(r,\theta) = r^\nu g(\theta) \tag{317}$$

where $f(\theta)$ and $g(\theta)$ are angular functions to be determined. Substituting into the equilibrium equations $\nabla \cdot \sigma = 0$ yields ordinary differential equations for f and g that depend parametrically on ν.

The boundary conditions on the wedge faces ($\theta = \pm\alpha$) select particular solutions. For stress-free faces, the angular functions must satisfy homogeneous conditions. A non-trivial solution exists only for discrete values of ν, determined by a transcendental eigenvalue equation involving α and the Poisson ratio.

Effective Description Near the Apex

The coarse-graining map in this context takes the elastic solution at scale r and relates it to the solution at scale br. The similarity ansatz (317) ensures that this relation is purely multiplicative: the field at scale br is b^ν times the field at scale r, with the same angular dependence.

This multiplicative structure is the hallmark of RG covariance. The "effective coupling" at each scale is encoded in the amplitude of the singular field, and the scaling exponent ν determines how this amplitude transforms. The angular functions $f(\theta)$ and $g(\theta)$ specify the "shape" of the fixed-point solution.

Step 3: Theory Space for Fracture

The theory space for fracture problems is parametrized by quantities that characterize the stress field near the crack tip or wedge apex. These play the role of couplings in the RG sense.

The Stress Intensity Factor

For a crack in a two-dimensional elastic body, the stress field near the tip takes the universal form

$$\sigma_{ij}(r,\theta) = \frac{K}{\sqrt{2\pi r}} f_{ij}(\theta) + O(r^0) \tag{318}$$

where K is the stress intensity factor and $f_{ij}(\theta)$ are universal angular functions that depend only on the loading mode (tensile, shear, or anti-plane). The stress intensity factor K is the single parameter that

characterizes the singular field, regardless of the overall geometry of the body or the detailed loading.

The stress intensity factor plays the role of a relevant coupling. Its value determines whether a crack will propagate.

In fracture mechanics terms, K is an "external" parameter determined by the far-field loading and geometry. But from the RG perspective, K is a coupling that runs with scale. The effective stress intensity at scale r is $K_{\text{eff}}(r) = K/\sqrt{r}$, which grows as we zoom in toward the crack tip.

Theory Space for the Wedge

For the elastic wedge, the theory space is more complex. Multiple singular modes may exist, each with its own exponent ν_n and amplitude A_n. The stress field is a superposition:

$$\sigma_{ij}(r,\theta) = \sum_n A_n r^{\nu_n - 1} g_{ij}^{(n)}(\theta). \tag{319}$$

The amplitudes A_n are the "couplings" of the problem, and the exponents ν_n are their scaling dimensions.

The most singular mode (smallest ν_n) dominates as $r \to 0$. Less singular modes become increasingly irrelevant at short distances, just as irrelevant operators in field theory decay under the RG flow. The fixed-point behavior is controlled by the leading singular mode.

Material Parameters

The material enters through elastic moduli (Young's modulus E, Poisson ratio ν) and, for fracture, through the fracture toughness K_c. In the linear elastic regime far from failure, these parameters are fixed and do not run with scale. Near the crack tip, however, nonlinear effects and microstructural details modify the effective material response.

The fracture toughness K_c represents a critical value of the stress intensity factor beyond which the crack propagates. It is determined by the energy required to create new fracture surface. The ratio K/K_c is the control parameter that determines whether the system is subcritical (stable crack) or critical (propagating crack).

Step 4: Beta Functions for Crack Growth

The beta function for fracture problems describes how the stress field or crack geometry evolves as we change scale or, equivalently, as time progresses during crack propagation.

Static Beta Function

For the elastic wedge under fixed loading, there is no dynamical evolution; the problem is static. The "beta function" in this case simply

encodes the scaling of the amplitude with distance from the apex:

$$\frac{\mathrm{d}\ln A}{\mathrm{d}\ln r} = \nu - 1. \tag{320}$$

The exponent $\nu - 1$ is the analogue of the anomalous dimension. When $\nu < 1$, the stress diverges at the apex, corresponding to a relevant perturbation that grows toward short distances.

Static problems have "trivial" beta functions that simply count the power-law exponent. The non-triviality enters through the eigenvalue determination of that exponent.

The Paris Law

For fatigue crack growth, the dynamical evolution is captured by the Paris law, an empirical relation between crack growth rate and stress intensity factor range:

$$\frac{\mathrm{d}c}{\mathrm{d}N} = C(\Delta K)^m \tag{321}$$

where C and m are material constants and ΔK is the range of stress intensity factor during a load cycle. The Paris exponent m typically lies between 2 and 4 for metals.

The Paris law is the statement that in the intermediate asymptotic regime, crack growth rate depends only on the local stress intensity, not on the details of specimen geometry or loading history. This universality is the signature of fixed-point behavior. The exponent m cannot be determined by dimensional analysis; it is an anomalous dimension arising from the microscopic physics of crack advance.

The Beta Function for Crack Length

Treating the crack length c as a dynamical variable and the number of cycles N as "time," the Paris law becomes a beta function:

$$\beta_c \equiv \frac{\mathrm{d}c}{\mathrm{d}N} = C(\Delta K)^m. \tag{322}$$

The stress intensity factor ΔK itself depends on c through the geometry of the specimen. For a center crack of length $2c$ in an infinite plate under uniform far-field stress σ,

$$\Delta K = \Delta\sigma\sqrt{\pi c}. \tag{323}$$

Substituting gives $\beta_c = C' c^{m/2}$, a power-law beta function.

The Paris law beta function is power-law in form, analogous to the perturbative beta functions of field theory.

This beta function has no finite fixed point for $m > 0$: the crack length accelerates without bound until catastrophic failure. The "fixed point" behavior is instead the power-law form itself, which is maintained throughout the intermediate asymptotic regime even as c grows.

Step 5: Fixed Points and Critical Behavior

The fixed-point structure of fracture problems determines the universal features of failure.

The Wedge Eigenvalue Problem

For the elastic wedge, the scaling exponents ν are eigenvalues of a boundary-value problem. Substituting the ansatz (317) into the equations of plane elasticity yields

$$\nu^2 + 2\nu(1 - \cos 2\alpha) + (1 - 2\cos 2\alpha) = 0 \tag{324}$$

for anti-symmetric modes under certain boundary conditions. The solutions depend on the wedge angle α and cannot be determined by dimensional analysis alone.

For the crack limit $\alpha = \pi$ (zero internal angle), the eigenvalue is $\nu = 1/2$, recovering the inverse-square-root stress singularity of fracture mechanics. For other angles, ν varies continuously with geometry. This continuous dependence of the exponent on a control parameter is characteristic of self-similar solutions of the second kind.

The eigenvalue nature of the scaling exponent is the mathematical realization of anomalous dimensions. The eigenvalue problem arises from boundary conditions, not from loop corrections.

Universality in Fatigue

The Paris law exhibits a form of universality: the power-law relation (321) holds for a wide variety of materials and loading conditions, with material-specific constants C and m. Within a given material class (say, aluminum alloys), the exponent m is approximately constant even though C varies with alloy composition.

This universality is analogous to that of critical exponents in phase transitions. Just as the Ising model exponents are the same for uniaxial ferromagnets and liquid-gas critical points, the Paris exponent is the same for different specimens of the same material class. The "universality class" is determined by the dominant failure mechanism at the crack tip.

The Cohesive Zone Model

The RG structure becomes clearer in the cohesive zone model, which regularizes the crack-tip singularity by introducing a process zone of size d where the material response is nonlinear. The crack tip is no longer a mathematical singularity but a region where damage accumulates according to a cohesive law.

In this model, the stress intensity factor K is the relevant coupling that grows toward the crack tip, while d provides an ultraviolet cutoff. The scaling of K with distance from the cohesive zone edge determines the fracture behavior. The Paris exponent m emerges from matching the outer linear elastic solution to the inner cohesive zone solution, analogous to matching in effective field theory.

Intermediate Asymptotics in Solid Mechanics

The concept of intermediate asymptotics, developed by Barenblatt, provides the physical interpretation of RG fixed points in continuum mechanics.

The Intermediate Regime

Between the very short scales where microstructure dominates and the very long scales where finite-size effects enter, there exists an intermediate asymptotic regime where the solution is self-similar. In this regime, the details of boundary conditions and material microstructure are irrelevant; only the universal scaling behavior matters.

For the elastic wedge, the intermediate regime is $a \ll r \ll L$ where a is the microstructural scale and L is the overall dimension. In this regime, the stress field follows the power-law form with exponent determined by the eigenvalue analysis. The microstructure at $r \sim a$ cuts off the singularity, while the finite boundaries at $r \sim L$ modify the far field, but neither affects the intermediate scaling.

Intermediate asymptotics is the solid mechanics term for the basin of attraction of an RG fixed point.

Barenblatt's Classification

Barenblatt distinguished two types of self-similar solutions. Solutions of the first kind have exponents fully determined by dimensional analysis; an example is the heat kernel solution $T \sim t^{-1/2} f(x/\sqrt{\kappa t})$. Solutions of the second kind have exponents that cannot be so determined; they are eigenvalues of boundary-value problems.

The elastic wedge and Paris law are both self-similar solutions of the second kind. The exponents are "anomalous" in the sense that they encode information about the dynamics beyond dimensional counting. The RG provides the framework for computing these anomalous exponents: they are eigenvalues of the linearized flow around a fixed point.

Connection to Field Theory

The anomalous dimensions of field theory are the quantum or statistical analogues of Barenblatt's second-kind exponents. Both arise when the naive dimensional analysis fails and the true scaling must be computed dynamically. Both can be interpreted as eigenvalues: of the stability matrix in field theory, of the angular boundary-value problem in elasticity.

This parallel is not coincidental. The mathematics of self-similarity is universal across physical domains. The RG provides the unifying language that connects the intermediate asymptotics of continuum me-

chanics to the universality of critical phenomena and the running of couplings in quantum field theory.

Summary

This chapter has applied the RG recipe to scaling phenomena in solid mechanics. The elastic wedge problem exemplifies self-similar solutions of the second kind, where the scaling exponent is an eigenvalue that cannot be determined by dimensional analysis alone. The angular boundary-value problem plays the role of the RG fixed-point analysis, with the eigenvalue ν determining the strength of the stress singularity.

Fatigue crack growth provides a dynamical example where the Paris law serves as the beta function. The universality of the Paris exponent within material classes reflects fixed-point behavior in the space of damage models. The cohesive zone model regularizes the crack-tip singularity, providing an ultraviolet cutoff analogous to the lattice spacing in field theory.

The concept of intermediate asymptotics unifies these examples. Between the microscopic scale where material discreteness matters and the macroscopic scale where boundary conditions dominate, there exists a regime of self-similar scaling controlled by RG fixed points. Barenblatt's classification into first and second kinds maps directly onto the distinction between engineering and anomalous dimensions in the RG framework.

Solid mechanics thus provides another domain where the geometric RG framework applies with full force. The same five-step recipe that organized the anharmonic oscillator and will organize the remaining applications in Part II applies here as well. The mathematical unity across these diverse physical contexts is the central message of this book.

Conformal Field Theory: The 2D Ising Model

The two-dimensional Ising model holds a special place in the history of physics as one of the few exactly solvable interacting systems. At its critical point, it exhibits conformal invariance and provides a beautiful testing ground for the RG framework. This chapter applies the five-step recipe of Chapter I from multiple perspectives, demonstrating how the same physics emerges whether we use real-space blocking, field theory, conformal methods, or free fermion techniques.

The scale hierarchy (Step 1) ranges from the lattice spacing a to the diverging correlation length ξ. Coarse-graining (Step 2) can be implemented via Kadanoff's block-spin transformation, momentum-shell integration, or operator product expansion. Theory space (Step 3) has coordinates (K, H) representing temperature and magnetic field. The beta functions (Step 4) follow exactly from conformal invariance at the fixed point. Fixed-point analysis (Step 5) reveals the critical point with its exact scaling dimensions $\Delta_\sigma = 1/16$ and $\Delta_\varepsilon = 1/2$.

The 2D Ising model was solved exactly by Onsager in 1944, one of the great achievements of theoretical physics.

The Lattice Model

Consider a square lattice with spin variables $\sigma_i = \pm 1$ at each site. The Hamiltonian is

$$H = -J \sum_{\langle i,j \rangle} \sigma_i \sigma_j - h \sum_i \sigma_i \tag{325}$$

where $J > 0$ is the ferromagnetic coupling, h is an external magnetic field, and $\langle i, j \rangle$ denotes nearest neighbors.

Scale Identification

Following Step 1 of the recipe, we identify the scales. The lattice spacing a provides the UV cutoff, below which the discrete nature of the spins matters. The correlation length ξ provides the IR scale, diverging at the critical point as $\xi \sim |T - T_c|^{-\nu}$ with the critical exponent $\nu = 1$.

Temperature is the control parameter. At $T = T_c$ and external field $h = 0$, the system sits at the critical point where fluctuations occur on all length scales from a to $\xi = \infty$. The dimensionless couplings are

$K = J/(k_B T)$ and $H = h/(k_B T)$, which parametrize the theory space for this model.

Kadanoff's Real-Space RG

The conceptually clearest approach to the RG in the Ising model is Kadanoff's block-spin transformation.

Block Spin Construction

Divide the lattice into blocks of $b \times b$ spins. Define a new "block spin" σ'_I for each block I using a majority rule:

$$\sigma'_I = \text{sign}\left(\sum_{i \in I} \sigma_i\right). \tag{326}$$

Kadanoff's blocking procedure makes the RG coarse-graining physically transparent.

After this transformation, the lattice has spacing $a' = ba$, and we have integrated out fluctuations at scales smaller than ba.

The RG Transformation

To preserve the partition function, the block spins must interact with effective couplings (K', H') determined by

$$Z(K, H; N) = Z(K', H'; N/b^2) \tag{327}$$

where N is the number of spins.

For the 2D Ising model, the RG transformation takes the form

$$K' = R_K(K, H), \tag{328}$$

$$H' = R_H(K, H). \tag{329}$$

Fixed Points and Critical Behavior

The critical point corresponds to a fixed point (K^*, H^*) where

$$K^* = R_K(K^*, 0), \quad H^* = 0. \tag{330}$$

Linearizing around the fixed point:

$$\begin{pmatrix} \delta K' \\ \delta H' \end{pmatrix} = \begin{pmatrix} \frac{\partial R_K}{\partial K} & \frac{\partial R_K}{\partial H} \\ \frac{\partial R_H}{\partial K} & \frac{\partial R_H}{\partial H} \end{pmatrix}_{K^*,0} \begin{pmatrix} \delta K \\ \delta H \end{pmatrix}. \tag{331}$$

The eigenvalues λ_t and λ_h of this matrix give the critical exponents via

$$\nu = \frac{\ln b}{\ln \lambda_t}, \quad \Delta_h = \frac{\ln \lambda_h}{\ln b} \tag{332}$$

where Δ_h is the scaling dimension of the magnetic field operator.

The critical exponents are eigenvalues of the linearized RG, exactly as developed in Chapter I.

The ϕ^4 Field Theory Approach

In the continuum limit, the Ising model is described by a scalar field theory.

Continuum Limit

Near the critical point, the lattice model can be replaced by a continuum action:

$$S[\phi] = \int d^2x \left[\frac{1}{2}(\nabla\phi)^2 + \frac{r}{2}\phi^2 + \frac{u}{4!}\phi^4 \right] \tag{333}$$

where $\phi(x)$ is a coarse-grained magnetization field.

This is the O(1) case of the O(N) model studied in Chapter II. The critical point corresponds to the Wilson-Fisher fixed point (which becomes nontrivial in $d < 4$).

Two-Dimensional Peculiarities

In $d = 2$, the ϕ^4 theory is super-renormalizable. The coupling u has dimension $[u] = 4 - d = 2$, making it strongly relevant. The RG flow drives the system rapidly away from the Gaussian fixed point toward a strongly coupled fixed point.

This is where exact methods and conformal field theory become essential.

The CFT Approach

At the critical point, the 2D Ising model possesses full conformal invariance, not just scale invariance.

Conformal Symmetry

In two dimensions, the conformal group is infinite-dimensional. Holomorphic coordinate transformations $z \to f(z)$ and antiholomorphic $\bar{z} \to \bar{f}(\bar{z})$ form two copies of the Virasoro algebra with generators L_n and $\bar{L}_n$ satisfying:

$$[L_m, L_n] = (m-n)L_{m+n} + \frac{c}{12}m(m^2-1)\delta_{m+n,0}. \tag{334}$$

The central charge c appears in the anomalous term. For the Ising CFT:

$$c = \frac{1}{2}. \tag{335}$$

The central charge c is the most important invariant of a 2D CFT, encoding the number of degrees of freedom.

Primary Operators

The spectrum of the Ising CFT consists of primary operators $\mathcal{O}_\Delta$ labeled by their scaling dimensions Δ. The identity operator $\mathbb{1}$ has $\Delta = 0$, as required by conformal invariance. The spin field σ represents the local magnetization and has the non-trivial scaling dimension $\Delta = 1/16$. The energy density ε measures the local deviation from criticality and has scaling dimension $\Delta = 1/2$. These dimensions are exact, determined by the representation theory of the Virasoro algebra, not by perturbative calculations.

Connection to RG

The CFT perspective provides a complete solution to the RG at the fixed point. Scaling dimensions are eigenvalues of the dilation operator $D = L_0 + \bar{L}_0$, which generates scale transformations in the conformal algebra. Correlation functions are completely determined by conformal symmetry up to a finite number of constants, the OPE coefficients. The operator product expansion provides the connection structure discussed in Chapter I, relating operators at different points in spacetime.

The correlation length exponent can be read off directly from the scaling dimension of the energy operator:

$$\nu = \frac{1}{2 - \Delta_\varepsilon} = \frac{1}{2 - 1/2} = 1. \tag{336}$$

This exact result confirms that the 2D Ising model is in a universality class distinct from mean field theory, which predicts $\nu = 1/2$.

The exact exponents from CFT confirm that 2D Ising is in a universality class distinct from mean field theory.

Grassmann Variables and Free Fermions

A remarkable feature of the 2D Ising model is its equivalence to a theory of free fermions.

The Transfer Matrix

The partition function can be written as

$$Z = \operatorname{Tr} T^M \tag{337}$$

where T is the transfer matrix acting on a row of spins and M is the number of rows.

The transfer matrix can be diagonalized using a Jordan-Wigner transformation to fermionic variables.

Grassmann Representation

Define Grassmann (anticommuting) variables $\psi_i, \bar{\psi}_i$ satisfying $\{\psi_i, \psi_j\} = \{\bar{\psi}_i, \bar{\psi}_j\} = \{\psi_i, \bar{\psi}_j\} = 0$.

The partition function becomes a Gaussian integral over Grassmann variables:

$$Z = \int \prod_i d\bar{\psi}_i d\psi_i \, e^{-S_F} \tag{338}$$

with the free fermion action

$$S_F = \sum_{\langle i,j \rangle} \bar{\psi}_i M_{ij} \psi_j. \tag{339}$$

The mapping to free fermions makes the Ising model exactly solvable, but the same technique does not generalize to higher dimensions.

Relation to CFT

The continuum limit of the free fermion theory is a CFT with $c = 1/2$. The spin field σ is not part of the free fermion theory but can be constructed as a "disorder operator" that creates a branch cut in the fermion propagator.

This construction explains why $\Delta_\sigma = 1/16$ is not a simple multiple of the fermion dimension.

RG Near the Critical Point

Away from criticality, the RG flow describes how the Ising model approaches or departs from the critical fixed point.

Relevant Perturbations

The critical theory has two relevant perturbations corresponding to the two relevant directions in the linearized RG. Temperature deviation adds a term $\delta\mathcal{L} \sim t\,\varepsilon(x)$ to the Lagrangian, with $t \propto T - T_c$ measuring the distance from criticality. A magnetic field adds $\delta\mathcal{L} \sim h\,\sigma(x)$, breaking the $\mathbb{Z}_2$ symmetry. Both perturbations are relevant because $\Delta_\varepsilon = 1/2$ and $\Delta_\sigma = 1/16$ are both less than the spatial dimension $d = 2$.

Beta Functions

Near the critical point, the beta functions for the dimensionless couplings are:

$$\beta_t = (2 - \Delta_\varepsilon) t = \frac{3}{2} t, \tag{340}$$

$$\beta_h = (2 - \Delta_\sigma) h = \frac{15}{8} h. \tag{341}$$

These are determined exactly by the scaling dimensions.

The exact beta functions confirm the structure derived in Chapter I.

The Zamolodchikov Metric and c-Theorem

The 2D Ising model provides a concrete example of the geometric structures in Part I.

The Metric on Theory Space

Following Chapter I, the Zamolodchikov metric on the (t, h) coupling space is:

$$G_{ij} = \int d^2x \, |x|^4 \langle \mathcal{O}_i(x) \mathcal{O}_j(0) \rangle \tag{342}$$

where $\mathcal{O}_1 = \varepsilon$ and $\mathcal{O}_2 = \sigma$.

At the critical point, conformal invariance completely determines the two-point functions:

$$\langle \varepsilon(x) \varepsilon(0) \rangle = \frac{C_\varepsilon}{|x|^{2\Delta_\varepsilon}} = \frac{C_\varepsilon}{|x|} \tag{343}$$

and similarly for σ.

The c-Function

The Zamolodchikov c-function interpolates between fixed points:

$$C(t, h) = c_{\text{UV}} - (\text{positive contribution from flow}) \tag{344}$$

The c-theorem ensures that c decreases monotonically along any RG trajectory.

For flows in the (t, h) plane, C decreases from its value at the Ising fixed point ($c = 1/2$) to zero in the ordered or disordered phases.

Comparing the Four Approaches

The 2D Ising model admits four distinct but equivalent treatments, each illuminating different aspects of the physics. The fact that all four give identical physical predictions is a powerful consistency check on the RG framework.

Kadanoff real-space RG: This approach directly implements coarse-graining on the lattice by grouping spins into blocks and defining new effective spins for each block. The method provides an intuitive geometric picture of the RG transformation and gives approximate critical exponents that become exact in certain limits or with improved blocking schemes. Its main limitation is the accumulation of errors from truncating the growing number of couplings generated at each step.

ϕ^4 field theory: The continuum limit replaces the discrete spin variable with a continuous field $\phi(x)$, connecting to the general framework of Chapter II. In two dimensions, the field theory is strongly coupled (since $\varepsilon = 4 - d = 2$ is large), making perturbation theory less reliable than in higher dimensions. Nevertheless, the ϕ^4 formulation provides

the natural bridge to quantum field theory methods and relates the Ising model to the universal O(1) symmetry class.

CFT: At the critical point, the 2D Ising model becomes a conformal field theory with central charge $c = 1/2$. The infinite-dimensional Virasoro symmetry completely determines all scaling dimensions and correlation functions, providing exact non-perturbative results. The CFT approach is most powerful for two-dimensional systems where conformal symmetry is especially constraining; it identifies the Ising CFT as the first in the discrete series of minimal models.

Grassmann/fermion: The mapping to free fermions, possible only in two dimensions, makes the model exactly solvable via standard quadratic path integral methods. This provides a rigorous benchmark for comparing approximate methods and demonstrates that the critical behavior emerges from the massless fermion dispersion relation. The fermion representation also reveals the topological structure underlying the model and connects to modern developments in fermionic topological phases.

All four approaches give the same physical predictions for critical exponents, correlation functions, and thermodynamic quantities. This remarkable consistency demonstrates both the universality of critical phenomena and the internal coherence of the RG framework.

The equivalence of these four approaches—lattice, field theory, CFT, and free fermions—is a deep manifestation of universality.

Connection to the Geometric Framework

The Ising model illustrates every aspect of Part I:

Chapter Connections

Scale and Dilation (Chapters I, I): The lattice spacing provides the UV scale; the correlation length provides the IR scale. Scaling dimensions classify operators.

RG Equation (Chapter I): The Kadanoff transformation directly implements the RG. Beta functions are determined by scaling dimensions.

Fixed Points (Chapter I): The critical point is a fixed point of the RG. Eigenvalues of the linearization give critical exponents.

Theory Space (Chapter I): The (t, h) plane is the theory space. The Zamolodchikov metric gives it Riemannian structure.

Irreversibility: The c-theorem ensures irreversibility with $c = 1/2$ at the Ising fixed point.

Connections (Chapter I): The OPE provides the connection structure, relating operators at different points.

Summary

The 2D Ising model demonstrates the five-step RG recipe in an exactly solvable setting. The scale hierarchy (Step 1) extends from lattice spacing to correlation length. Coarse-graining (Step 2) can be implemented in multiple ways: Kadanoff blocking, field-theoretic methods, CFT, or free fermion techniques. Theory space (Step 3) is the two-dimensional (t, h) plane. The beta functions (Step 4) are determined exactly by conformal invariance. Fixed-point analysis (Step 5) reveals the critical point with central charge $c = 1/2$ and exact scaling dimensions.

The power of the Ising model as a testing ground lies in the consistency of all approaches. Real-space, field theory, CFT, and fermion methods all give identical results, confirming the universality of the RG framework. The exact scaling dimensions $\Delta_\sigma = 1/16$ and $\Delta_\varepsilon = 1/2$ provide non-trivial tests: these are not simple fractions but emerge from the representation theory of the Virasoro algebra. The c-theorem is realized explicitly, with the central charge $c = 1/2$ at the critical point decreasing to $c = 0$ in the ordered or disordered phases.

The geometric framework of Part I achieves exact realization in this celebrated system. The stability matrix eigenvalues give critical exponents. The Zamolodchikov metric can be computed from two-point functions. The gradient flow structure and c-theorem hold exactly. The OPE provides the connection structure of Chapter I. The Ising model demonstrates that the abstract geometric RG framework produces concrete, exact predictions when applied to systems with sufficient symmetry.

Statistical Field Theory: The O(N) Model

The O(N) model is the canonical example for perturbative RG in statistical field theory, and this chapter applies the five-step recipe of Chapter I in detail. The model describes systems with an N-component order parameter and exhibits a rich phase structure including continuous phase transitions. By working through the recipe systematically, we will see how the abstract framework of Part I produces concrete predictions for critical exponents that have been verified experimentally.

The scale hierarchy (Step 1) ranges from the UV cutoff Λ (the lattice scale) to the IR correlation length ξ. Coarse-graining (Step 2) proceeds by integrating out high-momentum modes in thin shells, the Wilsonian approach. Theory space (Step 3) is parametrized by the mass-squared r and quartic coupling u. The beta functions (Step 4) are computed perturbatively using the ϵ-expansion. Fixed-point analysis (Step 5) reveals the Gaussian and Wilson-Fisher fixed points, with the latter controlling critical behavior in $d < 4$.

The O(N) model encompasses many physical systems: $N = 1$ is Ising, $N = 2$ is XY (superfluids), $N = 3$ is Heisenberg (magnets), $N = 4$ is relevant to electroweak theory.

The O(N) Symmetric Field Theory

The Euclidean action for the O(N) model in d dimensions is

$$S[\phi] = \int d^d x \left[\frac{1}{2} (\partial_\mu \phi^a)(\partial^\mu \phi^a) + \frac{r_0}{2} \phi^a \phi^a + \frac{u_0}{4!} (\phi^a \phi^a)^2 \right] \tag{345}$$

where ϕ^a ($a = 1, \ldots, N$) is an N-component real scalar field, r_0 is the bare mass squared, and u_0 is the bare quartic coupling. Repeated indices are summed.

Scale Identification

Following Step 1 of the recipe, we identify the scales. The momentum cutoff Λ provides the UV scale where the continuum description breaks down, typically corresponding to the inverse lattice spacing in a microscopic model. The correlation length ξ provides the IR scale characterizing the decay of correlations, which diverges at the critical point.

The scale parameter $s = \ln(\Lambda/\mu)$ measures the logarithm of the ratio between the cutoff and the renormalization scale μ. As we integrate out modes and reduce the effective cutoff, s increases. The dimensionless couplings $r = r_0/\Lambda^2$ and $u = u_0\Lambda^{d-4}$ are the natural variables for the RG, with the powers of Λ chosen to make them dimensionless in d dimensions.

Canonical Scaling Dimensions

From the action (345), we read off the canonical (engineering) dimensions using the principle of Chapter I.

For the action to be dimensionless:

$$[\phi] = \frac{d-2}{2}, \quad [r_0] = 2, \quad [u_0] = 4 - d. \tag{346}$$

The canonical dimension of u_0 determines whether the ϕ^4 interaction is relevant, irrelevant, or marginal at the Gaussian fixed point.

The critical dimension $d_c = 4$ is where u_0 becomes dimensionless. For $d < 4$, the coupling is relevant at the Gaussian fixed point, driving the system to a nontrivial interacting fixed point.

The Wilson-Fisher Fixed Point

We now derive the famous Wilson-Fisher fixed point using the ε-expansion, where $\varepsilon = 4 - d$.

One-Loop Beta Functions

Using standard perturbative techniques involving dimensional regularization and the minimal subtraction scheme, the beta functions to one loop are:

$$\beta_r \equiv \mu \frac{\partial r}{\partial \mu} = -2r + \frac{(N+2)u}{6(4\pi)^2} + O(u^2), \tag{347}$$

$$\beta_u \equiv \mu \frac{\partial u}{\partial \mu} = -\varepsilon u + \frac{(N+8)u^2}{6(4\pi)^2} + O(u^3). \tag{348}$$

The Gaussian fixed point at $u^* = 0$, $r^* = 0$ has

$$\frac{\partial \beta_u}{\partial u}\Big|_{u^*=0} = -\varepsilon \tag{349}$$

which is negative for $d < 4$, confirming that the Gaussian fixed point is unstable.

Box 13.1: One-Loop Beta Function Derivation

The diagrams: The one-loop corrections arise from two Feynman diagrams:

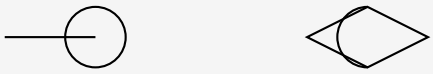

(a) Tadpole → mass renorm

(b) Sunset → coupling renorm

Mass correction (tadpole): The vertex $\frac{u_0}{4!}(\phi^a\phi^a)^2$ contains the term $\frac{u_0}{2}(\phi^a\phi^a)\delta^{bc}\phi^b\phi^c$. Contracting two ϕ fields in a loop:

$$\delta r = \frac{u_0}{2} \cdot N \cdot \int \frac{d^dk}{(2\pi)^d} \frac{1}{k^2 + r} = \frac{(N+2)u_0}{6} \cdot I_1 \tag{350}$$

where $I_1 = \int d^dk/(k^2 + r)$ has a pole $\sim 1/\varepsilon$ in $d = 4 - \varepsilon$, and the factor $(N + 2)$ arises from the O(N) index contractions.
Coupling correction (sunset): The four-point vertex correction involves two internal propagators. After O(N) index algebra:

$$\delta u = -\frac{(N+8)u_0^2}{36} \cdot I_2 \tag{351}$$

where I_2 is the sunset integral, also with a $1/\varepsilon$ pole.
Renormalization and beta function: In the $\overline{\text{MS}}$ scheme, the counterterms cancel the poles. The renormalized couplings satisfy:

$$r_0 = \mu^2 Z_r r, \qquad u_0 = \mu^\varepsilon Z_u u \tag{352}$$

with $Z_r = 1 - \frac{(N+2)u}{6(4\pi)^2\varepsilon} + O(u^2)$ and $Z_u = 1 + \frac{(N+8)u}{6(4\pi)^2\varepsilon} + O(u^2)$.
The beta function from $\mu\partial_\mu u_0 = 0$:

$$\beta_u = \mu\frac{\partial u}{\partial \mu} = -\varepsilon u + u \cdot \mu\frac{\partial}{\partial \mu} \ln Z_u = -\varepsilon u + \frac{(N+8)u^2}{6(4\pi)^2} \tag{353}$$

Physical interpretation: The $(N + 2)$ factor in β_r counts the number of field components that can run in the tadpole loop. The $(N + 8)$ factor in β_u arises from the sum over three distinct index structures in the four-point function.

The Nontrivial Fixed Point

Setting $\beta_u = 0$ in equation (348) gives the Wilson-Fisher fixed point:

$$u^* = \frac{6(4\pi)^2\varepsilon}{N+8} + O(\varepsilon^2). \tag{354}$$

The Wilson-Fisher fixed point exists for $\varepsilon > 0$ (i.e., $d < 4$) and governs continuous phase transitions.

At this fixed point, the stability matrix (equation **??**) has eigenval-

ues:

$$\lambda_r = 2 - \frac{(N+2)\varepsilon}{N+8} + O(\varepsilon^2), \tag{355}$$

$$\lambda_u = \varepsilon + O(\varepsilon^2). \tag{356}$$

The eigenvalue $\lambda_r > 0$ indicates that r is a relevant perturbation (temperature deviation from criticality). The correlation length exponent is

$$\nu = \frac{1}{\lambda_r} = \frac{1}{2} + \frac{(N+2)\varepsilon}{4(N+8)} + O(\varepsilon^2). \tag{357}$$

Critical Exponents and Universality

The critical exponents characterize the singular behavior near the phase transition.

Standard Critical Exponents

Near the critical point at $r = r_c$:

$$\xi \sim |r - r_c|^{-\nu}, \qquad \text{(correlation length)} \tag{358}$$

$$\chi \sim |r - r_c|^{-\gamma}, \qquad \text{(susceptibility)} \tag{359}$$

$$\langle \phi \rangle \sim (-r + r_c)^{\beta}, \qquad \text{(order parameter)} \tag{360}$$

$$G(r) \sim r^{-(d-2+\eta)}, \qquad \text{(correlation function)} \tag{361}$$

The critical exponents depend only on d and N, not on microscopic details. This is universality.

The anomalous dimension η arises from the field renormalization and is given by

$$\eta = \frac{(N+2)\varepsilon^2}{2(N+8)^2} + O(\varepsilon^3). \tag{362}$$

This is precisely the anomalous dimension discussed in Chapter I, arising from the scale dependence of the field normalization.

Scaling Relations

The critical exponents satisfy scaling relations (Chapter I):

$$\gamma = \nu(2 - \eta), \tag{363}$$

$$\alpha = 2 - d\nu, \tag{364}$$

$$\beta = \frac{\nu(d - 2 + \eta)}{2}. \tag{365}$$

These relations are consequences of the RG structure and hold for any fixed point, not just Wilson-Fisher.

Large-N Limit and the Metric

The large-N limit provides a solvable example where the geometry of theory space can be computed exactly.

Large-N Saddle Point

In the limit $N \to \infty$ with uN held fixed, the path integral is dominated by a saddle point. Introducing an auxiliary field $\sigma = \phi^a \phi^a$, the effective action becomes

$$S_{\text{eff}}[\sigma] = \frac{N}{2}\left[\text{Tr}\ln(-\nabla^2 + r + \sigma) - \int d^d x \frac{\sigma^2}{4u}\right]. \tag{366}$$

The saddle point equation $\delta S_{\text{eff}}/\delta\sigma = 0$ determines the gap equation for the effective mass.

Fisher Information Metric

Following Chapter I, we can compute the metric on the space of couplings from the two-point function:

$$G_{ij} = \frac{1}{N}\langle \mathcal{O}_i \mathcal{O}_j \rangle \tag{367}$$

where $\mathcal{O}_i$ are operators conjugate to the couplings.

The Fisher information metric coincides with the Zamolodchikov metric in suitable limits.

In the large-N limit, this metric can be computed explicitly from Gaussian fluctuations around the saddle point. The result takes the form

$$ds^2 = G_{rr}(r,u)dr^2 + 2G_{ru}(r,u)dr\,du + G_{uu}(r,u)du^2 \tag{368}$$

with specific functions that can be determined from the correlation functions.

RG Flow as Gradient Flow

For $d = 2$, the O(N) model is a conformal field theory at criticality, and Zamolodchikov's c-theorem applies directly.

The c-Function

Zamolodchikov showed that there exists a function $C(r,u)$ satisfying:

$$\frac{dC}{ds} = -G_{ij}\beta^i\beta^j \leq 0 \tag{369}$$

where $s = \ln\mu$ is the RG scale.

The c-function monotonically decreases along RG trajectories, proving irreversibility.

At fixed points, $\beta^i = 0$ and C takes the value of the Virasoro central charge. At the Gaussian fixed point, the central charge is $c = N$, reflecting the N free scalar degrees of freedom. At the Wilson-Fisher fixed point in two dimensions (when it exists), the central charge satisfies $c < N$, reflecting the reduced number of effective degrees of freedom at strong coupling. This demonstrates that the RG flow is always "downhill" in the central charge.

Connection to Entropy

The decrease of c can be interpreted as a loss of degrees of freedom under coarse-graining. As we integrate out short-distance fluctuations, the effective theory has fewer active degrees of freedom, just as entropy increases in thermodynamics.

The Anharmonic Oscillator Revisited

The one-dimensional version of the O(N) model with $N = 1$ is precisely the anharmonic oscillator introduced in Chapter I.

From Partition Function to RG

The partition function

$$Z = \int_{-\infty}^{\infty} dx\, e^{-\beta(\frac{1}{2}\omega^2 x^2 + \frac{\lambda}{4}x^4)} \tag{370}$$

can be analyzed using the same RG techniques. In zero dimensions (quantum mechanics at finite temperature), there is no momentum integral, so the beta functions arise purely from the measure.

The anharmonic oscillator provides the simplest example of the RG in field theory, with all essential features present.

Strong Coupling Expansion

For large λ, the perturbative expansion fails, but the RG allows systematic improvement. The effective coupling at scale μ satisfies

$$\mu \frac{d\lambda_{\text{eff}}}{d\mu} = \beta_\lambda(\lambda_{\text{eff}}) \tag{371}$$

which can be integrated to resum the perturbation series.

This is the statistical mechanics analog of the secular term resummation in the ODE version (Chapter I).

Connection to the Geometric Framework

We now summarize how the O(N) model illustrates all aspects of the geometric framework.

Theory Space

The coupling space (r, u) is a two-dimensional manifold. The RG flow

$$\dot{r} = \beta_r(r, u), \tag{372}$$

$$\dot{u} = \beta_u(r, u) \tag{373}$$

defines a vector field on this manifold.

Fixed Points and Scaling

The Gaussian and Wilson-Fisher fixed points organize the flow, serving as the endpoints of RG trajectories. The stability matrix at each fixed point determines the local flow structure completely. Its eigenvalues distinguish relevant directions (unstable under the flow) from irrelevant directions (stable under the flow). The critical exponents follow directly from these eigenvalues through the relation $\Delta_a = d - \lambda_a$. The number of relevant perturbations determines the universality class: systems requiring the same number of tuned parameters to reach the fixed point belong to the same class.

The Metric

The Zamolodchikov metric provides a natural Riemannian structure on theory space. The RG flow is a gradient flow with respect to this metric, with the c-function as the potential.

Connections

Scheme changes correspond to coordinate transformations on theory space. The connection (Chapter I) ensures that physical quantities are scheme-independent.

Renormalons and the Mass Gap

The perturbative ε-expansion for the O(N) model, like all asymptotic series in field theory, exhibits renormalon singularities in its Borel transform. The singularity positions follow from the one-loop beta function coefficient:

$$\zeta_k = \frac{k}{\beta_1} = \frac{6k(4\pi)^2}{N+8}, \qquad k = 1, 2, 3, \ldots \tag{374}$$

The renormalon structure of the O(N) model mirrors the general framework of Chapter I—the positions follow from the RGE, not from summing diagrams.

These renormalons have physical significance. The dynamically generated mass gap m_{gap} in the O(N) model (relevant for $N > 2$ in two dimensions) is a non-perturbative effect invisible to any finite order of perturbation theory. It appears in the transseries as:

$$m_{\text{gap}} \sim \Lambda\, e^{-1/(|\beta_1| g_*)} \tag{375}$$

where Λ is the UV cutoff and g_* is the coupling at the Wilson-Fisher fixed point.

The cancellation of ambiguities between the perturbative series and the mass gap sector illustrates the general principle of Chapter I: the imaginary parts from Borel resummation must cancel against contributions from non-perturbative sectors for physical observables to be real.

Summary

The O(N) model demonstrates the five-step RG recipe in its natural habitat: statistical field theory near continuous phase transitions. The scale hierarchy (Step 1) extends from the microscopic cutoff Λ to the diverging correlation length ξ. Coarse-graining (Step 2) integrates out momentum shells in the Wilsonian approach. Theory space (Step 3) has coordinates (r, u) with the RG flow defining a vector field. The beta functions (Step 4) are computed via the ϵ-expansion, yielding equations (347) and (348). Fixed-point analysis (Step 5) reveals the Wilson-Fisher fixed point (354) with universal critical exponents.

The chapter has invoked every element of the geometric framework from Part I. Canonical scaling dimensions follow from the dilation group analysis of Chapter I. Beta functions emerge from scale covariance as developed in Chapter I. Fixed points and stability analysis apply the machinery of Chapter I. The Zamolodchikov metric and gradient flow structure connect to the geometry of Chapter I. The c-theorem establishes irreversibility of the flow.

The one-dimensional limit of the O(N) model with $N = 1$ is precisely the anharmonic oscillator partition function that introduced the RG in Chapter I. This connection closes the pedagogical loop: the abstract framework produces concrete, testable predictions for critical phenomena that agree with experiment to high precision. The correlation length exponent ν in three dimensions, for example, has been measured in superfluid helium and agrees with the theoretical prediction to several decimal places.

Strongly Correlated Electrons: The Hubbard Model

The Hubbard model captures the essential physics of strongly correlated electron systems, where the interplay between electron kinetic energy and on-site repulsion produces a rich phase diagram. This chapter applies the five-step recipe of Chapter I to a condensed matter system where strong correlations challenge perturbative methods and reveal the full power of RG thinking. The functional RG provides a non-perturbative approach that interpolates between weak and strong coupling.

The scale hierarchy (Step 1) compares the bandwidth $W \sim zt$ to the interaction strength U. Coarse-graining (Step 2) can proceed from weak coupling (integrating out high-energy particle-hole excitations) or strong coupling (integrating out doubly occupied states). Theory space (Step 3) includes the ratio U/t, the filling, and temperature. The beta functions (Step 4) are computed via perturbative or functional methods. Fixed-point analysis (Step 5) reveals multiple competing phases: Fermi liquid, Mott insulator, superconductor, and possibly strange metal.

The Hubbard model was introduced independently by Hubbard, Gutzwiller, and Kanamori in 1963 to explain magnetism and metal-insulator transitions.

The Hubbard Hamiltonian

The Hubbard model describes electrons hopping on a lattice with an on-site repulsion:

$$H = -t \sum_{\langle i,j \rangle, \sigma} (c^\dagger_{i\sigma} c_{j\sigma} + \text{h.c.}) + U \sum_i n_{i\uparrow} n_{i\downarrow} \tag{376}$$

where $c^\dagger_{i\sigma}$ creates an electron with spin σ at site i, $n_{i\sigma} = c^\dagger_{i\sigma} c_{i\sigma}$ is the number operator, t is the hopping amplitude, and $U > 0$ is the on-site Coulomb repulsion.

Scale Identification

Following Step 1 of the recipe, we identify the scales. The bandwidth $W \sim zt$ (where z is the coordination number) sets the kinetic energy scale, characterizing how much energy an electron gains by delocalizing across the lattice. The interaction U is the potential energy scale,

the cost of putting two electrons on the same site. The dimensionless coupling $u = U/W$ measures the relative strength of interactions: when $u \ll 1$ kinetic energy dominates and electrons form a Fermi liquid, while when $u \gg 1$ interactions dominate and electrons localize into a Mott insulator.

The scale parameter can be taken as the energy cutoff Λ or temperature T. As we lower Λ or T, the effective coupling can flow to strong or weak values depending on the bare parameters and dimensionality.

The ratio U/t controls whether electrons behave as itinerant metals or localized moments.

Limiting Cases

The physics depends dramatically on the ratio U/t and the electron filling.

Weak Coupling: $U \ll t$

For small U, electrons form a Fermi liquid with renormalized parameters. Standard perturbation theory in U/t applies, and the system is metallic.

Strong Coupling: $U \gg t$

For large U, double occupancy is energetically suppressed. At half-filling (one electron per site on average), the system becomes a Mott insulator with localized spins. The effective low-energy theory is the Heisenberg antiferromagnet:

$$H_{\text{eff}} = J \sum_{\langle i,j \rangle} \mathbf{S}_i \cdot \mathbf{S}_j \tag{377}$$

with exchange coupling $J = 4t^2/U$.

The Mott Transition

As U/t increases from zero, the system undergoes a metal-insulator transition (Mott transition) at some critical value $(U/t)_c$. This is a quantum phase transition driven by the competition between kinetic and potential energy.

RG for the Hubbard Model

Several RG approaches have been developed for the Hubbard model.

Weak Coupling RG

For $U \ll t$, perturbative RG can be developed around the free electron fixed point. The beta function for the interaction strength depends on

the dimensionality and band structure.

In one dimension with a linear spectrum near the Fermi points, the RG equations for the coupling constants g_i (characterizing different scattering processes) take the form:

$$\frac{dg_1}{d\ell} = -g_1^2 + \cdots, \tag{378}$$

$$\frac{dg_2}{d\ell} = -2g_1 g_2 + \cdots, \tag{379}$$

where $\ell = \ln(\Lambda_0/\Lambda)$ is the logarithmic scale.

The 1D Hubbard model is exactly solvable by the Bethe ansatz, providing a benchmark for RG calculations.

Strong Coupling RG

For $U \gg t$, one starts from the atomic limit and treats hopping as a perturbation. The RG generates effective interactions at lower energy scales.

The key insight is that high-energy virtual excitations (creating double occupancies) are integrated out, generating the superexchange coupling J and other effective interactions.

Fixed Points and Phase Diagram

Applying the framework of Chapter I:

One Dimension

In 1D at half-filling, the repulsive Hubbard model flows toward a Mott insulating fixed point for any $U > 0$. The fixed point is described by a Luttinger liquid with gapless spin excitations governed by the effective Heisenberg antiferromagnetic coupling, and gapped charge excitations reflecting the Mott gap that prevents charge transport. Away from half-filling, the system remains metallic but as a Luttinger liquid rather than a Fermi liquid, with power-law correlations rather than quasiparticle excitations.

Two Dimensions

The 2D Hubbard model is believed to describe high-temperature superconductivity in the cuprates. The RG analysis reveals a complex phase diagram with multiple competing phases. At half-filling and sufficiently strong coupling $U > U_c$, the system forms an antiferromagnetic Mott insulator. Upon doping away from half-filling, d-wave superconductivity may emerge from the pairing of electrons mediated by antiferromagnetic fluctuations. At weak coupling, the system exhibits Fermi liquid behavior with well-defined quasiparticles.

The phase diagram involves multiple competing fixed points, and no single analytical method captures all regimes. Numerical methods including quantum Monte Carlo, dynamical mean-field theory, and tensor networks complement the analytical RG, each providing insight into different corners of parameter space.

The 2D Hubbard model remains one of the great unsolved problems in condensed matter physics.

Infinite Dimensions

In the limit $d \to \infty$ (with proper scaling of t), the Hubbard model becomes exactly solvable via dynamical mean-field theory (DMFT). This provides a nonperturbative benchmark for understanding the Mott transition. A sharp first-order Mott transition occurs at $(U/W)_c \approx 1.5$, with a metal-insulator coexistence region where both phases are locally stable. The crossover from itinerant to localized behavior can be traced continuously as U/W increases, with spectral weight transferring from coherent quasiparticle peaks to incoherent Hubbard bands.

Functional RG Approach

The functional renormalization group provides a systematic nonperturbative framework for the Hubbard model. This approach, based on an exact flow equation for the effective action, allows interpolation between weak and strong coupling.

The Effective Action

Define the generating functional for connected Green's functions $W[J]$ and its Legendre transform, the effective action $\Gamma[\phi]$. Introducing a regulator R_Λ that suppresses modes below the scale Λ:

$$\Gamma_\Lambda[\phi] = \sup_J \left(J \cdot \phi - W_\Lambda[J] \right) - \Delta S_\Lambda[\phi] \tag{380}$$

where ΔS_Λ is the regulator contribution.

The Flow Equation

The exact RG equation for Γ_Λ is:

$$\frac{\partial \Gamma_\Lambda}{\partial \Lambda} = \frac{1}{2} \mathrm{Tr} \left[\left(\Gamma_\Lambda^{(2)} + R_\Lambda \right)^{-1} \frac{\partial R_\Lambda}{\partial \Lambda} \right] \tag{381}$$

where $\Gamma_\Lambda^{(2)}$ is the second functional derivative of the effective action.

The functional RG provides a nonperturbative framework valid at any coupling strength.

Truncation and Results

Practical calculations require truncating the effective action to a finite number of coupling constants. Common truncations include the static

four-point vertex, which captures magnetic and pairing instabilities; the frequency-dependent vertex, which captures dynamic correlations; and self-energy effects, which capture spectral weight transfer between coherent and incoherent excitations. More sophisticated truncations include momentum dependence and higher-order vertices.

The functional RG has successfully predicted several key features of the Hubbard model phase diagram. Antiferromagnetic order emerges at half-filling when the nesting of the Fermi surface enhances magnetic susceptibility. Upon doping, d-wave pairing can arise from antiferromagnetic fluctuations acting as a pairing glue. Pseudogap behavior in the underdoped regime, where spectral weight is suppressed near the Fermi level even above the superconducting transition, also emerges naturally from the functional RG flow.

Connection to the Anharmonic Oscillator

There is a deep connection between the Hubbard model and the anharmonic oscillator of Chapter I.

Path Integral Representation

In the coherent state path integral, the Hubbard model becomes:

$$Z = \int \mathcal{D}[\bar{c}, c]\, e^{-S[\bar{c},c]} \tag{382}$$

with action containing quadratic (kinetic) and quartic (interaction) terms.

This has the same structure as the ϕ^4 theory, with fermionic (Grassmann) fields instead of bosonic ones. The RG analysis proceeds similarly, with complications from the Fermi surface geometry.

Local vs. Itinerant Physics

The competition between t (promoting delocalization) and U (promoting localization) mirrors the competition between kinetic and potential energy in the anharmonic oscillator. The RG identifies which physics dominates at low energies.

Emergent Phenomena

The Hubbard model exhibits emergent phenomena that arise from the RG flow.

Antiferromagnetism

At half-filling with moderate U, antiferromagnetic order emerges below a Néel temperature T_N. The RG shows that antiferromagnetic

fluctuations are relevant perturbations that flow to strong coupling.

Superconductivity

Upon doping, the antiferromagnetic fluctuations can mediate an effective attractive interaction between electrons, potentially leading to superconductivity. The RG identifies the pairing symmetry (typically d-wave in 2D cuprates).

The mechanism of high-temperature superconductivity remains one of the outstanding problems in physics.

Strange Metal

In certain parameter regimes, the Hubbard model may flow toward a "strange metal" fixed point characterized by non-Fermi liquid behavior: linear-in-T resistivity, anomalous scaling of transport properties, and absence of well-defined quasiparticles.

Connection to the Geometric Framework

We now connect the Hubbard model to the geometric framework of Part I.

Theory Space

The theory space for the Hubbard model includes the interaction strength U/t, the electron filling n (from empty to half-filled to fully occupied), temperature T or equivalently the energy scale Λ, and in extended models, longer-range interactions and additional orbitals. The RG flow traces a trajectory through this high-dimensional space, with different regions flowing to different fixed points.

Fixed Points and Phases

Different phases correspond to different fixed points in theory space. The Fermi liquid is described by a free fermion fixed point with renormalized parameters including the quasiparticle mass and Landau interaction parameters. The Mott insulator corresponds to a strong coupling fixed point with localized spins and a charge gap. The superconductor is a BCS-type fixed point with Cooper pairing. A strange metal phase, if it exists, would correspond to a non-Fermi liquid fixed point with anomalous scaling and no well-defined quasiparticles. Phase transitions are crossovers between basins of attraction of these different fixed points.

Stability Analysis

At each fixed point, the stability matrix of Chapter I determines the fate of perturbations. Relevant perturbations destabilize the phase and drive transitions to other fixed points. Irrelevant perturbations flow to zero and do not affect the long-distance physics. Marginal perturbations require higher-order analysis to determine their ultimate behavior.

For the Fermi liquid fixed point in dimensions $d > 1$, forward scattering is marginal, corresponding to the renormalization of Landau parameters. BCS pairing is marginally relevant at zero temperature in the presence of an attractive interaction, explaining why arbitrarily weak attraction leads to superconductivity.

The Metric on Theory Space

While less developed than in CFT, a metric on the coupling space can be defined from susceptibilities:

$$G_{ij} = \frac{\partial^2 F}{\partial g^i \partial g^j} \tag{383}$$

where F is the free energy density and g^i are the couplings.

This metric diverges at phase transitions (critical points), reflecting the singular behavior of the thermodynamic potentials.

Summary

The Hubbard model demonstrates the five-step RG recipe in strongly correlated systems where perturbation theory is insufficient. The scale hierarchy (Step 1) compares kinetic energy t to interaction U. Coarse-graining (Step 2) can proceed perturbatively from weak or strong coupling, or non-perturbatively via functional methods. Theory space (Step 3) includes U/t, filling, and temperature. The beta functions (Step 4) are computed via weak-coupling RG, strong-coupling expansion, or the Wetterich equation (381). Fixed-point analysis (Step 5) reveals competing phases: Fermi liquid, Mott insulator, superconductor, and possibly strange metal.

The competition between kinetic and potential energy scales creates a rich phase diagram with the metal-insulator (Mott) transition as its central feature. Different phases correspond to different fixed points in theory space, with phase transitions representing crossovers between basins of attraction. Emergent phenomena including magnetism and superconductivity arise naturally from the RG flow, even when they are not visible in the microscopic Hamiltonian.

The Hubbard model demonstrates that the geometric RG framework extends to strongly correlated quantum systems, providing organizing principles even when perturbative calculations fail. The functional RG offers non-perturbative access to the full phase diagram, interpolating between weak and strong coupling limits. The same five-step recipe that organized the anharmonic oscillator applies here, though the implementation requires more sophisticated machinery.

Quantum Electrodynamics

Quantum electrodynamics (QED) is the relativistic quantum field theory of the electromagnetic interaction, and it was here that renormalization was first developed as a systematic procedure. This chapter applies the five-step recipe of Chapter I to QED, showing how the abstract geometric framework of Part I manifests in the physical phenomenon of charge screening. The extraordinary agreement between QED predictions and experiment provides the most precise test of quantum field theory.

The scale hierarchy (Step 1) ranges from the electron mass m (the IR scale) through the renormalization scale μ to the UV cutoff Λ. Coarse-graining (Step 2) integrates out high-momentum modes, generating effective couplings. Theory space (Step 3) is parametrized by the fine structure constant α and the electron mass m. The beta function (Step 4) is computed from vacuum polarization, yielding $\beta_\alpha = 2\alpha^2/(3\pi) + O(\alpha^3)$. Fixed-point analysis (Step 5) reveals that $\alpha^* = 0$ is an IR-stable fixed point, explaining why electromagnetism appears weakly coupled at everyday energies.

QED achieved unprecedented agreement between theory and experiment, with the electron magnetic moment predicted to better than one part in a trillion.

The QED Lagrangian

The QED Lagrangian density is

$$\mathcal{L} = \bar{\psi}(i\gamma^\mu D_\mu - m)\psi - \frac{1}{4}F_{\mu\nu}F^{\mu\nu} \tag{384}$$

where ψ is the electron field, A_μ the photon field, $D_\mu = \partial_\mu + ieA_\mu$ the covariant derivative, $F_{\mu\nu} = \partial_\mu A_\nu - \partial_\nu A_\mu$ the field strength, and m the electron mass.

Scale Identification

Following Step 1 of the recipe, we identify the scales. The energy scale μ characterizes the typical momentum transfer in a scattering process; this is the scale at which we probe the electromagnetic interaction. The electron mass $m \approx 0.511$ MeV provides an IR scale below which

electron-positron pairs cannot be created, setting a threshold for vacuum polarization effects.

The cutoff Λ is the UV scale where the effective field theory description breaks down and new physics must enter. In practice, QED is embedded in the electroweak theory at scales of order 100 GeV. The dimensionless coupling is the fine structure constant $\alpha = e^2/(4\pi) \approx 1/137$, whose small value makes perturbation theory extraordinarily successful.

Canonical Scaling Dimensions

Following the analysis of Chapter I, we determine the canonical dimensions from the Lagrangian.

In $d = 4$ dimensions:

$$[\psi] = \frac{3}{2}, \quad [A_\mu] = 1, \quad [e] = 0, \quad [m] = 1. \tag{385}$$

The dimensionlessness of e in $d = 4$ makes QED marginal at the classical level, with quantum corrections determining its fate.

The charge e is classically dimensionless, indicating that the interaction is marginal. Quantum corrections will determine whether the coupling is marginally relevant or irrelevant.

Running of the Coupling

The beta function describes how the effective coupling changes with energy scale.

Vacuum Polarization

The photon propagator receives quantum corrections from virtual electron-positron pairs. These corrections are summarized by the vacuum polarization tensor $\Pi_{\mu\nu}(q)$:

$$\Pi_{\mu\nu}(q) = (q^2 g_{\mu\nu} - q_\mu q_\nu)\Pi(q^2). \tag{386}$$

The function $\Pi(q^2)$ contains a logarithmic dependence on momentum:

$$\Pi(q^2) = -\frac{\alpha}{3\pi} \ln \frac{q^2}{m^2} + \text{finite terms} \tag{387}$$

for $|q^2| \gg m^2$.

Vacuum polarization represents the "dressing" of the photon by virtual particles, screening the bare charge.

The QED Beta Function

The beta function for α is obtained from the RG equation (Chapter I):

$$\beta_\alpha \equiv \mu \frac{d\alpha}{d\mu} = \frac{2\alpha^2}{3\pi} + O(\alpha^3). \tag{388}$$

This positive beta function indicates that α increases with energy scale (UV) and decreases toward lower energies (IR).

Physical Interpretation

The running coupling can be integrated:

$$\alpha(\mu) = \frac{\alpha(m)}{1 - \frac{2\alpha(m)}{3\pi} \ln(\mu/m)}. \tag{389}$$

At low energies $\mu \ll m$, virtual pairs cannot be created, and α approaches its observed value $\alpha \approx 1/137$. At high energies, the coupling increases due to charge screening by virtual pairs.

Fixed Points and the Landau Pole

Applying the framework of Chapter I to QED reveals important features.

The Gaussian Fixed Point

The only perturbatively accessible fixed point is $\alpha^* = 0$ (the Gaussian or free theory). At this fixed point:

$$\frac{\partial \beta_\alpha}{\partial \alpha}\Big|_{\alpha=0} = 0. \tag{390}$$

The coupling is marginal at leading order. The positive coefficient in (388) makes it marginally irrelevant in the IR: the theory flows toward the free fixed point at low energies.

The Gaussian fixed point is an IR attractor for QED, explaining why electromagnetism appears weakly coupled at everyday energies.

The Landau Pole

From equation (389), the coupling diverges at the "Landau pole":

$$\Lambda_{\text{Landau}} = m \exp\left(\frac{3\pi}{2\alpha(m)}\right) \sim 10^{286}\ \text{GeV}. \tag{391}$$

This enormously high scale is far beyond any accessible energy, but the existence of the Landau pole indicates that QED cannot be a complete theory valid at all energies.

UV Incompleteness and Resurgent Self-Completion

The Landau pole suggests that QED requires a UV completion—but there are two qualitatively different possibilities.

Wilsonian completion. New physics takes over before the coupling becomes strong. In the Standard Model, QED is embedded in the electroweak theory at scale ~ 100 GeV, far below the Landau pole.

Non-Wilsonian completion via resurgence. The transseries framework of Chapter I offers an alternative. The perturbative beta function

$\beta_\alpha = 2\alpha^2/(3\pi) + O(\alpha^3)$ is asymptotic, with renormalon singularities in its Borel transform at positions:

$$\zeta_k = \frac{3\pi k}{2}, \qquad k = 1, 2, 3, \ldots \tag{392}$$

When these renormalon contributions are included, the full transseries beta function becomes:

$$\beta_{\text{full}}(\alpha) = \beta_{\text{pert}}(\alpha) + \sum_k C_k \, e^{-3\pi k/(2\alpha)} R_k(\alpha) \tag{393}$$

The Landau pole may be an artifact of perturbation theory. The resurgent completion could reveal a UV fixed point, rendering QED self-consistent without new particles.

For certain values of the transseries parameters C_k, this effective beta function can vanish at a finite coupling α^*_{NP}—a **non-perturbative fixed point**. At this fixed point, QED becomes scale-invariant without the coupling diverging.

Whether such a fixed point exists in QED is an open question. If it does, it would represent **non-Wilsonian UV completion**: the theory is consistent to arbitrarily high energies without requiring new heavy particles. The Landau pole would be an artifact of truncating the transseries, not a genuine inconsistency.

This connects to the broader theme of Chapter I: fixed points may exist beyond perturbation theory, visible only through the resurgent structure of the RG equation.

Anomalous Dimensions

Beyond the running of α, quantum corrections also modify the scaling dimensions of operators.

Electron Field Anomalous Dimension

The electron propagator receives corrections that modify its scaling behavior. The anomalous dimension γ_ψ is defined through:

$$\mu \frac{d}{d\mu} \psi_R = \gamma_\psi \psi_R \tag{394}$$

where ψ_R is the renormalized field.

At one loop in QED:

$$\gamma_\psi = \frac{\alpha}{4\pi}(3 - \xi) \tag{395}$$

where ξ is the gauge parameter. In Landau gauge ($\xi = 0$), $\gamma_\psi = \frac{3\alpha}{4\pi}$.

The anomalous dimension represents the deviation from classical scaling due to quantum fluctuations.

Electron Mass Running

The electron mass also runs with scale:

$$\mu \frac{dm}{d\mu} = -\frac{3\alpha}{\pi} m + O(\alpha^2). \tag{396}$$

This indicates that the electron mass is a relevant perturbation: at the IR fixed point ($\alpha = 0$), massive electrons decouple from massless photons.

Ward Identities and Gauge Invariance

Gauge invariance imposes powerful constraints on the RG flow.

The Ward-Takahashi Identity

The conservation of the electromagnetic current implies:

$$q^\mu \Gamma_\mu(p', p) = e[S^{-1}(p') - S^{-1}(p)] \tag{397}$$

where Γ_μ is the vertex function and S is the electron propagator.

This identity ensures that the charge renormalization Z_1 equals the electron field renormalization Z_2:

$$Z_1 = Z_2. \tag{398}$$

Ward identities are consequences of gauge symmetry that constrain the form of quantum corrections.

Consequences for the RG

The Ward identity has profound consequences for the structure of the RG in QED. The electric charge is universally defined and scheme-independent, a remarkable constraint that does not hold for arbitrary couplings. The beta function (388) is gauge invariant, taking the same form in any gauge. Only one independent renormalization constant—Z_3 for the photon field—determines the running of α, dramatically simplifying the structure of theory space. This exemplifies how symmetries constrain the geometry of theory space, as discussed abstractly in Chapter I.

The Lamb Shift and Anomalous Magnetic Moment

The RG framework in QED makes precise predictions that have been verified experimentally.

The Lamb Shift

The energy levels of hydrogen receive corrections from vacuum polarization and electron self-energy. The splitting between the $2S_{1/2}$ and $2P_{1/2}$ states (which are degenerate in the Dirac theory) is:

$$\Delta E_{\text{Lamb}} \approx \frac{\alpha^5 m_e c^2}{6\pi} \left[\ln \frac{1}{\alpha^2} - \ln 2 + \frac{5}{6} \right] \approx 1057 \text{ MHz}. \tag{399}$$

This prediction agrees with experiment to high precision.

Anomalous Magnetic Moment

The electron magnetic moment is predicted to differ from the Dirac value $g = 2$:

$$a_e \equiv \frac{g-2}{2} = \frac{\alpha}{2\pi} + O(\alpha^2). \tag{400}$$

The anomalous magnetic moment of the electron is the most precisely tested prediction in all of physics.

Including higher-order corrections (which require sophisticated RG techniques), the theoretical prediction agrees with the experimental value to better than one part in 10^{12}.

QED in External Fields

QED in strong external fields provides another arena for RG methods.

Schwinger Effect

In a constant electric field E, virtual electron-positron pairs can become real if the field is strong enough. The pair production rate per unit volume is:

$$w = \frac{\alpha E^2}{\pi^2} \sum_{n=1}^{\infty} \frac{1}{n^2} e^{-\frac{\pi m^2 n}{eE}}. \tag{401}$$

This nonperturbative effect lies beyond the perturbative RG but can be understood through instanton methods.

Euler-Heisenberg Effective Action

At energies below the electron mass, the physics is described by an effective action for the electromagnetic field alone:

$$\mathcal{L}_{\text{eff}} = -\frac{1}{4}F^2 + \frac{\alpha^2}{90m^4}\left[(F^2)^2 + \frac{7}{4}(F\tilde{F})^2\right] + \cdots \tag{402}$$

where $\tilde{F}^{\mu\nu} = \frac{1}{2}\epsilon^{\mu\nu\rho\sigma}F_{\rho\sigma}$ is the dual field strength.

This is the effective theory obtained after integrating out electrons, implementing the RG procedure discussed in Chapter I.

Connection to the Geometric Framework

We now explicitly connect QED to the geometric framework of Part I.

Theory Space

The coupling space for QED includes (α, m) and gauge-fixing parameters. The essential physics is captured by the flow of α:

$$\frac{d\alpha}{ds} = \beta_\alpha(\alpha) \tag{403}$$

where $s = \ln(\mu/m)$ is the scale parameter.

Fixed Points

QED has a single perturbative fixed point at $\alpha^* = 0$, the free theory. The stability analysis of Chapter I reveals the character of perturbations around this fixed point. The coupling α is marginally irrelevant, flowing to $\alpha^* = 0$ in the IR; this explains why electromagnetism appears weakly coupled at low energies. The electron mass m is a relevant perturbation: massive electrons decouple at energies below their mass, leaving only massless photons.

Gradient Flow Structure

In four dimensions, the a-theorem governs RG flows. While the full proof is technical, the decrease of the a-anomaly coefficient from UV to IR is consistent with QED flowing toward the free theory.

Connections and Scheme Dependence

The renormalization scheme choice (MS, $\overline{\text{MS}}$, on-shell, etc.) corresponds to a choice of coordinates on theory space. The connection (Chapter I) ensures that physical observables are scheme-independent.

The Ward identity provides additional structure, constraining the allowed coordinate transformations to preserve gauge invariance.

Summary

QED demonstrates the five-step RG recipe in its original domain: relativistic quantum field theory. The scale hierarchy (Step 1) extends from the electron mass to the UV cutoff. Coarse-graining (Step 2) integrates out high-momentum virtual particles. Theory space (Step 3) is parametrized by the fine structure constant and electron mass. The beta function (Step 4), equation (388), describes charge screening by vacuum polarization. Fixed-point analysis (Step 5) reveals that the Gaussian fixed point $\alpha^* = 0$ is an IR attractor.

The chapter has demonstrated every element of the geometric framework in a gauge theory setting. The running of α according to the beta function provides the prototypical example of a running coupling. The Landau pole indicates UV incompleteness, showing that QED cannot be valid at arbitrarily high energies. Anomalous dimensions arise from loop corrections to propagators. Ward identities from gauge invariance constrain the structure of the RG flow, providing an example of how symmetries restrict the geometry of theory space.

The extraordinary precision of QED predictions represents the triumph of the RG approach. The electron anomalous magnetic moment has been computed to five-loop order and agrees with experiment to

better than one part in 10^{12}. This agreement confirms that the abstract geometric framework of Part I, when implemented through systematic perturbative calculations, achieves predictive power unprecedented in the history of physics.

Part III

Synthesis

The Unity of Scale

We have now traversed a wide landscape of physical systems, from chaotic ordinary differential equations through turbulent fluids and fracture mechanics in solids, from critical phenomena in statistical mechanics to quantum field theories and strongly correlated electrons. The common thread running through all of these is the renormalization group and the five-step recipe of Chapter I. This final chapter synthesizes the diverse applications into a unified picture, constructing a dictionary that reveals the structural parallels. We highlight the universal features, acknowledge what remains context-dependent, and point toward open problems and future directions.

The unity of physics lies not in shared material constituents but in shared mathematical structures. The RG is one of the most profound such structures.

A Dictionary of Correspondences

We begin by constructing an explicit dictionary relating the seven systems studied in Part II, following the five-step recipe from Chapter I.

Scale Parameters

Each system has a natural scale parameter:

System	Scale Parameter
Lorenz	Time t (or log time $s = \ln t$)
Navier-Stokes	Length scale ℓ (or wavenumber k)
Fracture/Solids	Distance from crack tip r (or stress intensity)
O(N) model	Momentum cutoff Λ (or $\mu = \ln \Lambda$)
2D Ising	Block size b (or correlation length ξ)
QED	Energy scale μ
Hubbard	Energy cutoff Λ (or temperature T)

Despite these different physical interpretations, all scale parameters enter the RG equation in the same way:

$$\frac{\mathrm{d}g^i}{\mathrm{d}s} = \beta^i(g) \tag{404}$$

where s is the logarithm of the relevant scale.

Couplings and Theory Space

Each system has a natural set of "couplings" that parameterize theory space:

System	Couplings
Lorenz	(σ, ρ, β) or amplitude/phase
Navier-Stokes	Effective viscosity ν_{eff}, forcing spectrum
Fracture/Solids	Wedge angle α, cohesion modulus K_c
O(N) model	(r, u) or $(T - T_c, \lambda)$
2D Ising	$(K, H) = (J/k_B T, h/k_B T)$
QED	(α, m)
Hubbard	$(U/t, n)$ filling

The dimensionality of theory space reflects the number of physically distinct parameters in each system.

Fixed Points

Fixed points organize the flow in each system:

System	Key Fixed Points
Lorenz	Origin, convective fixed points, strange attractor
Navier-Stokes	Kolmogorov fixed point (K41 scaling)
Fracture/Solids	Self-similar crack tip, Paris law scaling
O(N) model	Gaussian, Wilson–Fisher
2D Ising	Disordered, ordered, critical (CFT)
QED	Gaussian ($\alpha^* = 0$)
Hubbard	Fermi liquid, Mott insulator, strange metal

Scaling Dimensions and Eigenvalues

At each fixed point, the stability matrix has eigenvalues that classify perturbations:

System	Relevant	Irrelevant
Lorenz	Driving (ρ)	Damping (some modes)
Navier-Stokes	Large-scale forcing	Small-scale viscosity
Fracture/Solids	Wedge angle	Higher stress multipoles
O(N) model	Temperature deviation	Higher ϕ^n couplings
2D Ising	$T - T_c$, magnetic field	All others
QED	Electron mass	Higher-dim. operators
Hubbard	Fixed-point dependent	Fixed-point dependent

Universal Structures

Beyond the dictionary of correspondences, certain mathematical structures appear universally.

The Lie Group Structure

As developed in Chapter I, scale transformations form a Lie group. The infinitesimal generator acts on observables:

$$\mathcal{D} = s\frac{\partial}{\partial s} + \beta^i \frac{\partial}{\partial g^i} + \Delta_{\mathcal{O}} \tag{405}$$

where $\Delta_{\mathcal{O}}$ is the scaling dimension of the observable.

This structure is common to all six systems. The specific form of β^i differs, but the algebraic structure is universal.

The Geometry of Theory Space

As developed in Chapters I and I, theory space carries a natural geometric structure that makes the RG coordinate-independent. A metric G_{ij}, defined from two-point functions or susceptibilities, measures the "distance" between nearby theories. A connection Γ^k_{ij} ensures covariance under reparameterization, allowing us to compare quantities at different scales in a scheme-independent way. The RG flow itself is a vector field with the beta function as its components, generating trajectories through theory space.

The geometry of theory space provides coordinate-independent characterizations of RG flows.

In 2D CFT (including the Ising model), this geometry is especially rich. The Zamolodchikov metric and the OPE-derived connection are fully determined by conformal symmetry, providing exact results that serve as benchmarks for the general framework.

Irreversibility

The gradient flow structure and c-theorems (Chapter I) establish that RG flows are irreversible:

$$\frac{\mathrm{d}C}{\mathrm{d}s} \leq 0 \tag{406}$$

where C is the c-function (2D) or a-function (4D).

This irreversibility manifests differently in each system but has the same origin. In the Lorenz system, it appears as Lyapunov function decrease and phase space contraction. In Navier-Stokes turbulence, it appears as the energy cascade from large to small scales and the associated entropy production. In the O(N) model and Ising CFT, it appears as the decrease of the central charge, directly counting the reduction in effective degrees of freedom. In QED and the Hubbard model, it appears as the decrease of effective degrees of freedom as high-energy modes are integrated out.

Universality

Perhaps the most striking feature is universality: different microscopic systems can flow to the same fixed point and exhibit identical long-

distance behavior.

In the O(N) model and Ising model, this explains why different magnetic materials have the same critical exponents. In turbulence, it explains the universality of Kolmogorov scaling. In QED, it underlies the scheme independence of physical predictions.

Resurgence and Non-Perturbative Completeness

A universal feature developed in Chapter I deserves emphasis: the **transseries structure** of RG flows. In every system where the beta function is computed perturbatively, the result is an asymptotic series—factorially divergent, with zero radius of convergence. Yet this divergence is not a failure but a feature.

Resurgence unifies perturbative and non-perturbative physics: each determines the other through the alien calculus.

The general pattern across all systems:

- The **Borel transform** converts divergent series to convergent ones
- **Renormalon singularities** at $\zeta_k = k/\beta_1$ obstruct naive resummation
- **Transseries** including exponentially suppressed sectors provide the complete solution
- **Ambiguity cancellation** between perturbative and non-perturbative sectors ensures physical reality

This adds a new entry to our dictionary:

Perturbative physics	Non-perturbative physics
Power series in g	Exponentially small in $1/g$
Feynman diagrams	Instantons, renormalons
Perturbative fixed points	Non-perturbative fixed points
Convergent sums (finite orders)	Transseries (all sectors)
Naive Lie group	Resurgent completion of Lie group

The resurgent perspective reveals that perturbative and non-perturbative physics are not separate domains but two aspects of a single unified structure. The perturbative coefficients "know" about non-perturbative effects through their large-order behavior; non-perturbative sectors are constrained by the requirement of ambiguity cancellation with the perturbative series. This is **resurgence**—the mutual determination of all sectors of the transseries.

Structural Stability

The classification of operators into relevant, irrelevant, and marginal is fundamentally a **structural stability analysis**. A model is structurally stable with respect to a perturbation δg^i if the perturbation is irrelevant—it decays under RG flow and does not affect long-distance physics.

Structural stability analysis determines which simplifications in a model are justified and which are not.

This perspective explains the robustness of RG predictions. When we compute critical exponents using a simplified model—neglecting certain higher-order interactions, approximating a lattice by a continuum, or truncating an infinite-dimensional theory space—the result is reliable if the neglected terms are irrelevant. The RG provides a principled way to assess which simplifications are safe and which destroy essential physics.

Conversely, relevant perturbations signal structural *instability*: the simplified model misses qualitatively important effects. The critical surface is precisely the locus of structurally unstable points—even infinitesimal relevant perturbations drive the system to qualitatively different behavior.

For the anharmonic oscillator, structural stability manifests concretely:

- **Irrelevant perturbations:** Adding higher-order terms like x^5 or x^6 to the potential does not change the universality class at weak coupling. The amplitude still decays to zero, and the phase still accumulates nonlinearly—only the numerical coefficients change.
- **Relevant perturbations:** Changing the sign of λ from positive to negative is a relevant perturbation. For $\lambda > 0$, the potential confines; for $\lambda < 0$, trajectories escape to infinity. This is a qualitative change—a different universality class entirely.

The structural stability framework thus provides both confidence (irrelevant details can be safely neglected) and caution (relevant parameters must be treated exactly). This is why the RG is predictive despite our ignorance of microscopic details.

What is Context-Dependent

While the mathematical structure is universal, specific features depend on the physical context.

The Beta Function

The explicit form of $\beta^i(g)$ depends on the system, requiring different calculational techniques in each case. For the Lorenz equations, the beta function is derived from averaging over fast oscillations and multiple-scale analysis. For Navier-Stokes, it comes from shell models or the Yakhot-Orszag ε-expansion. For the O(N) model, it is calculated from Feynman diagrams using dimensional regularization. For the 2D Ising model, it is known exactly from conformal field theory. For QED, it arises from vacuum polarization loop corrections. For the Hubbard model, it requires fermionic loop calculations or functional methods.

Dimensionality

The spatial dimension d plays a crucial role in determining what methods apply and what behavior emerges. In $d = 1$, many systems are exactly solvable: the Hubbard model via Bethe ansatz, the Ising model trivially. In $d = 2$, conformal symmetry provides exact results for the Ising CFT and the c-theorem guarantees irreversibility. In $d = 3$, where most physical systems live, analytical methods are limited and numerical approaches become essential. In $d = 4$, the upper critical dimension for ϕ^4 theory and many other systems, couplings are marginal and logarithmic corrections appear.

The dependence on dimensionality reflects the balance between fluctuations and mean-field behavior.

Symmetries

Symmetries constrain the RG flow, reducing the dimensionality of theory space and relating different correlation functions. Gauge symmetry in QED leads to Ward identities that constrain renormalization, ensuring that only one independent renormalization constant determines the running of α. The O(N) symmetry of the vector model reduces the number of independent couplings by requiring that all components of the field be treated equivalently. Conformal symmetry in the 2D Ising model completely determines the fixed-point theory, fixing all scaling dimensions and OPE coefficients. Fermi statistics in the Hubbard model shapes the Fermi surface through Pauli exclusion, fundamentally affecting the structure of the RG flow.

The Anharmonic Oscillator: A Microcosm

The anharmonic oscillator, our simple example from Chapter I, captures the essence of all six applications.

ODE Perspective

The dynamical problem $\ddot{x} + \gamma\dot{x} + \omega^2 x + \lambda x^3 = 0$ exhibits all the essential features of RG. Naive perturbation theory produces secular terms that grow without bound, requiring RG resummation just as in the Lorenz system and turbulence. The resummation yields amplitude equations with beta functions governing the slow evolution. Limit cycles and fixed points of the amplitude flow correspond to scale-invariant behavior, with the approach to equilibrium governed by stability eigenvalues.

Statistical Mechanics Perspective

The partition function $Z = \int e^{-\beta(\frac{1}{2}\omega^2 x^2 + \frac{\lambda}{4}x^4)} \mathrm{d}x$ exhibits the same RG structure in statistical language. Couplings run with temperature just as in the O(N) model and Ising CFT. Fixed points correspond to scale-invariant probability distributions. The connection to ϕ^4 field theory in zero dimensions makes the correspondence with higher-dimensional field theory explicit. The unity of the RG is already present in this simplest example.

Connections to Other Fields

The RG framework extends beyond the systems we have studied.

String Theory and Gravity

In string theory, the worldsheet theory is a 2D CFT, and the RG governs its behavior. The Ricci flow, which evolves a metric according to $\partial_t g_{ij} = -2R_{ij}$, appears as the one-loop beta function for sigma models, connecting geometry and RG.

In the AdS/CFT correspondence, the RG scale of the boundary theory corresponds to the radial direction in the bulk. This "geometric RG" provides a new perspective on the emergence of spacetime.

Condensed Matter Beyond Hubbard

The RG applies to many condensed matter systems beyond the Hubbard model. Topological phases and their protected edge states can be understood through RG flows that preserve topological invariants. Disordered systems and localization transitions involve RG flows in the space of random Hamiltonians. Quantum critical points in heavy fermion materials exhibit non-Fermi liquid behavior controlled by interacting fixed points. Strange metals may represent entirely new fixed points with no quasiparticle description.

The RG continues to reveal new physics in condensed matter, especially in strongly correlated systems.

Biology and Complex Systems

The RG philosophy of coarse-graining and emergence extends beyond physics to complex systems more broadly. Neural networks exhibit large-scale dynamics that emerge from microscopic synaptic interactions, amenable to RG-inspired analysis. Population genetics and evolution involve scale hierarchies from individual mutations through populations to species. Ecological systems and species interactions span scales from individual organisms to ecosystems. Economic systems and market dynamics show collective behavior emerging from

individual decisions. While the mathematical formalism may differ from the field-theoretic RG, the conceptual framework of scale hierarchies and effective descriptions remains powerful.

Open Problems

Despite tremendous progress, fundamental questions remain.

Non-Perturbative Fixed Points

Many important fixed points lie outside perturbative reach, requiring new theoretical and computational methods. The 3D Ising fixed point is known only numerically through Monte Carlo simulations and the conformal bootstrap, despite being the most physically relevant case. Possible non-Fermi liquid fixed points in strongly correlated electron systems have been proposed but not conclusively identified. The conformal window in non-abelian gauge theories, where asymptotic freedom coexists with an infrared fixed point, remains incompletely understood.

Resurgent fixed points. Chapter I introduced the possibility of non-perturbative fixed points emerging from the transseries completion of the beta function. Key open questions include: Does QED possess a resurgent UV fixed point that resolves the Landau pole? Can the transseries parameters C_k be determined from physical principles beyond ambiguity cancellation? Are there experimentally accessible signatures of resurgent fixed points? The interplay between the conformal bootstrap (which constrains fixed points from above) and resurgence (which reveals them from below) remains largely unexplored.

Turbulence

Fully developed turbulence remains one of the great unsolved problems in classical physics. The origin and precise values of intermittency corrections to Kolmogorov scaling are not understood from first principles. The structure of the turbulent fixed point, if one exists in a precise sense, has not been characterized. Connections to integrability and exactly solvable models remain tantalizing but incomplete.

Quantum Gravity

The RG for gravity faces profound conceptual challenges. Whether there exists a UV fixed point (the asymptotic safety scenario) that would render gravity non-perturbatively renormalizable is an open question. How the RG interplays with spacetime diffeomorphisms, which mix scales in a gauge-dependent way, remains unclear. The

correct counting of degrees of freedom in quantum gravity, which the RG requires, is itself problematic. Quantum gravity may require a fundamental extension of RG ideas rather than a straightforward application.

Quantum gravity may require a fundamental extension of RG ideas.

The Broader Significance

The renormalization group represents one of the deepest conceptual advances in theoretical physics, not merely as a calculational tool but as a shift in how we approach physical theories.

Intrinsic Structure vs. Observer-Dependent Description

Every effective description involves choices: where we place the renormalization scale μ, how we parameterize theory space, which regularization scheme we use. These choices affect numerical values. The coupling constant λ of the anharmonic oscillator *runs* with scale—its numerical value depends on these conventions.

Some quantities run with scale and depend on conventions. Others—fixed points, eigenvalues, critical exponents—are intrinsic to the physics itself.

But not everything runs. The *fixed points* of the RG flow are scale-invariant by definition—they do not change under rescaling. The *eigenvalues* at these fixed points, which determine how perturbations grow or decay, are independent of how we parameterize theory space. The critical exponents, universal amplitude ratios, and scaling functions that characterize a universality class are scheme-independent physical quantities that can be measured experimentally.

This distinction—between what runs and what does not—lies at the heart of the RG's predictive power. The running quantities carry the arbitrary conventions we introduced; the fixed-point structure reveals the physics underneath.

For the anharmonic oscillator, this distinction is concrete. The coupling λ depends on how we define the effective theory at a given scale. But the fixed point at $A = 0$ (representing the equilibrium state) and the eigenvalue $-\gamma/2$ that governs approach to equilibrium are intrinsic properties of the physical system. Any valid RG scheme must reproduce these values.

More generally, the RG transforms observer-dependent descriptions into observer-independent knowledge. What matters is not the value of a coupling at some arbitrary scale, but how couplings flow, where the flow terminates, and how it behaves near those endpoints. This is why different regularization schemes—dimensional regularization, lattice cutoffs, Pauli-Villars—all yield the same physical predictions despite assigning different values to intermediate quantities.

Emergence and Reduction

The RG provides a precise mathematical framework for understanding how macroscopic phenomena emerge from microscopic constituents. It explains both why reduction (deriving macro from micro) sometimes works and why effective theories at different scales can be largely independent.

The key insight is that microscopic details can be "irrelevant" in the technical RG sense: they decay under the flow and leave no trace at macroscopic scales. This explains the remarkable fact that we can understand phase transitions without knowing the detailed form of interatomic potentials, or that we can describe hydrodynamics without tracking individual molecular collisions.

Universality and Laws of Nature

The universality revealed by the RG suggests that the laws of physics, as we observe them, may be low-energy effective descriptions rather than fundamental truths. The microscopic theory could be quite different from what we infer from experiments, yet flow to the same IR physics.

This is both humbling and liberating. It is humbling because it suggests we may never know the "true" microscopic theory. It is liberating because it means our effective descriptions are robust: even if we are wrong about the microscopic details, the macroscopic predictions remain valid.

Information and Coarse-Graining

The irreversibility of RG flow is intimately connected to information loss under coarse-graining. The c-theorems quantify this loss, connecting the RG to information theory and thermodynamics.

The RG connects to the second law: both express the irreversibility of coarse-graining and the loss of fine-grained information.

The semi-group structure of the RG (Chapter I) reflects this irreversibility: we can coarse-grain but not "fine-grain." Once microscopic information is averaged away, it cannot be recovered. This is the RG manifestation of the second law of thermodynamics—the arrow of time in the space of models.

Conclusion

This book has developed the renormalization group as a unified geometric framework for understanding scale in physical systems. Starting from the simple notion that physics depends on the scale at which we observe it, we built a mathematical apparatus involving Lie groups, differential geometry, and flow equations. This apparatus applies with

equal validity to chaotic dynamics in the Lorenz system, turbulent flows governed by Navier-Stokes, phase transitions in the O(N) model and 2D Ising model, quantum electrodynamics, strongly correlated electrons in the Hubbard model, and fracture mechanics in solids. The common mathematical structure underlying these diverse phenomena is the RG flow on theory space, with fixed points representing scale-invariant physics and eigenvalues determining universal critical behavior.

The RG teaches us that understanding physics at one scale gives insight into physics at all scales.

The renormalization group is not merely a calculational technique but a way of thinking about physical systems. It reveals the hidden simplicity behind apparent complexity, the emergence of universal behavior from diverse microscopic origins, and the deep connections between seemingly unrelated areas of physics.

As we have seen, the RG framework continues to generate new insights and applications. From its origins in handling infinities in quantum field theory to its current role as a unifying principle across physics, the renormalization group stands as one of the great intellectual achievements of the twentieth century, with much still to be discovered in the twenty-first.

"The enormous usefulness of mathematics in the natural sciences is something bordering on the mysterious, and there is no rational explanation for it."

— Eugene Wigner

Mathematical Toolkit

This appendix provides a compact reference for the mathematical tools used throughout the book. Each topic is treated in the main text and this serves as a quick-lookup resource rather than a standalone introduction.

This appendix collects definitions, formulas, and key results for quick reference. The material has been developed throughout Part I and is gathered here for convenience.

Asymptotic Series and Gevrey Classes

Asymptotic Expansions

A formal series $\tilde{f}(z) = \sum_{n=0}^{\infty} a_n z^n$ is **asymptotic** to a function $f(z)$ as $z \to 0$ if:

$$\left| f(z) - \sum_{n=0}^{N-1} a_n z^n \right| \leq C_N |z|^N \tag{407}$$

for each N and $|z|$ sufficiently small. We write $f(z) \sim \tilde{f}(z)$.

Gevrey Classes

A series is **Gevrey of order** s (written Gevrey-s) if its coefficients satisfy:

$$|a_n| \leq C \cdot K^n \cdot (n!)^s \tag{408}$$

for some constants $C, K > 0$.

Gevrey-0: Convergent series with $|a_n| \leq CK^n$.

Gevrey-1: Factorially divergent with $|a_n| \leq CK^n \cdot n!$. This is the generic case in physics.

Gevrey-s for $s > 1$: Faster than factorial growth, less common.

Borel Transform and Laplace Transform

The Borel Transform

Given a formal series $\tilde{f}(z) = \sum_{n=0}^{\infty} a_n z^n$, its **Borel transform** is:

$$\hat{f}_B(\zeta) = \sum_{n=0}^{\infty} \frac{a_n}{n!} \zeta^n \tag{409}$$

For Gevrey-1 series, the Borel transform has finite radius of convergence and can be analytically continued.

The Laplace Transform

The **Laplace transform** of $g(\zeta)$ along direction θ is:

$$\mathcal{L}_\theta[g](z) = \int_0^{e^{i\theta}\infty} e^{-\zeta/z} g(\zeta)\, d\zeta \tag{410}$$

Borel-Laplace Resummation

The **Borel sum** of $\tilde{f}$ along direction θ is:

$$\mathcal{S}_\theta[\tilde{f}](z) = \mathcal{L}_\theta[\hat{f}_B](z) = \int_0^{e^{i\theta}\infty} e^{-\zeta/z} \hat{f}_B(\zeta)\, d\zeta \tag{411}$$

This recovers a function from a divergent series when no singularities obstruct the integration path.

Singularities in the Borel Plane

Types of Singularities

Common singularities in the Borel plane of physical theories include the following.

Instantons: Singularities at $\zeta = S_{\text{inst}}$ (classical instanton action). These encode tunneling effects and typically have the form:

$$\hat{f}_B(\zeta) \sim \frac{c}{(\zeta - S)^\alpha} \log(\zeta - S) + \text{regular} \tag{412}$$

Renormalons: Singularities at $\zeta = k/\beta_1$ (multiples of inverse one-loop beta function). These arise from factorial growth induced by RG running:

$$\hat{f}_B(\zeta) \sim \frac{1}{(1 - \beta_1 \zeta)^p} \tag{413}$$

IR renormalons: Singularities on the positive real axis, obstructing naive Borel resummation.

UV renormalons: Singularities on the negative real axis, not obstructing resummation but encoding UV sensitivity.

Stokes Phenomena

Stokes Lines

A **Stokes line** is a direction in the z-plane where the integration contour for Borel-Laplace resummation crosses a singularity in the Borel plane. For a singularity at ζ_*, the Stokes line occurs at:

$$\arg(z) = \arg(\zeta_*) \tag{414}$$

The Stokes Automorphism

When crossing a Stokes line, the resummation changes discontinuously. The **Stokes automorphism** $\mathfrak{S}$ acts on the transseries parameter:

$$\mathfrak{S} : \sigma \mapsto \sigma + S_\omega \tag{415}$$

where S_ω is the **Stokes constant** associated with the singularity at ω.

Stokes Constants

The Stokes constant encodes the "residue" of the ambiguity in crossing a singularity. It relates different sectors of the transseries and is computed from:

$$S_\omega = 2\pi i \cdot \mathrm{Res}_\omega[\hat{f}_B] \tag{416}$$

for simple poles, with generalizations for branch points.

Transseries

Definition

A **transseries** combines perturbative and non-perturbative sectors:

$$\tilde{f}(z, \sigma) = \sum_{k=0}^{\infty} \sigma^k e^{-kS/z} \hat{f}^{(k)}(z) \tag{417}$$

where $\hat{f}^{(0)}$ is the perturbative series, $\hat{f}^{(k)}$ for $k \geq 1$ are instanton sectors, σ is the transseries parameter, and S is the instanton action.

More General Form

Multi-instanton transseries with multiple types of non-perturbative effects:

$$\tilde{f}(z, \{\sigma_i\}) = \sum_{n_1, n_2, \ldots} \prod_i \sigma_i^{n_i} e^{-(\sum_i n_i S_i)/z} \hat{f}^{(n_1, n_2, \ldots)}(z) \tag{418}$$

Reality Conditions

For real z, physical observables must be real. This constrains transseries parameters:

$$\text{If } \bar{\sigma} = \sigma^*, \text{ then } \overline{\tilde{f}(z, \sigma)} = \tilde{f}(\bar{z}, \bar{\sigma}) \tag{419}$$

Alien Calculus

The Alien Derivative

The **alien derivative** Δ_ω probes the singularity at $\zeta = \omega$ in the Borel plane. It extracts the coefficient relating the perturbative sector to the

instanton sector:

$$\Delta_\omega \hat{f}^{(0)} = S_\omega \hat{f}^{(1)} \tag{420}$$

where S_ω is the Stokes constant.

The Bridge Equation

The alien derivative is related to ordinary differentiation along transseries directions:

$$\Delta_\omega \tilde{f} = S_\omega \cdot \frac{\partial \tilde{f}}{\partial \sigma} \tag{421}$$

This is the **bridge equation**. It connects the Borel plane structure to the transseries parameter space.

Properties

The alien derivative satisfies a Leibniz rule:

$$\Delta_\omega(fg) = (\Delta_\omega f)g + f(\Delta_\omega g) \tag{422}$$

Multiple alien derivatives compose:

$$\Delta_{\omega_1}\Delta_{\omega_2} = \Delta_{\omega_2}\Delta_{\omega_1} \tag{423}$$

Median Resummation

Lateral Resummations

When a singularity lies on the positive real axis, define:

$$\mathcal{S}_\pm[\tilde{f}](z) = \mathcal{L}_{0^\pm}[\hat{f}_B](z) \tag{424}$$

by integrating just above or below the real axis.

The Median Resummation

The **median resummation** is the average:

$$\mathcal{S}_{\text{med}}[\tilde{f}](z) = \frac{1}{2}\left(\mathcal{S}_+[\tilde{f}] + \mathcal{S}_-[\tilde{f}]\right) \tag{425}$$

This gives a real result when the singularities come in conjugate pairs.

Ambiguity Cancellation

The difference between lateral resummations is:

$$\mathcal{S}_+[\tilde{f}] - \mathcal{S}_-[\tilde{f}] = 2\pi i \cdot \text{Disc}[\hat{f}_B] \tag{426}$$

For physical observables, this ambiguity must cancel against contributions from other sectors of the transseries.

Beta Functions and RG Flow

Definition

The **beta function** for coupling g^i is:

$$\beta^i(g) = \mu \frac{dg^i}{d\mu} = \frac{dg^i}{d\ell} \tag{427}$$

where μ is the RG scale and $\ell = \log(\mu/\mu_0)$.

Fixed Points

A **fixed point** satisfies $\beta^i(g^*) = 0$ for all i.
Perturbative fixed points: $\beta_{\text{pert}}(g^*) = 0$.
Non-perturbative fixed points: $\beta_{\text{pert}}(g^*) \neq 0$ but $\beta_{\text{full}}(g^*) = 0$.

Stability

Near a fixed point, linearize: $\delta\dot{g}^i = B^i{}_j \delta g^j$ where $B^i{}_j = \partial\beta^i/\partial g^j|_{g^*}$.

The eigenvalues Δ_α of B classify directions. When $\Delta_\alpha > 0$ the direction is relevant, when $\Delta_\alpha < 0$ the direction is irrelevant, and when $\Delta_\alpha = 0$ the direction is marginal.

Connections and Monodromy

Connections

A **connection** $\Gamma^a{}_{bc}$ on parameter space specifies parallel transport:

$$\nabla_b V^a = \partial_b V^a + \Gamma^a{}_{bc} V^c \tag{428}$$

The **curvature** measures path dependence:

$$R^a{}_{bcd} = \partial_c \Gamma^a{}_{bd} - \partial_d \Gamma^a{}_{bc} + \Gamma^a{}_{ec}\Gamma^e{}_{bd} - \Gamma^a{}_{ed}\Gamma^e{}_{bc} \tag{429}$$

Monodromy

Monodromy is the transformation acquired by parallel transport around a closed loop:

$$M(\mathcal{C}) = \mathcal{P} \exp\left(\oint_{\mathcal{C}} \Gamma^a{}_{bc}\, dg^b \right) \tag{430}$$

Stokes as monodromy: The Stokes automorphism is monodromy around the Stokes line in extended parameter space.

Key Formulas Summary

Name	**Formula**
Gevrey-1 bound	$\lvert a_n\rvert \le CK^n n!$
Borel transform	$\hat{f}_B(\zeta) = \sum_n \frac{a_n}{n!}\zeta^n$
Laplace transform	$\mathcal{L}[g](z) = \int_0^\infty e^{-\zeta/z} g(\zeta)\, d\zeta$
Borel sum	$\mathcal{S}[\tilde{f}] = \mathcal{L}[\hat{f}_B]$
Transseries	$\tilde{f} = \sum_k \sigma^k e^{-kS/z} \hat{f}^{(k)}$
Bridge equation	$\Delta_\omega \tilde{f} = S_\omega \partial_\sigma \tilde{f}$
Beta function	$\beta^i = \mu\, dg^i/d\mu$
Fixed point	$\beta^i(g^*) = 0$
Callan-Symanzik	$(\mu\partial_\mu + \beta^i\partial_i + n\gamma)G_n = 0$
Operator mixing	$\mu\, d\mathcal{O}_a/d\mu = \gamma_a{}^b \mathcal{O}_b$

References for Further Reading

Asymptotic Analysis and Resurgence

The foundational work on resurgence is Écalle's treatise on analysable functions. Accessible introductions include Costin's monograph on exponential asymptotics and the lecture notes by Mariño on resurgence in quantum field theory. The paper by Aniceto, Başar, and Schiappa provides a modern physics perspective.

Renormalization Group

Wilson's original papers remain essential reading. The textbooks by Goldenfeld, by Cardy, and by Amit and Martín-Mayor provide comprehensive treatments. For the geometric perspective, see the papers by Zamolodchikov on the c-theorem and the reviews by Komargodski.

Differential Geometry

For connections and fiber bundles in physics contexts, see the books by Nakahara and by Frankel. The information geometry perspective is developed in the book by Amari.

Bibliography

G. I. Barenblatt. *Similarity, Self-Similarity, and Intermediate Asymptotics*. Consultants Bureau, New York, 1979.